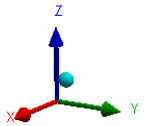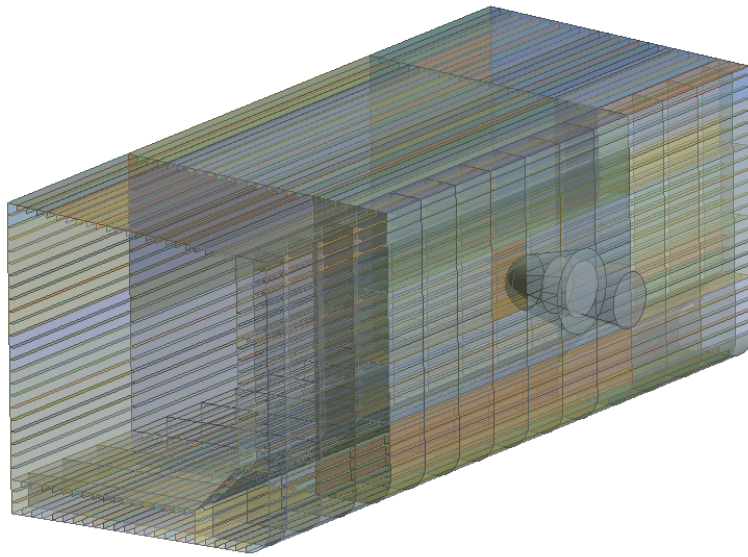# CHALMERS

Ice-Ship Collision in the Arctic Region

Master's Thesis in the Nordic Master in Maritime Engineering

CHI CHEN

Department of Shipping and Marine Technology
Division of Marine Technology
CHALMERS UNIVERSITY OF TECHNOLOGY
Göteborg, Sweden 2015
Master's thesis X-15/327

MASTER'S THESIS IN THE NORDIC MASTER IN MARITIME ENGINEERING

Ice-Ship Collision in the Arctic Region

CHI CHEN

Department of Shipping and Marine Technology
Division of Marine Technology
CHALMERS UNIVERSITY OF TECHNOLOGY
Göteborg, Sweden 2015

Ice-Ship Collision in the Arctic Region

CHI CHEN

Cover:
The ice-ship collision model in this master thesis report.

Ice-Ship Collision in the Arctic Region
Master's Thesis in the Nordic Master in Maritime Engineering
CHI CHEN
Department of Shipping and Marine Technology
Division of Marine Technology
Chalmers University of Technology

ABSTRACT

As the global warming enhance the ice melting in the Arctic region, it is easier to access the area once thought to be the forbidden zone for human beings. The shipping and offshore industry can have a lot benefits from the Arctic region. The Euro-Asian shipping route is shorter via the Arctic than traditional Suez Cannel Route. Furthermore, according to the data reported by the US Geological Survey, over one tenth of the undiscovered oil and around one third of the undiscovered natural gas reserves are believed to be stored in the Arctic region. There is a huge potential for the energy exploration in the Arctic. Due to the public concerns regarding the safety and environmental sensitive in this region, sailing and operation in the Arctic region has been attracted increasing attention. In marine industry, great challenge can also come from the technical immaturity related to the icebergs and low temperature effects, which are the major threats to the safe vessel operating in the Arctic region.

The iceberg with huge inertia can cause serious damage on vessels' structure if there is a collision happened between the ship and iceberg even though the ice is considered to be fragile. The low temperature can contribute to a higher steel yield stress but also lead to be brittle characteristics. The steel will have lower failure strain value due to low temperatures. In addition to these factors, the consequence of an ice-ship collision may be affected by other factors like the shape of the iceberg, boundary conditions, collisions etc.

In order to have a detail investigation into the collision in the Arctic region, FE simulation is implemented in this thesis project. It is expected that the collision will lead to non-linear deformation of the metal structure. The explicit simulation method is used to model the collision phenomena. The simulation is carried out by the FE software ANSYS Workbench Explicit using the dynamic explicit solver of AUTODYN. Many cases are raised in this thesis report to conclude the factors that influence the collision results. Different ambient conditions and collision scenarios are distinguished in those cases.

The optimization of operation and a ship structure for a better collision behaviour in the arctic region operation are also studied in this thesis report based on the results and analysis of the FE simulations.

Key words: Arctic, ice-ship collision, low temperature, non-linear FEA, optimization

II

Contents

Preface

This thesis is a part of the requirements for the master's degree in Nordic Master in Maritime Engineering at both Norwegian University of Science and Technology (NTNU), Trondheim, Norway and Chalmers University of Technology (Chalmers), Göteborg, Sweden. It has been carried out at the Division of Marine Technology, Department of Shipping and Marine Technology, Chalmers University of Technology between January and June of 2015.

I would like to acknowledge and thank my examiners and supervisors, Associate Professor Wengang Mao at the Department of Shipping and Marine Technology in Chalmers University of Technology and Professor Sören Ehlers at the Department of Marine Technology in Norwegian University of Science and Technology, for their excellent guidance and support throughout the work with this thesis. I would also like to show my thanks to Mr. Ivar Håberg, head of section in hull, stability and loadline at DNV GL Shanghai office. Without the profile of a CSR oil tanker he provided to me, it is impossible for me to build up the model for FE simulations. Mr. Junhua Zhang, once was my tutor in DNV GL Shanghai office during my summer internship 2014, also helped me to search the data I need. Moreover, I still get benefit from what Mr. Zhang guided me during my summer internship in the FE modelling at DNV GL Shanghai office.

During the building process of my master thesis, I also received many suggestions and advices. Professor Jonas Ringsberg at the Department of Shipping and Marine Technology in Chalmers University of Technology gave me many constructive advices after the mid-term review. Also my coordinator (Ph.D.) Mr. Per Hogström at the Department of Shipping and Marine Technology in Chalmers University of Technology gave me many guidance on the collision studies. I would also appreciate the help from Mr. Zhenhui Liu, the senior project engineer (Ph.D.) at REINERTSEN, Trondheim, Norway. He answered me many questions regarding his Ph.D. thesis, which is also focus on the ice-ship collisions.

I would also like to pay my tribute to all the people who organize the programme of Nordic Master in Maritime Engineering. Two years study at two excellent universities in Scandinavia will be one of my best memories in my life. Special thanks to Associate Professor Paul Anderson at the Department of Mechanical Engineering in Technical University of Denmark. He is the coordinator in general for the programme.

Finally, it should be noted that without the support from my friends and my family, it will be impossible for me to have such a nice study and life time abroad.

Göteborg, May 2015

Chi Chen

Notations

Abbreviations

AHSS	Advanced High Strength Sheet Steel
CFL	Courant-Friedrichs-Lwey (Conditions)
CN	Country code for China
CSR	Common Structural Rules
DNV GL	The name of a classification society
EPS	Equivalent Plastic Strain
FE	Finite Element
FEA	Finite Element Analysis
FPSO	Floating Production Storage Offloading
IACS	International Association of Classification Societies
NL	Country code for Netherlands
NSR	Northern Sea Route
NVA	Grade A steel defined by DNV
SCR	Suez Canal Route
TWIP	Twinning-Induced Plasticity Steel
USGS	U.S. Geological Survey

Roman upper letters

B	Breadth moulded
C_b	Block coefficient
D	Depth moulded
E	Young's modulus
F_i	Forces applied on the nodal points
$F(t)$	Load vector, as the function of time t
G	Shear Modulus
K	Bulk Modulus
L	Rule length
L_{bp}	Length between perpendiculars
L_{VE}	Virtual extensonrmeter when fracture occurs
R	Radius
RX	Degree of freedom regarding the rotation around X-axis
RY	Degree of freedom regarding the rotation around Y-axis
RZ	Degree of freedom regarding the rotation around Z-axis
T	Drought moulded
T_{ref}	Temperature at which zero thermal strains exist (at reference
V	Volume matrix
V_0	Initial volume matrix
W	Original width of the specimen
X	Degree of freedom regarding the displacement on X-axis
Y	Degree of freedom regarding the displacement on Y-axis
Z	Degree of freedom regarding the displacement on Z-axis

Roman lower letters

b_i Components of body acceleration

$b_{x,y,z}$ Body force tensor

c Damping matrix/ the sound speed in the local material/ Barba parameter

e Energy matrix

f Stability time step factor (0.9 by default)

k Stiffness matrix

l Element size

m Mass matrix/ mass attributed to the node

t Time/ thickness

Δt Time step

x Displacement in X, dot(s) above means the total derivative to time t

y Displacement in Y, dot(s) above means the total derivative to time t

z Displacement in Z, dot(s) above means the total derivative to time t

Greek lower letters

$\alpha^{se}(T_{ref})$ Secant coefficient of thermal expansion

ε Local/true strain

ε^{th} Thermal strain

ε_{ij} Strain tensor

ε_f Failure strain

ε_p Plastic strain

$\varepsilon_{p\max}$ Maximum equivalent plastic strain

κ Curvature

ν Poisson's ratio

ρ Density or density matrix

ρ_0 Initial density matrix

σ Local/true stress

σ_c Compressive Strength

σ_f Corresponding failure stress at the failure strain

σ_{ij} Stress tensor

σ_t Tensile Strength

1   Introduction

1.1 Backgrounds

The Arctic region is regarded as the last front line for the human beings exploration of energy and resources on the earth. USGS (2008) reports that 13% of the undiscovered oil and 30% of the undiscovered natural gas reserves are estimated located in the Arctic region. Although the oil and gas prices have dropped in the past year and the commercial drilling activities are suffering, it does not mean the exploration in the Arctic region is losing its value. As a rule of market, the low prices of fossil fuels will excite the consumption of them and in turns to push the prices higher in the future. Nevertheless, the new energy, like wind power, solar power, tide power and et cetera are developing, fossil fuels will be still the main energy resources for the human beings in the foreseeable future. Hence, in general, it is believed that global capital will still be interested in the exploration of fossil fuels resources. And the Arctic region is of course a hot spot to be investigated. However, for the next round investment on the traditional energy resources exploration, more sophisticated and advanced technologies will be required to keep the industry in a more sustainable development.

Moreover, the shipping industry also has great interest on the Arctic route. Due to the global warming, more ice melt during the summer in the Arctic region. Hence, shipping in the Arctic during the summer seems to be possible. The concept of Northern Sea Route (NSR) has been put forward for the discussion in recent years. Report of DNV GL shows the possibility to operate and sail in the Arctic in summer. To estimate the risk for the Arctic operation, DNV GL set safety and operability index to distinguish the danger and risk. From the illustration of the index, sailing through the Arctic region along the north coast line of Russia is less dangerous in July.
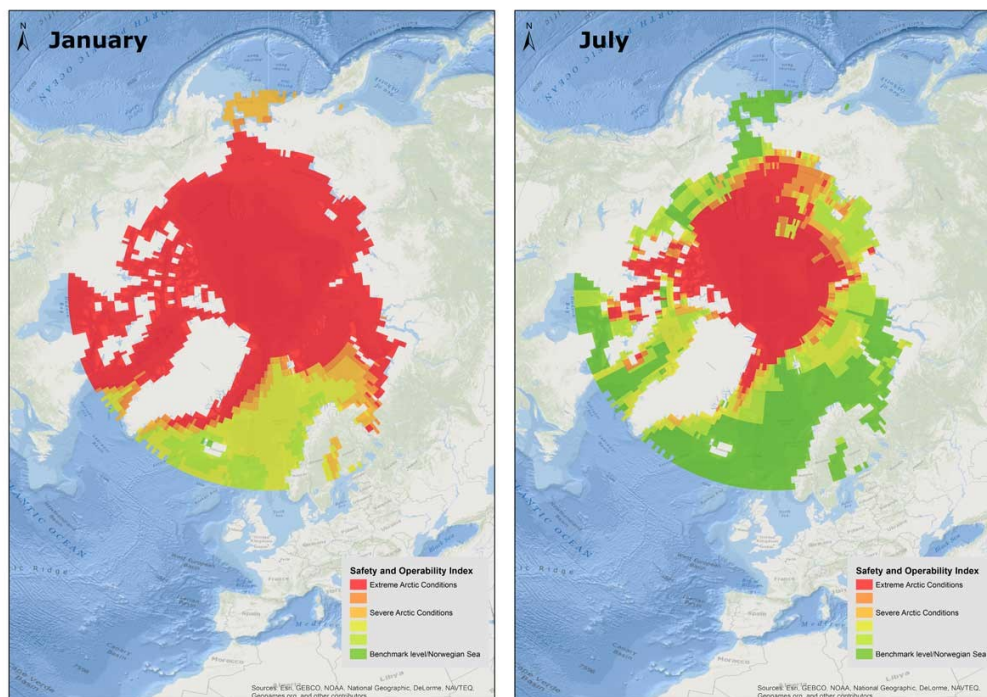

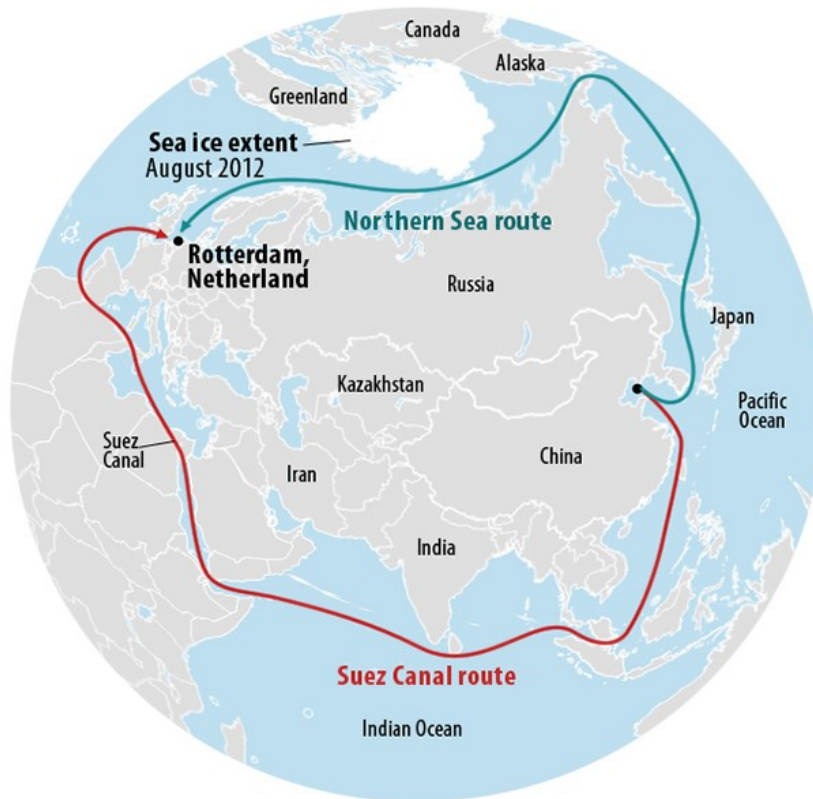*Figure 1-1 Safety operations index, from DNV GL*

Figure 1-2 NSR vs. SCR between Rotterdam (NL) and Dalian (CN)

The shipping between Europe and the Far East will benefit a lot from the NSR. For example, Rotterdam in Netherlands and Dalian in China are both big ports in their local region. And every year there is big amount of trade between Europe and China. The distance for Suez Canal Route (SCR) between the two ports is 24100km. And SCR crosses some dangerous areas like Gulf of Aden and Strait of Malacca. The security conditions are not optimistic due to the pirate activities. However, the distance of NSR is only 15400km between the two ports. More time and fuel can be saved for shipping via NSR. And there is almost no pirate threats on the European, Russian, Japanese, South Korean and Chinese water. Hence, the NSR has more advantages in the summer compared to SCR.

The Arctic energy exploration and shipping have a promising future, but the ice load and low temperature are still the priority challenges for the Arctic activities.

The Titanic disaster is still a topic and a landmark accident in the maritime history. The collision between iceberg or floating ice and ship structures are also the threats for vessels travelling in the Arctic region.

Moreover, the low temperature will also change the mechanical performance of materials, especially steels. Although the steel will have a high strength in low temperature, it will also become more brittle and easier to fail. Hence, the collision scenario under low temperature is more dangerous since it is easier for the material to fail.

CHALMERS, *Shipping and Marine Technology*, Master's Thesis

1.2 Motivation and Object

In order to have a sustainable development in the Arctic region, a safer and strong enough hull should be expected when sailing in the Arctic. It is not only a critical issue for the crew safety, but also an environmental issue. It is widely known that the leakage of the crude oil from a tanker will result in huge environmental disaster. The ecosystem in the Arctic region is vulnerable. That is to say the leakage in the Arctic region will have more serious influence than anywhere else.

Moreover, the environmental promotion is also at its highest peak ever. Frank Zelko (2013) reported that the Arctic drilling is already being disturbed by some extreme eco-organization like GREENPEACE. And it is now still a very controversial topic in the public. If crude oil leakage happens in the Arctic, it will have a high probability for the Arctic energy exploration to be stopped.

Although ice class is required in the Arctic sailing vessel, it cannot be sure that it will not fail under severe collision conditions. A worst case collision scenario will perform in this thesis project. That is to investigate if the hull structure will be damaged or even penetrated by the hitting ice. But to have a full scale collision experiment will be very expensive. Hence, the collision simulation will be carried out by the finite element analysis (FEA) software to see the result.

Lin and Abatan (1994) pointed out that the commercial FEA solvers are already well developed. ANSYS and ABAQUS are considered to be the most common used commercial FEA software. The calculation results from those FEA software are actually quite reliable. Hence, one of them, i.e. Ansys, is also chosen in this thesis project to carry out such simulations.

Although there are many research focus on the ice-ship collision, but they seldom take the low temperature into consideration. However, it is known that the low temperature will change the mechanical behaviour of materials, especially metals. In this thesis, a discussion will be illustrated on how the low temperature affects the collision. The overall objective of the thesis is to analyse the simulation of ice-ship collision under low temperature, and comes out with the optimization solution regarding both operational and structural aspects to prevent disaster scenario.

1.3 Procedures

To achieve the object, the collision simulation will be implemented. Vessel and iceberg are the two objects to be modelled in the simulation software. Hence, how to define the geometry and mechanical properties in the simulation process needs to be further discussed.

An oil tanker followed the common structural rules (CSR) is taken as the target vessel to be hit by the iceberg. The collision area is set to be the side structure of the parallel body of the tanker. And the collision position is near the water line. However, like all the inartificial things in the nature, the shape and properties of the iceberg is not easy to point out with a so called standard value. Therefore, there will be a specific chapter to discuss the problem in detail.

During the modelling process, some simplification will be taken in order to save the simulation time. It cannot be denied that an accurate model will have the result near the practical case. However, it is also known that a more accurate model also means more time consumption no matter on the model building or the calculation. Hence, how to balance the accuracy of the modelling and time consumption will be also illustrated in this thesis.

The collision scenarios are also another issue to be discussed. Under the sailing or porting conditions, the hitting iceberg or floating ice will come to the vessel with any reasonable angles or speeds. It is not possible to point out all of them. However, some special situations will be discussed in the thesis.

The results of those cases will be analysed. The analysis will focus on failure area, plastic deformation area on the vessel hull structure. The energy dissipation, velocity, and acceleration and etc. will be also under the monitoring.

Based on the analysed results, the risk-reduce methods both on operation and structure will be put on deck. Regulating the operation of the crew members can prevent the collision happen. In case of the collision between ice and vessels cannot be avoided, an optimized stiffened structure of the vessel will be suggested to resist the collision. It is expected that the optimized structure of the vessel can reduce the damage caused by the ice ship collision.
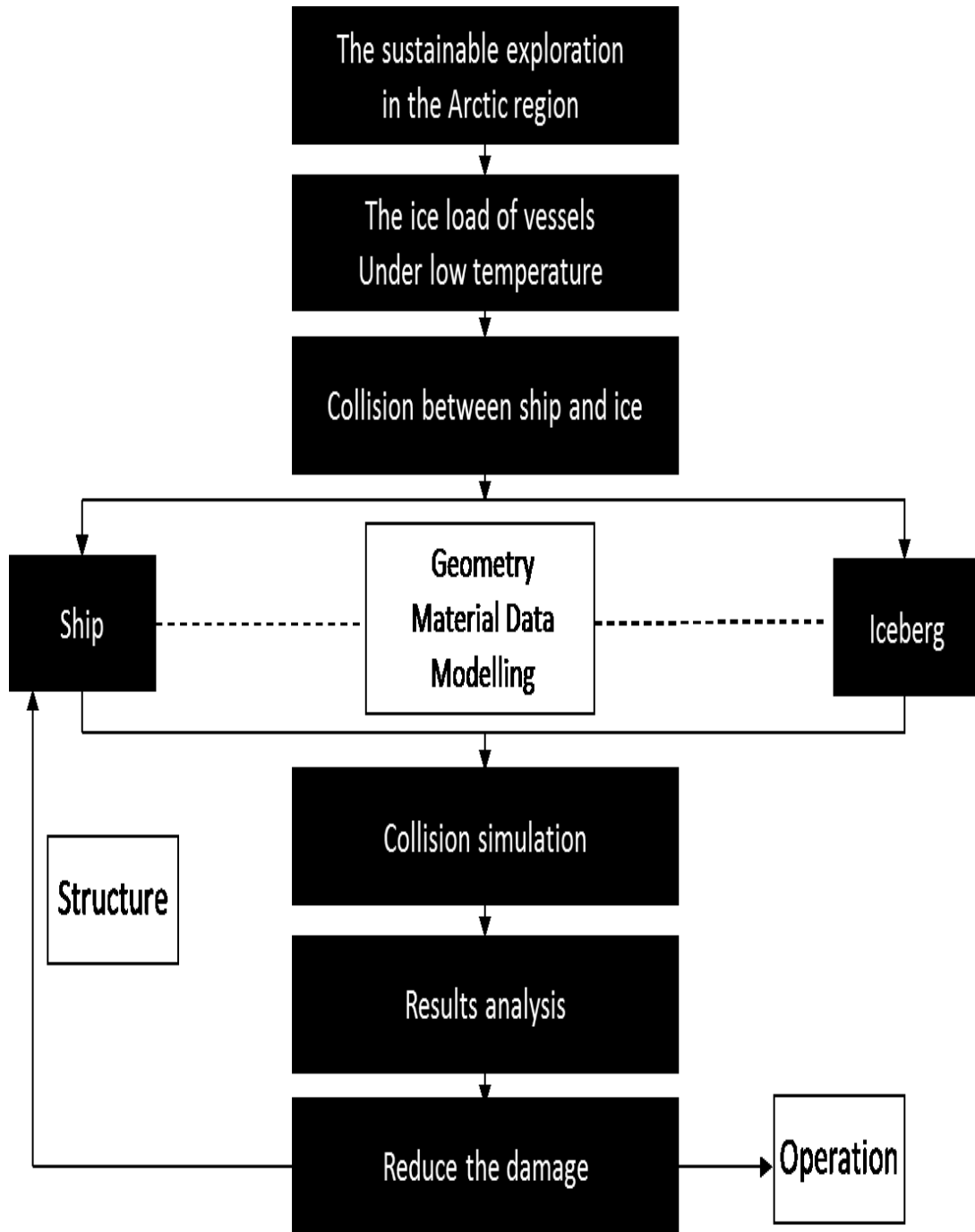
Figure 1-3 The general procedures used in this thesis

1.4 Limitation

Since time is the priority limitation for the project and all the process should be finished within 20 weeks, the results and optimization suggestions are also needed to be offered at the end of the project. It is known that every scientific or engineering research needs to spend plenty of time on it. And whether the results of the research are satisfied or not is unknown. It is the same thing in this thesis. 20 weeks are too short for a scientific research. There is still much future work to do.

The hull structure is another limitation. Due to the confidential issues, there is no public data can be checked for the structure details of oil tankers or FPSO. As a consequence, it is more difficult to find the detail information of an oil tanker with ice class. Thanks for the help from Mr. Ivar Håberg, DNV GL China, he provided me with a training handbook of Nauticus Hull. The profile of a common structural rule (CSR) oil tanker is provided. However, there is no ice class with the vessel. The vessel is more vulnerable to the ice load. Therefore, the collision from the iceberg can cause the damage easier. But in the other way, the collision mechanism can be observed more obviously. The effects of adding ice-class or other anti-collision equipment can also be verified. And more general collision problems can be derived from the case used in this thesis.

For the whole hull model, the same type steel will be used. The mechanical performance of the steel under different temperatures is not covered in all the range. But two specific temperatures are pointed out: 0°C and -30°C. Hence, the steel mechanical behaviour under those two temperature conditions will be defined in the specific region.

Due to the limitation of the authorized software in Chalmers, ANSYS Workbench Explicit is the main simulation tool for this master thesis. It is based on the solver AUTODYN.

2 Theories to Support the Collision Simulation

FEA will be used to simulate the collision phenomena. The basic idea of FEA is to discrete the physical properties of the material to numbers of elements. Loads and boundary conditions will be applied on the vertexes of those elements. And the results are based on the displacement of the vertexes on those elements.

Both "Implicit" and "Explicit" methods are used in the dynamic simulations via FEA. "Implicit" and "Explicit" are two kinds of integration methods used in dynamic simulations. Regarding the transient dynamic analysis, they are based on different basic formulations and process.

2.1 Introduction to Implicit and Explicit Methods

In order to clarify the compare "Implicit" and "Explicit" methods, the differences of them in motion equations and time integration will be illustrated.

2.1.1 Motion Equations

ANSYS, Inc (2013) provided the two basic motion formulations in ANSYS 15.0 Help Viewer. The basic equation of motion used in the implicit transient dynamic analysis:

$$m\ddot{x} + c\dot{x} + kx = F(t) \tag{2-1}$$

Where

m =   Mass matrix

x =   Displacement, dot(s) above means the total derivative to time t

c =   Damping matrix

k =   Stiffness matrix

$F(t)$ =   Load vector, as the function of time t

There are several motion equations from different aspect to support the explicit transient dynamics.

From the view of conservation of the mass:

$$\frac{\rho_0 V_0}{V} = \frac{m}{V} \tag{2-2}$$

Where

ρ_0 =   Initial density matrix

V_0 =   Initial volume matrix

V =   Volume matrix

m =   Mass matrix

From the view of conservation of the momentum relate the acceleration to the stress tensor

$$\rho\ddot{x} = b_x + \frac{\partial \sigma_{xx}}{\partial x} + \frac{\partial \sigma_{xy}}{\partial y} + \frac{\partial \sigma_{xz}}{\partial z} \qquad\qquad (2\text{-}3.1)$$

$$\rho\ddot{y} = b_y + \frac{\partial \sigma_{yx}}{\partial x} + \frac{\partial \sigma_{yy}}{\partial y} + \frac{\partial \sigma_{yz}}{\partial z} \qquad\qquad (2\text{-}3.2)$$

$$\rho\ddot{z} = b_z + \frac{\partial \sigma_{zx}}{\partial x} + \frac{\partial \sigma_{zy}}{\partial y} + \frac{\partial \sigma_{zz}}{\partial z} \qquad\qquad (2\text{-}3.3)$$

Where

ρ =   Density matrix

x, y, z =   Displacements in the corresponding directions

$b_{x,y,z}$ =   Body force tensor

σ_{ij} =   Stress tensor

Dot(s) above means the total derivative to time t

From the view of conservation of energy

$$\dot{e} = \frac{1}{\rho}\left(\sigma_{xx}\dot{\varepsilon}_{xx} + \sigma_{yy}\dot{\varepsilon}_{yy} + \sigma_{zz}\dot{\varepsilon}_{zz} + 2\sigma_{xy}\dot{\varepsilon}_{xy} + 2\sigma_{yz}\dot{\varepsilon}_{yz} + 2\sigma_{zx}\dot{\varepsilon}_{zx}\right) \qquad (2\text{-}4)$$

Where

e   =   Energy matrix

ρ =   Density matrix

σ_{ij} =   Stress tensor

ε_{ij} =   Strain tensor

Dot(s) above means the total derivative to time t

2.1.2   Time Integration

In the ANSYS Workbench Help Viewer, ANSYS, Inc (2013) indicates the time integration methods for implicit and explicit simulations.

In the linear problems of the implicit simulations, time integration is stable. However, the time step value will be changed to meet the requirement of the accurancy.

But for the nonlinear problems of the implicit simulations, solution will be obtained with a series of linear approximations. Normally, the linear approximation is based on Newton-Raphson method. However, the solution also requires the inversion of the nonlinear dyanmic equivalent stiffness matrix. And in order to achieve the convergence, smaller and iterative time steps are required. Even the convergence tools are employed in the simulation, it can not guarantee the convergence of the highly nonlinear problems.

The time integration method is more uniform in the explicit problems regardless of the linear or nonlinear problems.

Central difference time integration scheme, often referred to the Leapfrog method, is used in the Explicit Dynamic slover of the ANSYS Workbench.

The nodal acceleratios will be get by force divided by mass, after the forces on the mesh nodes have been obtained. Hence, the accelrations are

$$\ddot{x}_i = \frac{F_i}{m} + b_i \qquad\qquad (2\text{-}5)$$

Where

$\ddot{x}$ =   Components of nodal acceleration (i=1, 2, 3)

F_i =   Forces applied on the nodal points

b_i =   Components of body acceleration

m =   Mass attributed to the node

When the acceleration at time *m* has been determined, the velocity at time of *m+1/2* and displacement at time of *m+1* will be:

$$\dot{x}_i^{m+1/2} = \dot{x}_i^{m-1/2} + \ddot{x}_i^m \Delta t^m \tag{2-6}$$

$$x_i^{m+1} = \dot{x}_i^m + \dot{x}_i^{m+1/2} \Delta t^{m+1/2} \tag{2-7}$$

This method has advantages on nonlinear probelmes. Since the equations are uncoupled, they can be solved directly. That is also why the method can be called explicit. Also due to the equations are uncoupled, no convergence checks will be needed. And the inversion of the stiffness matrix is not required, because all nonlinearities are counted in the internal force vector.

To ensure the the accuracy and stability of the results, the value of the time step will be critial for the explicit problems. In the ANSYS Workbench Explicit, the time step is regulated by the CFL (Courant-Friedrichs-Lwey) conditions. Richard Courant et al. (1967) argues that the CFL condittion limit the disturbance or stress wave cannot travel farther than the smallest characteristic element dimension of the mesh in a time step. Hence the time step should fulfill the criteria:

$$\Delta t \leq f \cdot \left[\frac{h}{c} \right]_{min} \tag{2-8}$$

Where

Δt =   Time step

f =   Stability time step factor (0.9 by default)

h =   Characteristic dimension of an element

c =   The sound speed in the local material of the element

2.1.3 The Advantages of Explicit Dynamics

The nonlinear problems are more suitable to use explicit method. It will be more efficient and accurate. Moreover, Alexander Pett (2011) fingers out that explicit time integration will be more accurate and efficient when applying the simulations involving the propagation of shock wave, large strains and deformations, the nonlinear behaviour of materials, non-linear buckling, complex contacts and fragmentation. Therefore, the typical applications for the Explicit Dynamics are drop tests and impact or penetration.

It is highly expected during the simulation of ice-ship collisions that a non linear material performance will occur. The penetration and failure of the materials may also happen. Based on the evaluation and theory explaination of the implicit and explicit dyanmics, the explicit dynamic method will be chosen for the analysis of the ice-ship collision in this case.

2.2 Framework for the Solution

Much like the solution process of the structural static analysis in the finite element method, the model will be discretized into many mesh elements. And the material properties, loads, constraints and other initial conditions will be applied on the mesh. Then the time will be integrated, so it will have motion at the nodes of the mesh. The elements of the mesh will have deformation due to the motion of the nodes. The volume will be changed in those elements. And the rate of the deformation will produce the material strain rates. Hence, based on the strain vs. stress relationship, the stresses of the elements can be obtained. Then, the stresses will turn back to the internal nodal forces. The boundary conditions, body interaction and loads will give the state of the external nodal forces. Combined internal and external nodal forces, the nodal accelerations can be get with the nodal mass. Then, the accelerations will be integrated explicitly by time to have the new nodal velocities. The nodal velocities integrated with the time can have the new nodal positions. After this, another iterative begins.

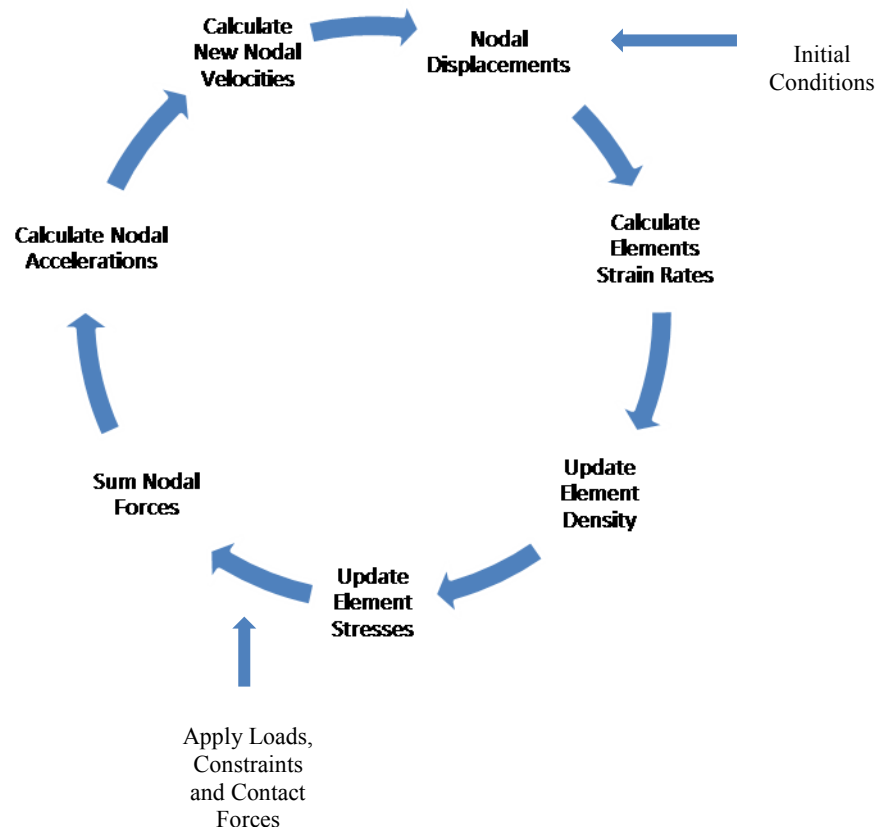The solution process can be represented by the cycle below:

Figure 2-1 Illustration of the framework for the solution

2.3 Introduction to the Materials

2.3.1 Properties of the Steel

Meyer and Chawla (2009) indicate that due to the low temperature, the movement of dislocation inside steels will become less active. Hence, the flow stress of the steel will be higher. The steel will have a higher yield stress and ultimate stress. Since the temperature in the Arctic region is much lower than the ductile-brittle transition temperature, the steel tend to be brittle when compared to the room temperature. Therefore, Ehlers and Østby (2012) point out the fracture strain will be lower with the decrease of the temperature. As a consequence, a different mechanical performance for the materials will be taken into consideration when researching the collision phenomenon in the low temperature conditions.

In this thesis, the NVA steel will be used. And the properties of the NVA steel will be entered into the simulation.

NVA steel is the grade A steel defined by DNV. It is the high strength steel for the offshore structures. And it is also one of the most used Arctic steel. In this thesis report, the physical and mechanical properties of the NVA steel are showed behind:

The properties in *Table 2-1* are not changed with the temperature.

For the density and specific heat, they verify a little in the range from -30°C to 0°C. And the material performance in the temperature range from -30°C to 0°C is the practical situation in the Arctic region.

For the Young's modulus, Meyer and Chawla (2009) illustrates that it is highly related to the bonding energies of the atoms in the metals. However, the temperature will not influence the bonding energies so much under the temperature range mentioned above. Hence the Young's Modulus does not depend on the temperature. Same theory can be applied to the Poisson Ratio.

Table 2-1 General Physics Properties for NVA Steel

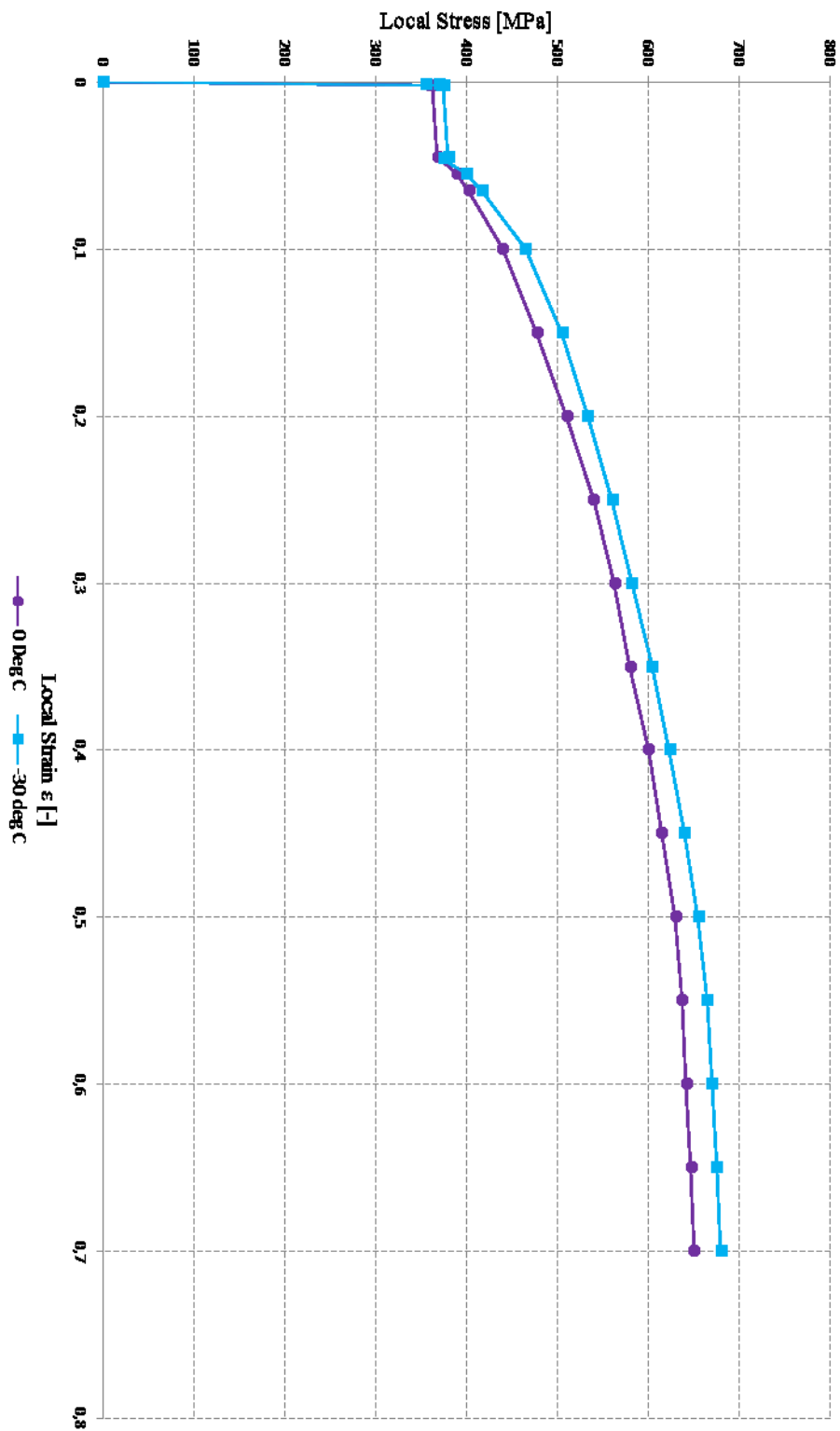| Name of the property	Value	Unit
Density	8000.00	Kg/m^3
Specific Heat	450.00	$J/(kg \cdot °C)$
Young's Modulus	210.00	GPa
Poisson Ratio	0.30	-

Figure 2-2 Local Stress vs. Local Strain of the NVA Steel

Table 2-2 Local Strain and Stress in Different Temperatures

Local Strain [-]	Local Stress [MPa]	
	0 °C	-30 °C
0	0	0
1.69E-3	355	355
1.76E-3	357	370
1.86E-3	359	372
2.00E-3	362	375
4.50E-2	368	380
4.60E-2	372	375
5.50E-2	389	400
6.50E-2	402	417
1.00E-1	440	465
1.50E-1	477	505
2.00E-1	510	533
2.50E-1	540	560
3.00E-1	563	582
3.50E-1	580	604
4.00E-1	600	623
4.50E-1	615	640
5.00E-1	630	655
5.50E-1	637	665
6.00E-1	642	670
6.50E-1	647	675
7.00E-1	650	680

The failure strain of the material is not only dependent on the temperature but also on the element size during the FE analysis. Hence, more discussion will be taken in the *Section 4*.

According to the common sense, the steel must burden plastic deformation and failure during the collision process. Hence, the non-linear mechanical performance of the steel is of great interest to be investigated.

2.3.2 Properties of the Ice

Since iceberg is the hitting object in the collision simulation. It is also very important to determine its properties, especially the mechanical aspects. The setting of the iceberg properties will definitely affect the final result of the collision simulation. However, it is very hard to find a standard or the values for the common use to the properties of the ice. Many properties like the density, Young's modulus and even ice belongs to isotropic or anisotropic material have controversial discussion in different papers.

There are many aspects can affect the properties of the ice in the iceberg. Liu (2011) indicates that age, sanity, strain rates, temperature, porosity, grain size etc. can contribute to vary the physical, especially the mechanical properties of the ice. As a consequence, it will be complicated to have a set of values which can be the represent of the properties of the ice.

However, the ambition of the author is not focus on the iceberg but ship structure. Hence, only one set of ice properties will be defined to make the iceberg simulation model as 'accurate' as possible.

In this case the iceberg will be treated as the fresh water iceberg. Hence, the density is set to be 900kg/m^3.

Sanderson (1988) refers that there is no significant difference of fresh water ice on the mechanical performance in each direction. And it is known that the icebergs in the Arctic region basically come from the glaciers. Hence, the ice can be set as isotropic material.

Erland (2001) illustrates that with the increase of the strain rate, the ice will become more brittle. And in this case, the ice will have the collision situation. That is to say the ice will suffer a very high strain rate. Therefore, the ice will be regarded as brittle material in this case. There is no plastic performance for the ice, but the fracture happens in the process of elastic strain.
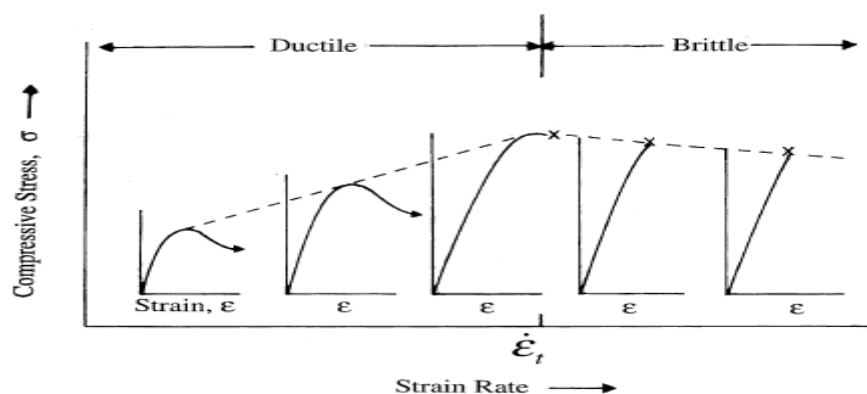

Figure 2-3 Ice strength vs. strain rate, from Schulson (2001)

In the paper of Gold (1988), the elastic modulus and Poisson's ratio of polycrystalline ice has been measured. In the experiment, the ice plates with diameter of 0.5m are subjected to biaxial bending at temperature of -10°C. The results show that the Young's modulus is in the rage of 9.7-11.2GPa. The Poisson's ratio is in the rage of 0.29-0.32. Liu et al. (2010) also argue that the Young's modulus of ice is 9.5GPa.

Based on the experimental results and some assumptions, the Young's modulus is set to be 10 GPa, and Poisson's ratio is 0.30 in this case.

To have a more detail view of the failure criteria of ice, Petrovic (2003) has a discussion mainly focus on the ice strength. He compares the ice strength with many factors like temperature, ice grain diameter, strain rate and ice test specimen volume. All of them can influence the ice strength. But in this case, only the temperature of ice can be settled. The failure criteria will be temperature based.

Haynes (1978) plots the relationship between ice strength and temperature. With the increasing of the temperature, the ice strength will be lower.
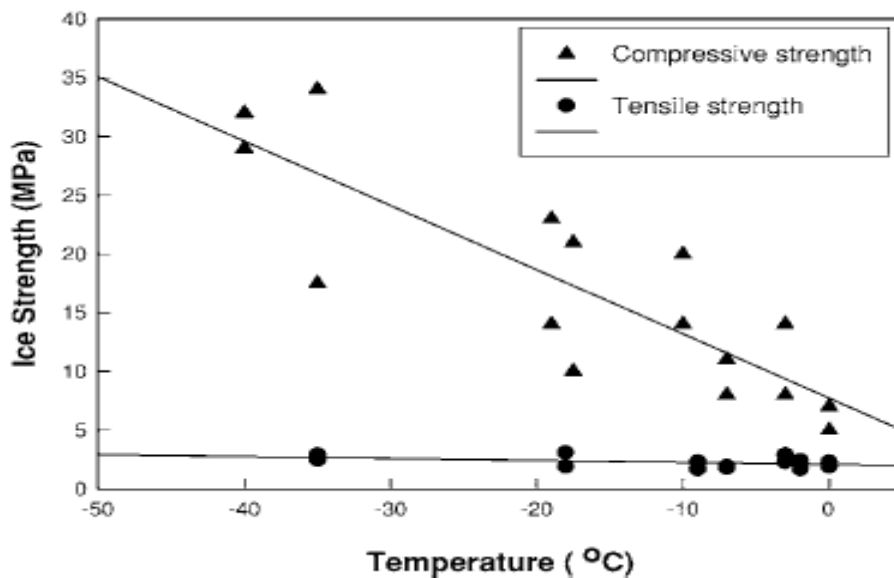

Figure 2-4 Tensile and compressive strength of ice vs. temperature, from Haynes (1978)

Hence, the failure criteria of the iceberg will be also based on the data presented in *Figure 2-4*.

Since the iceberg is in the water, an ambient temperature of 0°C is expected. The compressive strength will set to be 7MPa, and the tensile strength will set to be 2.5MPa.

Generally, the properties of ice are too complex. But the values of it can be set based on the assumptions and current research results. In this case the ice properties will follow the table below:

Table 2-3 Properties of Ice

Name of Properties	Symbol	Value	Unit
Density	ρ	900.00	Kg/m^3
Isotropic Elastic			
Young's Modulus	E	10.00	GPa
Poisson's Ratio	ν	0.30	-
Bulk Modulus	K	8.33	GPa
Shear Modulus	G	3.85	GPa
Failure Criteria			
Compressive Strength	σ_c	7.00	MPa
Tensile Strength	σ_t	2.50	MPa

Table 2-3 Properties of Ice

3   Structure of the Case Study Vessel

3.1 General Information of the Hull Structure

In this thesis report the side structure located in the parallel body of a CSR oil tank is taken into consideration. The data and scantling is taken from the training material of DNV GL software Nauticus Hull. There are several advantages for choosing a CSR oil tank as a target vessel for the collision simulation.

CSR oil tanks are the most popular design requirement. CSR is a regulation system defined by the cooperation of several world's biggest classification societies. It is not only a regulation system that belongs to the specific classification societies, but a common and general rules followed by the members in IACS (International Association of Classification Society). Hence, more new design will follow CSR.

The most popular topic for the Arctic exploration is energy resources. And the Arctic region is also called the last frontline for the energy discovery on the planet. It cannot be denied the main energy resource for the industry is oil. And it is also believed that the oil deposit in the Arctic region is rich. Hence, the production and transportation units are needed. The most common used production unit offshore for oil industry is FPSO (Floating Production Storage Offloading). However, many FPSOs are modified from oil tanks. And actually, FPSOs and oil tanks have many similarities in structure.

As a consequence, it has many practical advantages to take the CSR oil tank to be the target vessel for collision in the Arctic region.

General Information of the Oil Tanker

Table 3-1 Main Dimensions of the oil tanker

Name	Symbol	Value	Unit
Length between perpendiculars	L_{bp}	234.000	m
Rule Length	L	232.000	m
Breadth moulded	B	43.000	m
Depth moulded	D	21.000	m
Drought moulded	T	15.000	m
Block coefficient	C_b	0.840	-
Frame Spacing	-	4250.000	mm

The scantlings of the midship are showed in the following pictures. And the detail profile data of the stiffeners are in *Appendix A: Detail Information of the Side Structure*.
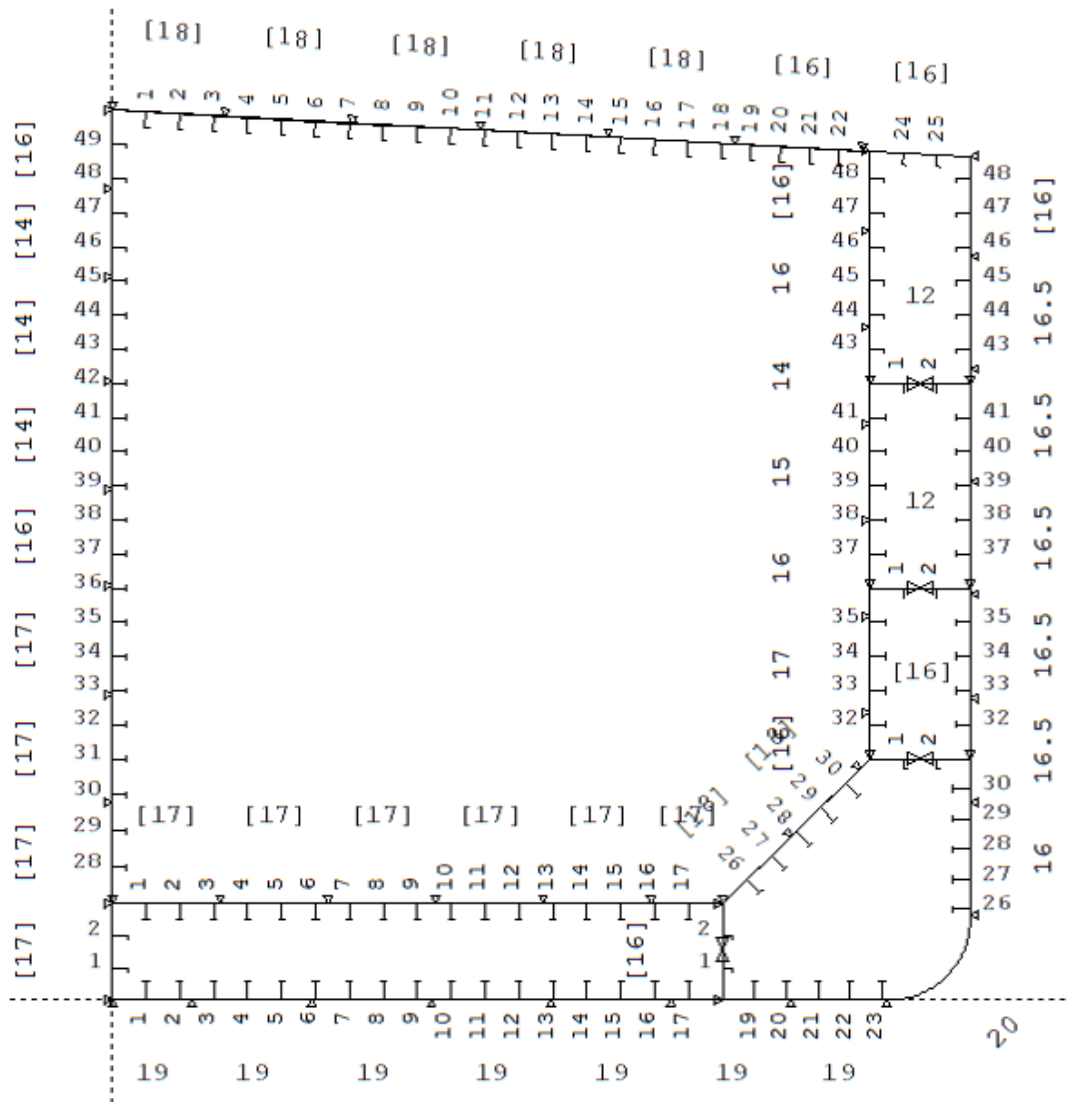
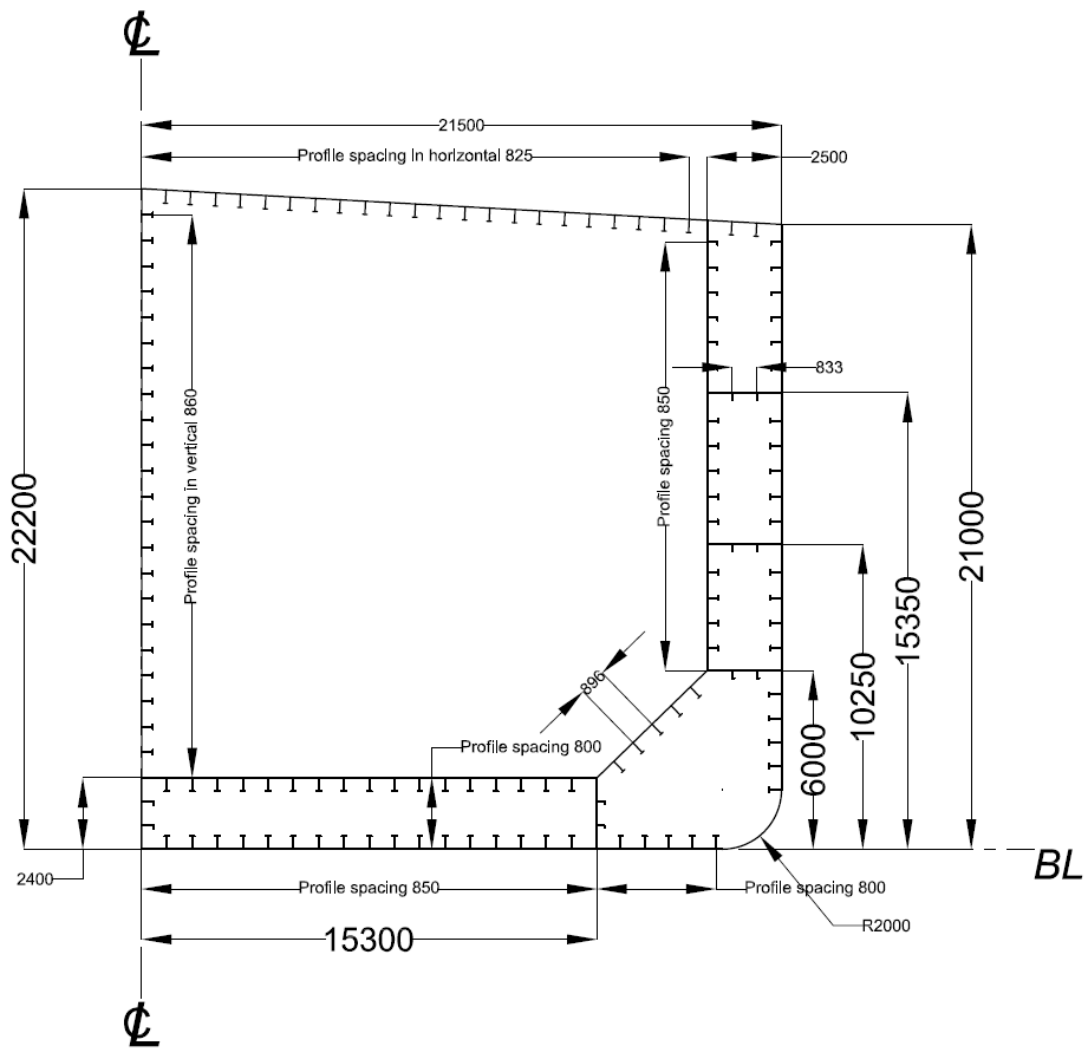*Figure 3-1 The scantling of the midship section with dimensions of plates*

Figure 3-2 Profile arrangement in the midship section

3.2 The side Structure for Collision Simulation

In this case, the side structure refers to the double side hull including the bulk in the bottom. All the stringers and stiffeners are also included. The frame spacing of the side structure is 4250mm. Hence, the web frames are arranged according to the frame spacing value.
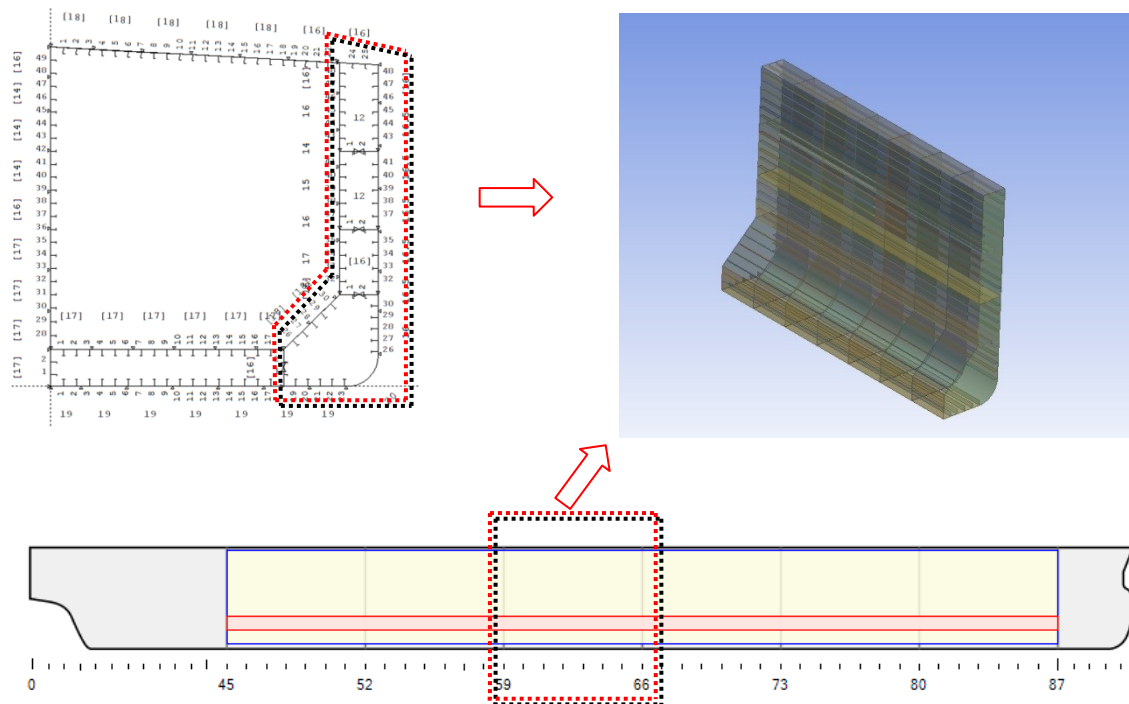

Figure 3-3 Illustration of the location of the side structure

And according to the CSR rules, the web frames are in the same thickness of 9 mm. And the thickness of the bulkheads will set to be 50 mm in order to simplify the problem.

4 Modelling

4.1 Introduction of the Simulation Model

In this simulation, an iceberg will hit on the side structure of the oil tanker. It is known that the collision is a dynamic process. And relative velocity of 2 m/s is assumed in this simulation. But in the model the vessel will be set as static. And the iceberg will be assigned an initial velocity. The mass of the iceberg is to be 2500t. And the initial velocity of the icebergs will be 2m/s along the Y direction of the vessel as the *Figure 4-1* shows. The gap between the iceberg tips to the plate will be 20mm at Y axis. The entire iceberg will have the same initial situation so that to guarantee the same initial kinetic energy.

There are two objects to be modelled in this simulation: the side structure of the oil tanker and the iceberg. The geometry and material characteristics of the ship side structure are well defined. And the boundary conditions of the side structure will also been defined based on assumptions. However, there are too many factors can reflect the definition of the iceberg.

In order to simplify the collision simulation, the iceberg will hit the side structure along the normal direction of the outside plates of the vessel. And the shapes of the iceberg will be set as a factor to influence the collision result. Different shapes of the iceberg will be tested in the simulation.

Regarding the collision, the simulation mainly focus on the collision happens near the waterline. The floating ice usually hit the vessel at the waterline position. However, simulations focus on the above waterline collision will also be implemented.
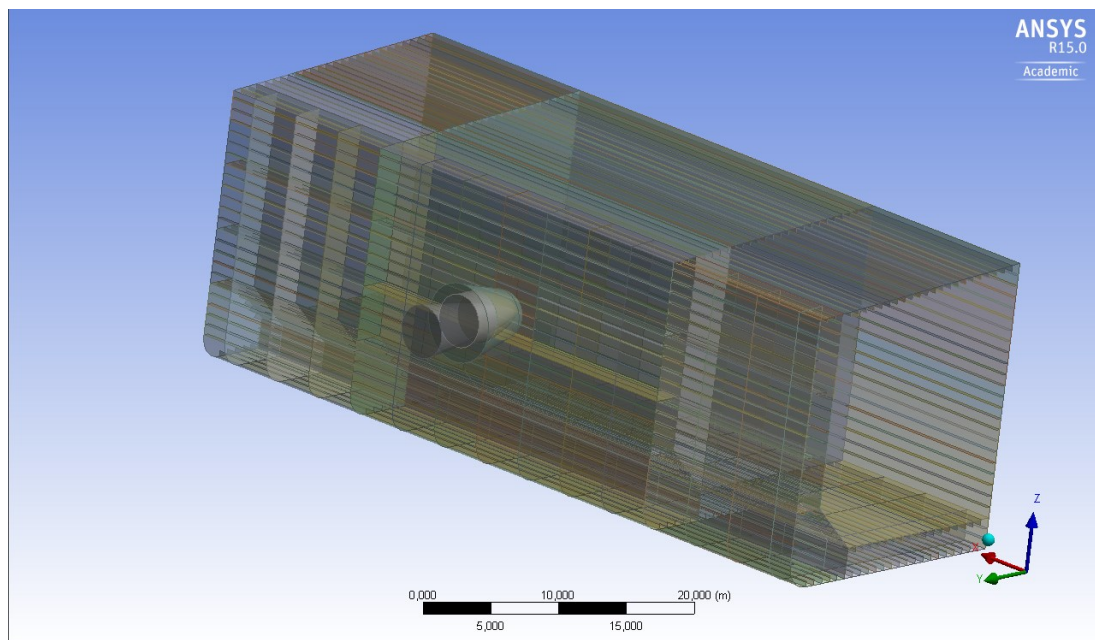

Figure 4-1 The collision model

4.2 Modelling of the Side Structure

4.2.1 The Geometry of the Hull Side Structure

In order to minimize the effect of boundary conditions and save the calculation time, the side structure of one tank is taken out to be investigated for the collision simulation. Also the bulk and keel parts are added to be the bottom of the side structure. Hence, the model can describe the practice situation as accurate as possible.

Main dimension of the side structure

Table 4-1 Main dimension of side structure

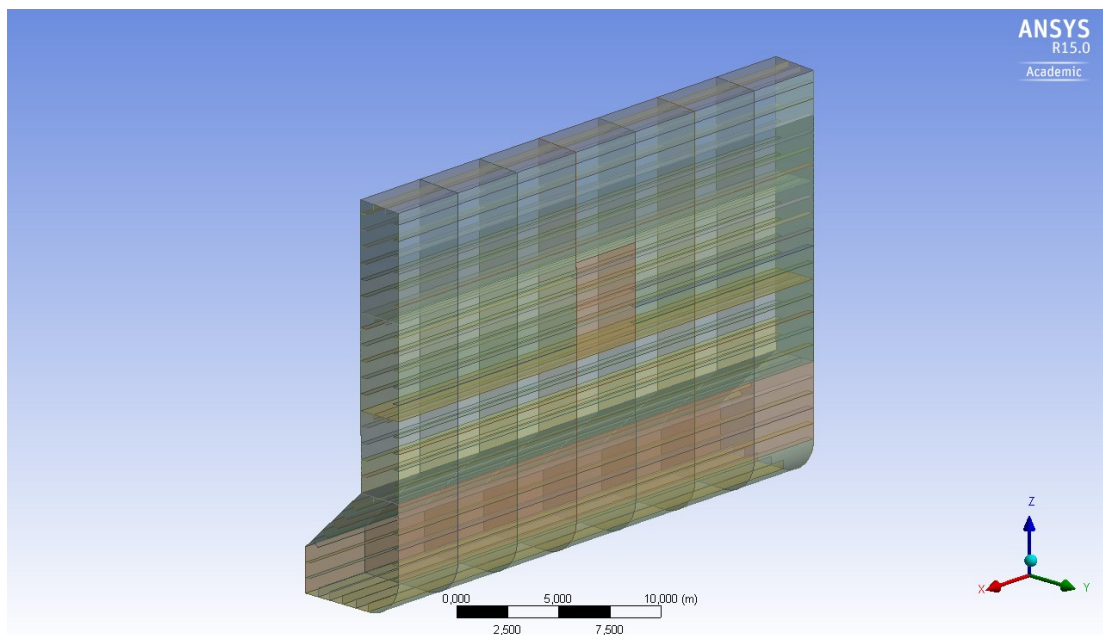| Name	Value	Unit
Length	29750	mm
Breadth (Upper)	2500	mm
Breadth (Bottom)	6200	mm
Height	21000	mm

Figure 4-2 Geometry of the side structure

The simplification of the stiffeners

The stiffeners of the side structure are mostly T-bars or L-bars. They are formed by webs and flanges. Two plates are joined together. The geometry configurations of T-bars and L-bars are complex than flat bars. Hence, it will increase the working load to build the model. Moreover, in the meshing process of the FEM (Finite Element Method), more elements will be created on the T-bars or L-bars. It also means more calculation time will be needed for the FEA (Finite Element Analysis).

In this thesis report, the iceberg is supposed to hit the side structure horizontally. The web of the stiffeners, which attached to the side plates, will play more important role in burdening the bending load due to the impact. That is to say the webs are the major elements for the impact resistance of the side structure. However, the flange of the stiffeners may not strengthen the impact resistance for the side structure. Based on this, there is a possibility for the stiffeners to be simplified.

In order to save the calculation time and put more attention on the mechanism of collision, those stiffeners have been simplified as a flat bar. Those flat bars have the same height as the corresponding stiffeners. However, the thickness of the flat bars has been added to make them have the similar moment of inertia. In this case, the difference between moment of inertia is controlled to be ±5%. In this way, the impact resistance of the side structure can be kept as similar as it was. The same strategy has been applied for the stiffeners attached to the deck, stringers, bottom, inner side, inner bottom and bulk plates.

This strategy is actually often used in the FEM modelling. And in this thesis report, the same strategy will used to simplify the stiffeners.

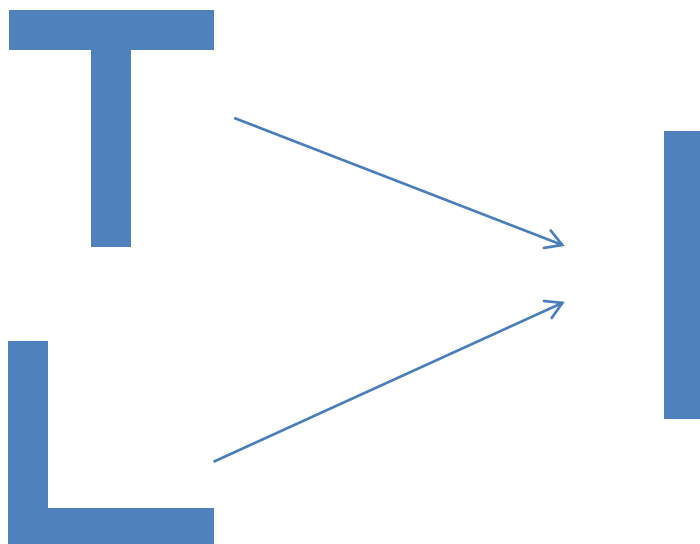The tables in Appendix A show the transverse of those stiffeners to the flat bars.

Figure 4-3 Transverse the T-bars and L-bars to Flat-bars to simplify the model

4.2.2 The Input of the Steel Material

The mechanical properties of NVA steel has introduced in *Section 2.3.1*. However, due to the limitation of ANSYS Workbench, the input data need of the steel need to be in more detail illustration.

Element Type

In the FEM simulation, the modelled objects should be assigned the element types. It is because element types differ the degrees of freedom of the nodes and also the algorithm during the calculation.

All the plates and stiffeners in the hull structure are defined as the shell element.

Thomas Nelson (2004) illustrates that it is a default setting that the shell element in ANSYS workbench will be defined as SHELL181. SHELL181 is recommended to model the thin shell structures. It has four nodes for an element. And each node has 6 degrees of freedom. Moreover, ANSYS Help Viewer indicates that SHELL181 is also suitable for linear, large rotation and also nonlinear applications. For the collision, it is highly expected that large deformation and nonlinear performance will happen to the material. Therefore, there is no need to change the default setting of the shell element.
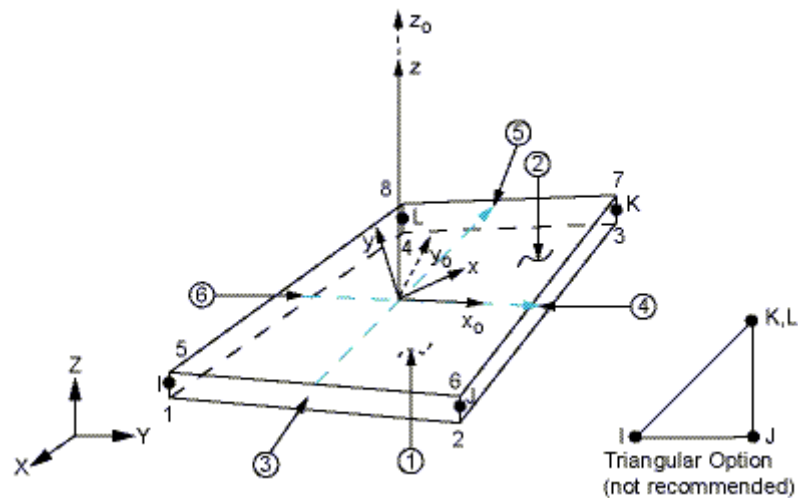

Figure 4-4 SHELL181, from ANSYS Help Viewer

In the ANSYS help manual, it regulates that the shell element can model the thin structures. And the thin structure is defined as one dimension is much smaller compared to the other two dimensions. However, ANSYS Help Viewer also indicates that there are no detail quantity regulations to indicate the level of 'smaller'. But it is a rule of thumb that if the dimension of the smallest edge divided by the thickness is bigger than 5, the plate can be modelled with shell element.

In this case, all the hull plates can be modelled in this way since it is much easy for them to fulfil the requirement. For the stiffeners, which are modelled as flat bars, they can also be defined as shell element. The ratio between height and thickness of the flat bars are in the range of 13.64 to 20.43. They are much bigger than the empirical value of 5. That is why the stiffeners can also be modelled as the shell element.

Physical Properties

In the ANSYS Workbench Explicit, the physical properties only refer to the density. In the temperature range from -30°C to 0°C, the density of the steel will not change too much. Hence, the density of the NVA steel is set to be 8000kg/m^3.

Linear Elastic

The NVA steel is an isotropic material. And the temperature difference does not influence the Young's modulus of the material. It has been discussed in *Section 2.3.1*. As a consequence, the bulk modulus and shear modulus of the NVA steel will be the same regardless of the temperature.

Table 4-2 Linear elastic properties of NVA steel

Name	Symbol	Value	Unit
Young's Modulus	E	210.0	GPa
Poisson's Ratio	N	0.3	-
Bulk Modulus	K	175.0	GPa
Shear Modulus	G	80.8	GPa

Plasticity

In the ANSYS Workbench, the function named Multilinear Isotropic Hardening can express the plastic property of the material. It requires at most ten straight lines to regress the strain vs. stress curve at the plastic region. However, different from the ordinary strain vs. stress curve. The input of the strain is required to be the plastic strain. Hence, the first pair of the input data should be 0 for the plastic strain but a positive number for the stress. And the next coming data should be the plastic strain and the corresponding stress. However, all the values should be the local strain and stress, that is to say the true strain and stress. Therefore, the stress will become larger with the increase of the strain.

The plastic strain follows the equation below:

$$\varepsilon_p = \varepsilon - \sigma / E \qquad\qquad (4\text{-}1)$$

Where

ε_p = Plastic strain

ε = Local/true strain

σ = Local/true stress

E = Young's modulus (For NVA steel, $E=210$ GPa regardless of temperature)

Due to the practice scenarios, the material data in 0°C and -30°C will be applied. Based on the data from *Table 2-2* in *Section 2.3.1* and *Equation 4-1*, the input data of NVA steel for Multilinear Isotropic Hardening in those two temperatures should follow the data below.

Table 4-3 Multilinear isotropic hardening data for NVA steel

0°C		-30°C	
Plastic Strain	Stress	Plastic Strain	Stress
[-]	[MPa]	[-]	[MPa]
0.000	355	0.000	370
0.043	368	0.044	375
0.100	443	0.100	491
0.200	519	0.200	579
0.300	564	0.300	631
0.400	596	0.400	668
0.500	621	0.500	696
0.600	641	0.600	720
0.700	659	0.700	739

Failure criteria for collision simulation

In the ANSYS Workbench, the only failure criteria for shell element is the Plastic Strain Failure. The software needs the input of the Maximum Equivalent Plastic Strain (EPS). However, the maximum EPS also related to the mesh size.

The NVA steel has been tested by e.g. Per Hogström (2009). The test of NVA steel was under the speed of 5 mm/min. The aim of the speed setting is to give an engineering strain of around 50% at the end of the test. The result of the test shows that the failure strain is related to the size of specimen. Actually, a formula has already been conducted by Yamada et al. (2005) to explain it.

$$\varepsilon_f = \ln\left(e^{\varepsilon_n} + c\,\frac{\sqrt{W \cdot t}}{L_{VE}} \right) \qquad\qquad (4\text{-}2)$$

Where

ε_f =   Failure strain

e =   Mathematical constant defined as the base of the natural logarithm

ε_n =   Necking strain

c =   Barba parameter

W =   Original width of the specimen

t =   Original thickness of the specimen

L_{VE} =   Virtual extensonrmeter when fracture occurs

From the *Equation 4-2*, the trend of the failure strain has been illustrated. If the specimens are in the same width and the thickness, the longer the specimen is, the lower failure strain will appear. The same theory is applied in the finite element simulations. That is to say the bigger mesh means the lower failure strain. Therefore different failure strains will be assigned based on the mesh sizes.

Sören Ehlers and Erling Østby (2012) has already given the failure strain vs. element length (mesh size) relationship for the standard NVA grade steel.

Table 4-4 Failure strain vs. element length (mesh size)

Element Length (Mesh Size)	Failure Strain	
mm	0°C	-30°C
1	1	0.885
5	0.642	0.565
10	0.531	0.46
15	0.472	0.408
20	0.435	0.385
25	0.405	0.36
30	0.384	0.345
35	0.362	0.322
40	0.348	0.31
45	0.34	0.3
50	0.335	0.295
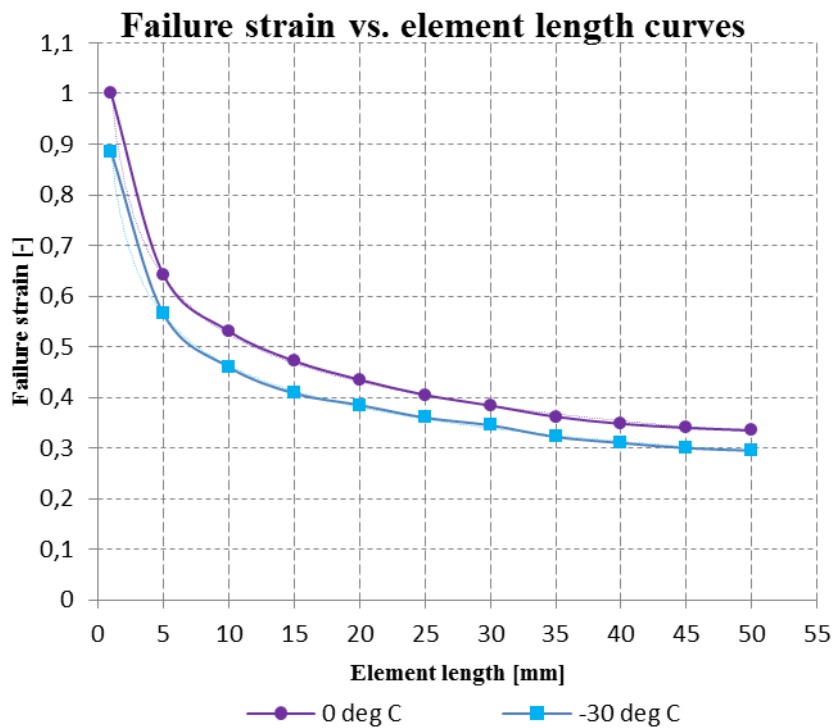
Figure 4-5 Failure strain vs. element length curves and trend lines

Two trend lines in power style are regressed from the data in *Table 4-4* to help the author to conduct the failure strains which will used in this case.

For the NVA grade steel in 0°C, it has a trend line of:

$$\varepsilon_f = 1.0107 l^{-0.285} \tag{4-3}$$

$$\varepsilon_f = 0.8863 l^{-0.282} \tag{4-4}$$

Where

ε_f =   Failure strain

l =   Element size in [mm]

However, in the ANSYS Workbench Explicit, the maximum equivalent plastic strain (ESP) is set to be the failure criteria. Hence, the *Equation 4-1 Calculation of plastic strain* is required for the calculation of the maximum ESP. The failure strain performed in *Equation 4-3* and *Equation 4-4* is the global failure strain not the plastic one. As a consequence, the maximum ESP should be calculated as the equation shows below:

$$\varepsilon_{p\,max} = \varepsilon_f - \sigma_f / E \tag{4-5}$$

Where

$\varepsilon_{p\,max}$ =   Maximum equivalent plastic strain

ε_f =   Failure strain

σ_f =   Corresponding failure stress at the failure strain

E =   Young's Modulus (For NVA steel, *E=210* GPa regardless of temperature)

In order to calculate the maximum ESP, the failure stress should be known. Another regression is carried out to simulate the curves of the material's plastic region. By this way, the stress at plastic region can be represented by the corresponding strain. And based on the data of *Table 2-2* in *Section 2.3.1*, a logarithmic form is used to regress the strain vs. stress curve in the plastic region. For the NVA grade steel in 0°C and -30°C, the regression formulas are *Equation 4-6* for 0°C and *Equation 4-7* for -30°C.

$$\sigma = 111.75 \ln(\varepsilon) + 698.27 \qquad (4\text{-}6)$$

$$\sigma = 128.6 \ln(\varepsilon) + 784.87 \qquad (4\text{-}7)$$

Where

σ = Local/true stress in [MPa]

ε = Local/true strain

Hence, combine *Equation 4-3, Equation 4-4, Equation 4-5, Equation 4-6,* and *Equation 4-7.* The final calculation formulas for maximum ESP can be obtained. *Equation 4-8* is for the 0°C and *Equation 4-9* for the -30°C

$$\varepsilon_{p\,max}^{0^0 C} = 1.0107 l^{-0.285} - \frac{111.75 \ln\left(1.0107 l^{-0.285}\right) + 698.27}{E} \qquad (4\text{-}8)$$

$$\varepsilon_{p\,max}^{-30^0 C} = 0.8863 l^{-0.282} - \frac{128.6 \ln\left(0.8863 l^{-0.282}\right) + 784.87}{E} \qquad (4\text{-}9)$$

Where

$\varepsilon_{p\,max}$ = Maximum equivalent plastic train

l = Element length/ Mesh size in [mm]

E = Young's Modulus (For NVA steel, $E=210$ GPa regardless of temperature)

Therefore, the failure criteria (maximum EPS) of the NVA grade steel can be calculated according to the temperature and the mesh size.

In the simulation, two sizes of mesh 100mm and 500mm are expected. Hence, the maximum EPS for those two size in 0°C and -30°C are acquired.

Table 4-5 Maximum EPS of NVA grade steel

Temperature	Mesh size	
°C	100mm	500mm
0	0.269	0.169
-30	0.239	0.151

4.3 Loads and Boundary Conditions

It is known that the boundary conditions of the simulation should be reliable enough to model the practical situation. Even when the vessel is in the static situation, gravity, static bending moment, thermal conditions, and water pressure will apply on the vessel structure. That is to say the structure has already under loads before the collision happens.

Due to the limitation of the ANSYS Workbench, not all the loads and boundary conditions can be applied on the ANSYS Workbench Explicit. For example, the thermal expansion coefficient cannot be assigned to the material during the Explicit simulation. Some simplification process should be implemented. In this section, the simplifications will be assumed with the explanations.

4.3.1 Static Analysis

Many classification societies like DNV GL will have approval jobs for the newly designed vessels. The static structural analysis is usually performed during the approval process of a CSR vessel. It is a process to check the strength and bulking issues of the hull structure. Normally, a part of vessel will be modelled in the finite analysis software. The static loading and boundary conditions will be the input. The strength and bulking check will follow in the post-process

It is known that the static loads should be also taken into the consideration to make the model as accurate as possible. However, it is also expected that more time will be needed for the simulation if the model has contained too many loads and boundary conditions. That is why in the simulation some factors have been simplified or excluded. In this case, the static check will also carry out to testify the boundary condition assumption of the model.

Baumans and Bøe (2012) point out that in the CSR vessels finite analysis check, a model of three holds is often built to verify the strength and bulking of the middle one. The investigated cargo is in the middle and completely built. And two half, in length, cargos joints the ends of the investigated cargo. Since the side structure of the parallel body of the CSR oil tanker is chosen as the modelled structure, the three cargos test will also be implemented in this case. Same strategies will be used in this case.

4.3.1.1 Static Factors

The bending moment due to sagging or hogging is one of the factors that should be taken into consideration. The bending moment occurs because the weight distribution of the vessel is not as the same as the buoyance distribution. It is an important factor for the global strength of the vessel.

In the local scope, water pressure, cargo pressure are the two routine factors to be taken into the consideration. Although these two factors have been already counted in the bending moment when focus on the global strength, they should also appear in the local analysis.

Another factor that should be taken into consideration is the thermal expansion of the materials. This factor is not considered when having the routine three holds checking. Normally, the model is in homogeneous temperature. And the temperature is the room temperature, which is around 20°C. But in this case, the upper hull will expose in the low temperature air of the Arctic region and the submerged part will also has the temperature near the ice point. Therefore, there are two aspects need to be considered when focus on the thermal expansion. First, the temperature distribution on the structure model is not homogeneous. That is also to say the material will expand in different levels at different places. Secondly, the whole structure is in under room temperature condition. The steel is considered to be in the thermal contraction condition. Due to the inhomogeneous temperature distribution and thermal contraction phenomenon, some parts of the side structure are not in stress free condition even exclude the gravity and bending moment.

Bending Moment

The bending moment acts on the three cargo model is the still-water bending moment. The design data of the vessel shows that

The maximum bending moment for hogging is 340000 kN·m

The maximum bending moment for sagging is 210000 kN·m

For the cross-section of the parallel body, where the model built in finite analysis software, the position of the centroid in Z direction is located in 9.256m. And the collision region in the model located in the range of 10.250m to 15.350m in Z direction. Hence, the collision region is above the natural axis of the cross section. Therefore, the bending moment for hogging should be investigated. In the hogging situation, the investigated plate is in tensile condition. Moreover, the maximum bending moment for hogging is much bigger than the sagging one. Hence, the vessel will be in a very extreme loading condition.

And the hogging moment apply on the remote points of both sides of the three cargo model. The remote points located on the centroids of the ends geometry. It is known that the neutral axis pass the centroid. And all the elements nodes at ends have a rigid connection to the remote points.
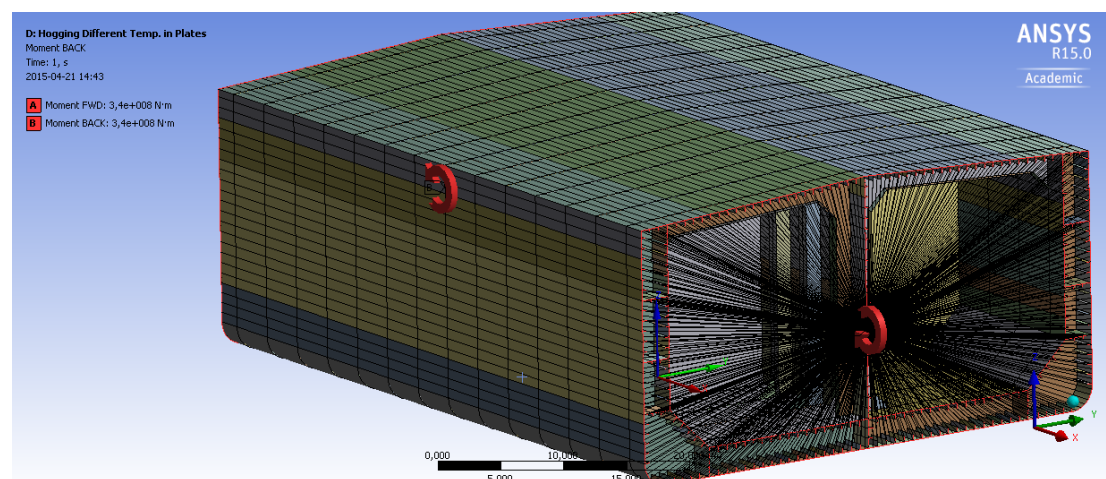

Figure 4-6 Bending moment for hogging (340000 kN·m) applied on the remote points of both ends

4.3.1.1.1 Water Pressure

The melded draught for the vessel is designed to be 15m. Hence, the static water pressure will be implemented on the outside and bottom plates. The density of the water will be as same as the sea water with a value of 1025kg/m^3. And the free surface will be set as the same height as the melded draught.
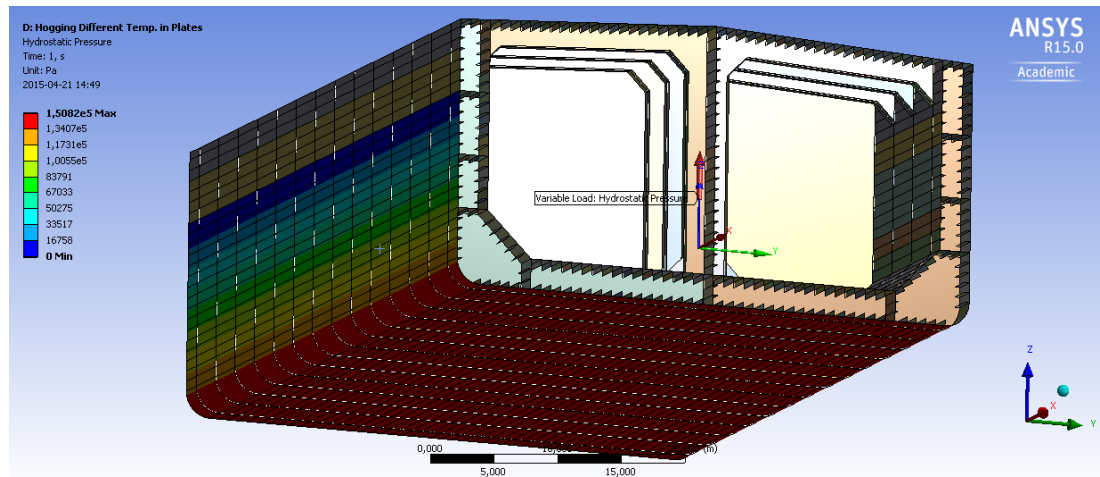

Figure 4-7 Hydrostatic pressure on the outer plates

4.3.1.1.2 Thermal Expansion Coefficient

The isotropic secant coefficient of thermal expansion (thermal expansion coefficient) is set to be 1.3×10^{-5}/°C and the reference temperature is 22°C (Western Washington University, 2009). Although the thermal expansion coefficient is not a constant at different temperature, in this case the temperature range does not affect the value of thermal expansion coefficient so much. Hence, the thermal expansion coefficient could be set as a constant. The programme will calculate the thermal strain as follows:

$$\varepsilon^{th} = \alpha^{se}\left(T_{ref}\right) * \left(T - T_{ref}\right)$$

(4-10)

Where:

ε^{th} =   Thermal strain

T_{ref} =   Temperature at which zero thermal strains exist (at reference temperature)

$\alpha^{se}\left(T_{ref}\right)$ =   Secant coefficient of thermal expansion

4.3.1.1.3 Temperature

The temperature distribution on the model is not in the same. In the Arctic region, the outer hull above the water line is under a very low temperature. However, the inside part will be in a higher temperature due to the insulation and heating system for the oil. But the underwater outer part will be in the temperature of 0°C. It is a common sense that the mixture of ice and water is the benchmark for 0°C. Although the sea water may change the value a little due to the salinity, still the temperature is around 0°C.

Therefore, a steady-state thermal model is built to judge the temperature distribution. Since the whole model is supposed to use the same type of metal NVA grade steel, all the plates and stiffeners will have the same thermal conductivity value.

According to the data provided by The Engineering ToolBox (2015), the carbon steel (max 0.5% C) has the thermal conductivity of 53.66W/(m·°C). And based on the Offshore Standard explained by DNV (2012), the NVA grade steel has a maximum 0.21% C. Hence thermal conductivity of 53.66W/(m·°C) can be set as the value applied on NVA steel.

Two situations are assumed for the thermal model.

a. Only the air (-30°C) and sea water (0°C) have thermal radiation to the model.
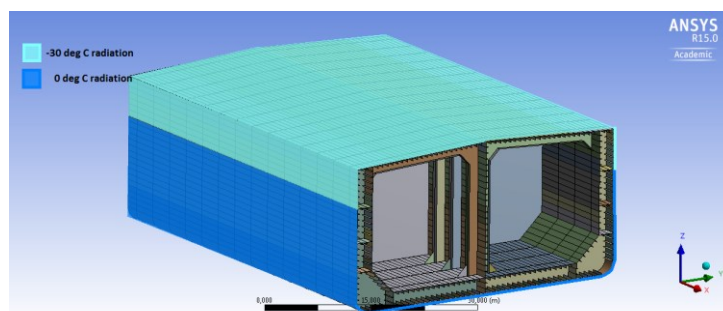b. Air (-30°C), sea water (0°C) and oil (0°C) inside all have thermal radiation to the model.
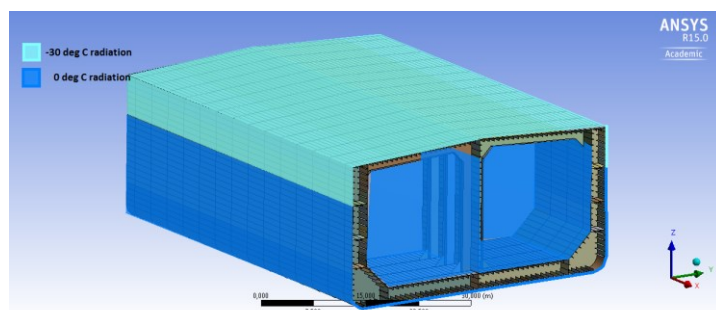

Figure 4-8 Thermal radiation situation a

Figure 4-9 Thermal radiation situation b

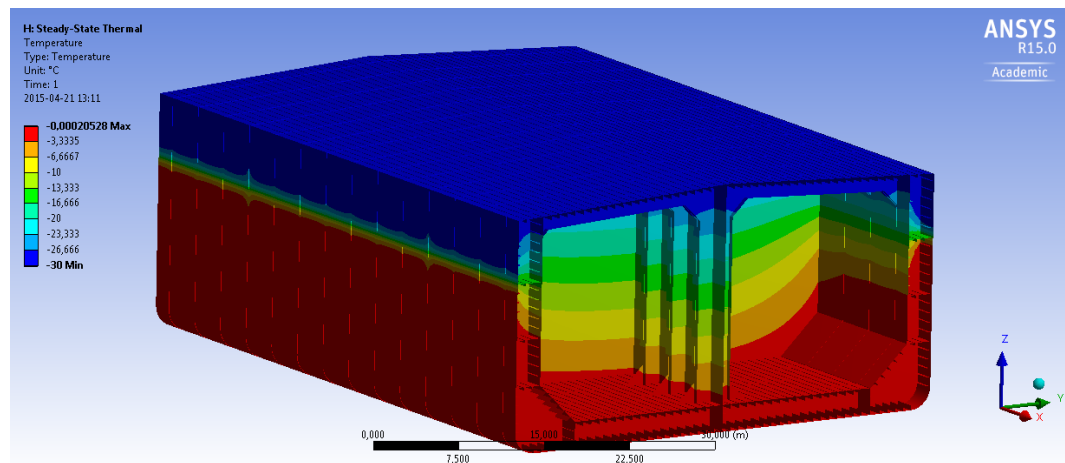The results of the steady state thermal check show as below:

Figure 4-10 Temperature result in situation a

In the situation a, the temperature of outer plates will have a rapid change near the water line. The plates expose to the air and corresponding attached stiffeners are in the temperature of -30°C. The plates submerged into the water have a temperature of 0°C. However, the temperature will change gradually for the inside part. The top beams are in the temperature around -30°C. But at the position near inner bottom and bulk, the temperature is in 0°C.
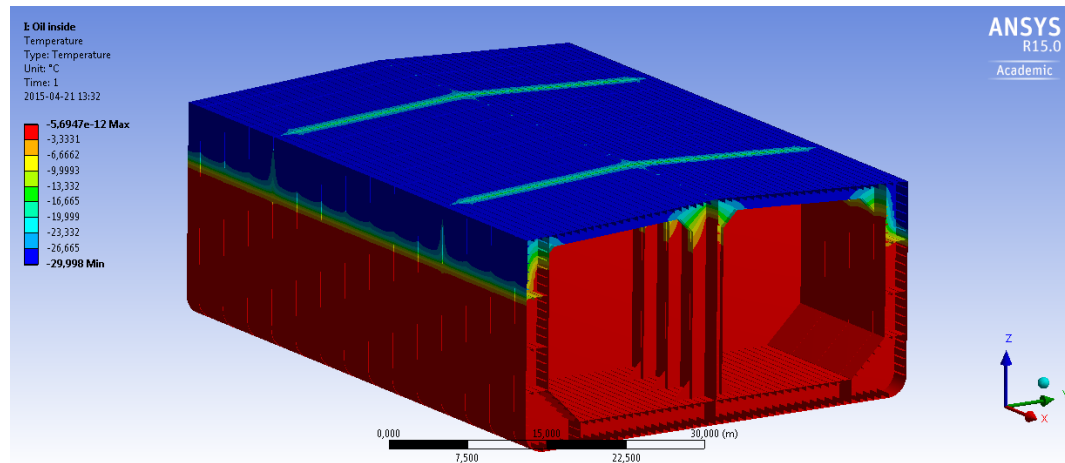
Figure 4-11 Temperature result in situation b

In the situation b, the temperature distribution on the out plates is as similar as the situation a. The temperature changes rapidly near the water line. However, due to the insulation and heating system inside the oil tanks, almost all the inner part is in temperature of 0°C except the top beams.

It is believed that if the oil tankers or FPSOs want to operate in the Arctic region, the storage space for the oil should be heated or insulated. Otherwise the oil or crude will be frozen. So the situation b is a more practical scenario.

Due to the limitation of ANSYS, the temperature distribution cannot be copied into static structural analysis exactly. Hence the thermal conditions, especially the temperature distribution, can only be roughly applied on the model. Based on the result of situation b, it is reasonable to set the plates expose to the air of temperature of -30°C. The corresponding stiffeners are in the same temperature. And the other parts of the vessel model are in the temperature of 0°C.
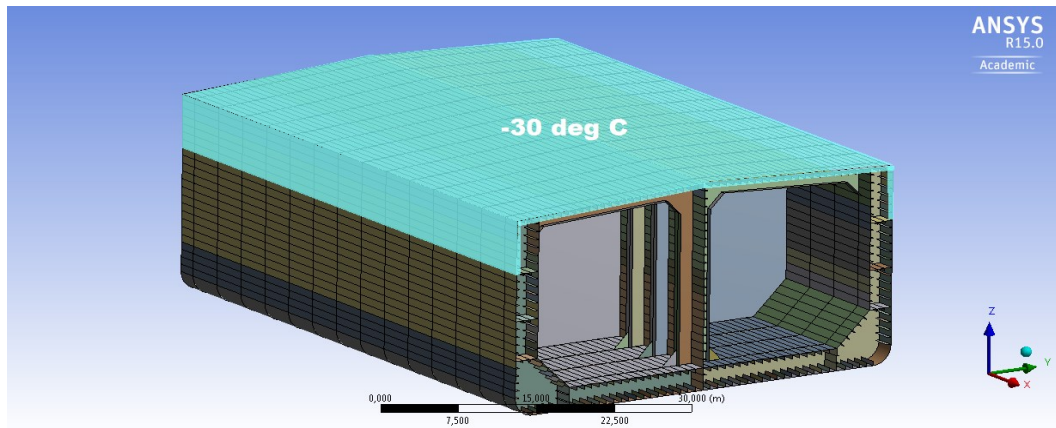

Figure 4-12 Temperature distribution applied in static structural analysis

4.3.1.2　The Boundary Conditions of the Static Analysis

Traditionally, the three cargo analysis will treat the hull structure as a beam being simply supported. And the bending moment will be loaded in both ends. The cargo pressure and outside water pressure are also included. In this case, the same strategy will be implemented.

All the nodes at the ends are rigid connected to the centroid points. Hence, it can be understood as a rigid plates connected to the ends. The boundary conditions will be applied on the centroid points, and the bending moment will also load on the centroid points.

Since the three cargos model is simply supported, the degrees of freedom in both ends will follow the table below.

Table 4-6 Boundary conditions of the static analysis

	X	Y	Z	RX	RY	RZ
FWD	Fixed	Fixed	Fixed	Fixed	Free	Fixed
BACK	Free	Fixed	Fixed	Fixed	Free	Fixed

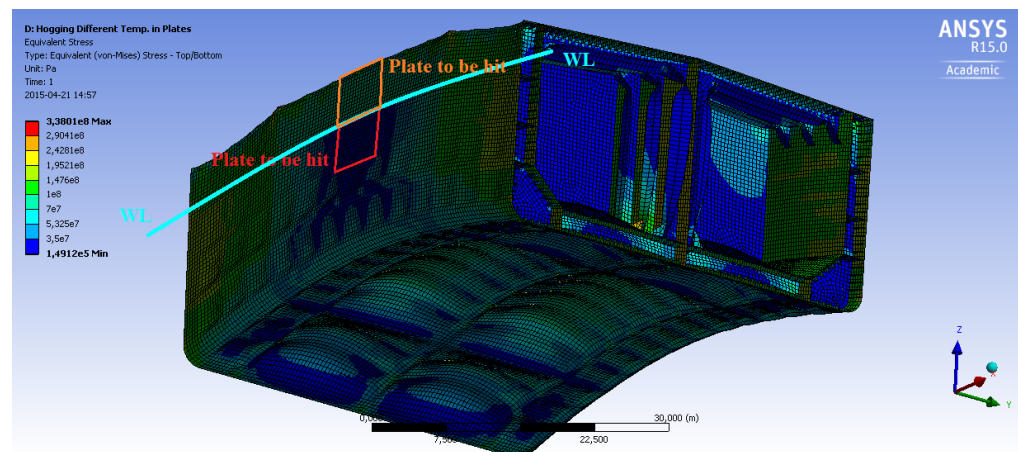### 4.3.1.3 The Result and Conclusion of the Static Analysis

Figure 4-13 Result of static structural analysis

According to the result of the quasi-static analysis, the hydrostatic pressure plays the most important role on the equivalent stress. And the region expose to the low temperature has a relatively low equivalent stress. That is because the low temperature leads the material to compress. It is a counter effect on tensile state, which caused by hogging. Therefore, the region does not have a high equivalent stress.

The result also shows a very optimistic situation. Except some corners, where the stress concentration can easily occur, the equivalent (Von Mises) stress is under the yield stress (355MPa for 0°C, 370MPa for -30°C). That is to say the hull structure is in well design in the strength wise.

The equivalent stress on the outer plate where the collision will occur is in the range from 0.15MPa-35Mpa for the under waterline part, and the values become larger above the waterline with a range from 70MPa to 100MPa. A conversional assumption is made that the yield stress for the steel is 355MPa, regardless of the temperature. For the underwater collision part, there is still a margin in the range from 90.14% to 99.96% regarding the yield stress. For the above water collision part, the margin is from 71.83% to 80.28%. And according to the material data provided in *Section 4.2.2*, the true failure stress for NVA at 0°C with the mesh size of 100mm is 553MPa. And the failure stress at -30°C with the mesh size of 100mm is 563MPa. As a consequence, there is a big margin in the range from 93.67% to 99.97% regarding the true failure stress at 0°C. And the margin is from 82.23% to 87.57% at the temperature of -30°C.

In the static analysis, all the loads are set to be the extreme condition. But still there is a big margin for the collision region regarding the equivalent stress no matter considering the yield stress or failure stress.

As a conclusion, the hydrostatic loads, bending moment loads and thermal expansion can be excluded in the collision simulation. The exclusion of those factors is not expected to influence the result of the collision simulation. But taking the static loads, which illustrated above, away will save time for the collision simulation.

4.3.2 Boundary Condition for the Side Structure

As a conclusion of the *Section 5.4.2*, the collision simulation will not take the hydrostatic load, global bending moment, and the thermal expansion into consideration. Therefore, those loads and effects will not apply on the side structure model.

The two ends of the side structure will be fixed supported. It is because the side structure is connected to the bulkheads. Bulkheads are considered to be the strongest element in the ship structure. It is reasonable that all the degrees of freedom have been fixed if the region is connected to the bulkheads.

All the shared edges, the rest of the hull structure connect to the side structure by sharing the edges, are also fixed supported. The bottom edges of bulk are connected to the inner bottom of the vessel, which is also a strong element. And the outer bottom, floors, deck beams and decks are all strong elements. That is the reason why the shared edges can be fixed supported.
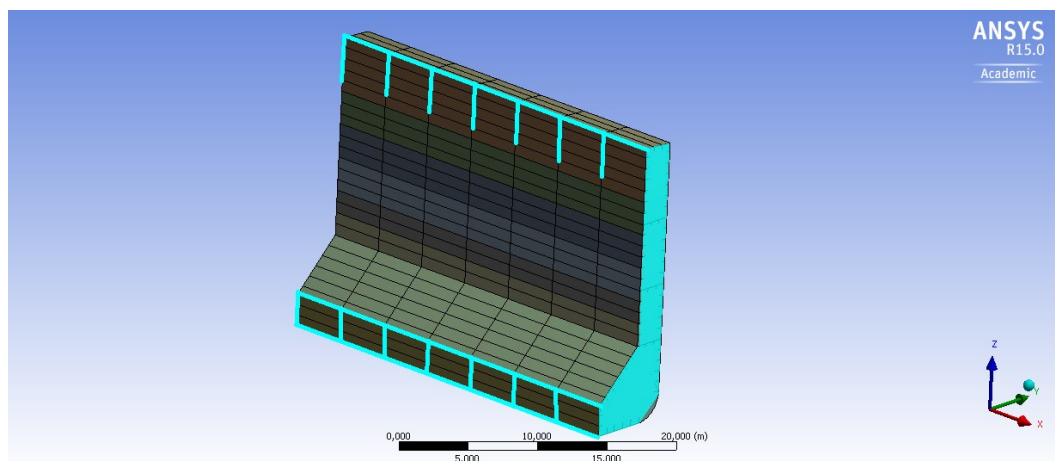

Figure 4-14 Boundary conditions: blue color represent fixed support

4.4 Iceberg Modelling

It has been mentioned in *Section 2.3.2* that the material characteristics of ice can differ significantly due to different ice properties, such as ice ages. In the current study, a set of ice material parameters have been defined based on the large literature study.

The shape of the iceberg is also another important factor to affect the collision performance. It is known that for the same material shaper objects may have higher probability to penetrate the hitting target. Therefore, a shape sensitivity check will also be carried out in this simulation.

4.4.1 Concept about the Iceberg Simulation

In order to save the computation time for the FEA, less number of mesh units is preferred. Hence, the iceberg does not need to be fully modelled.

In the simulation, the modelled iceberg will be divided to two parts: ice part and mass part. The ice part is the tip of the iceberg. This part is supposed to hit the side structure of the oil tanker. The properties of ice will be assigned to this part. However, since the volume of the ice part is limited, the mass of the ice part is much less than 2500t. Another mass part is attached to the end of the ice part to compensate the mass. Moreover, a much higher Young's Modulus will be assigned to the mass part. In this way, the mass part can be treated as a rigid.
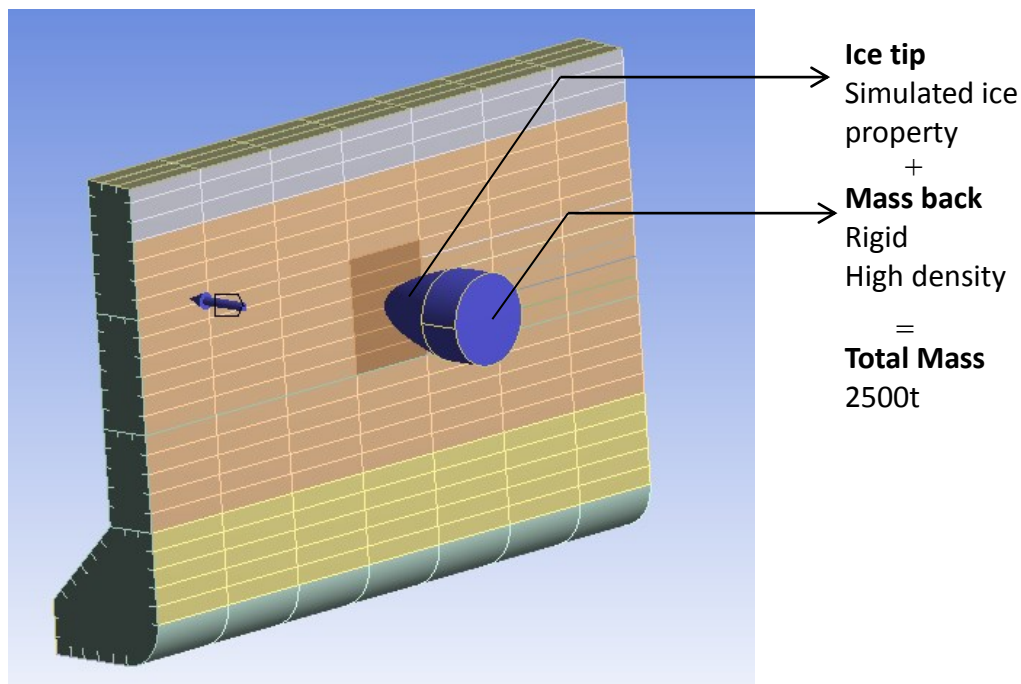

Figure 4-15 The simulation concept of the iceberg

4.4.2 The Input of the Ice Material

Element Type

It is known that the iceberg shall not be hollow inside. And there is not plate structure in the iceberg model. Therefore, solid element is assumed to be the element type of the iceberg, no matter the ice part or the mass part. Nelson and Wang (2004) indicate that the default type of solid element in ANSYS Workbench is SOLID186 or SOLID187.

ANSYS (2013) illustrates that the SOLID186 element is suitable for the homogeneous structural solid. And it is a higher order 20 nodes solid element in 3D. SOLID186 shows quadratic displacement behaviour. All the 20 nodes have 3 degrees of freedom of each. They are the translation in x, y and z direction. The element type can be applied in plasticity, large deflection and large strain. Since the collision will cause plastic deformation and also the large strain, it is suitable for the iceberg to be modelled with SOLID186.

The SOLID187 has a very similar property to SOLID186. But it is a 10 nodes element. In some level, the SOLID187 can be treated as the tetrahedral option of SOLID186.
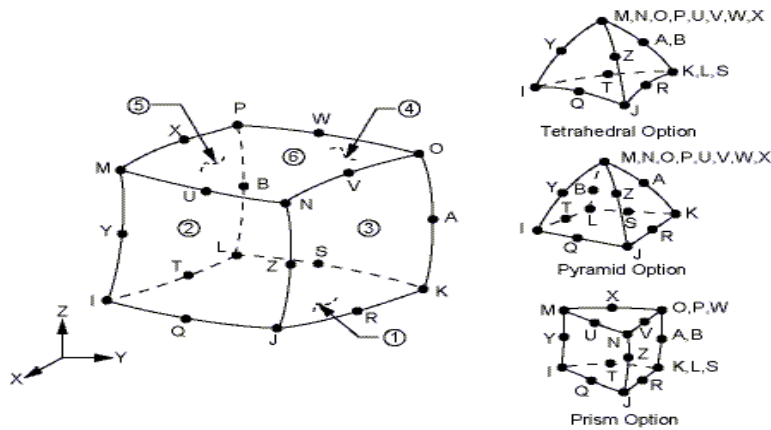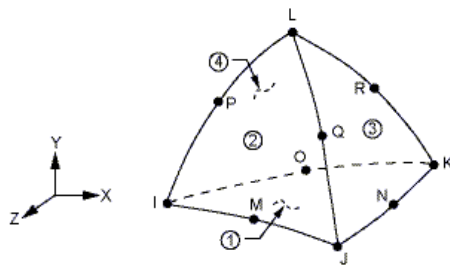

Figure 4-16 SOLID186, from ANSYS Help Viewer

Figure 4-17 SOLID187, from ANSYS Help Viewer

Physical Properties

The iceberg will be regarded in 0°C and formed by fresh water. Hence, the density is to be 900kg/m^3. And the density of the mass part will be varied to compensate the whole iceberg model to have a total mass of 2500t.

Linear Elastic

As discussed in *Section 2.3.2*, the ice will be treated as an isotropic material. And follow the data in *Table 2-3* the linear elastic properties for the simulated ice part should be:

Table 4-7 The linear elastic properties for the simulated ice part

Name of Properties	Symbol	Value	Unit
Young's Modulus	E	10.00	GPa
Poisson's Ratio	V	0.30	-
Bulk Modulus	K	8.33	GPa
Shear Modulus	G	3.85	GPa

However, the material makes mass part will have a very high Young's modulus so that it can be treated as a rigid.

Table 4-8 The linear elastic properties for the simulated mass part.

Name of Properties	Symbol	Value	Unit
Young's Modulus	E	1.00E5	GPa
Poisson's Ratio	V	0.30	-
Bulk Modulus	K	8.33E4	GPa
Shear Modulus	G	3.85E4	GPa

Plasticity

The ice part will be treated as brittle, hence there is no sense to discuss the plasticity of ice. And the mass part will be regarded as rigid. Therefore, there is no plasticity for the mass part also.

Failure

In the ANSYS Workbench, the failure strain is mesh size dependent. However the relationship between mesh size and failure strain is not indicated for ice. Therefore, it is no longer suitable to use the failure strain as the failure criteria. But the Maximum Tensile Pressure can be set as the failure criteria. And the Maximum Tensile Pressure is regulated suitable for the solid element.

And according to the data given by *Table 2-3*, the simulated ice will have a Maximum Tensile Pressure of 7 MPa.

For the mass part, rigid setting has been already made. Hence, there is no point to set the failure criteria.

4.5 Kinetic Situation

As introduced in *Section 4.1*, the iceberg will be assigned an initial velocity of 2m/s along the Y direction towards the side structure according to the vessel coordinate system. The side structure of the vessel will be set as static. Although during the practical collision, the vessel will not keep static in the water, it is still reasonable to have the assumption to fix the vessel.

The data of the vessel shows that it has a displacement of 130 000t. And the mass of iceberg is set to be 2500t with a velocity of 2m/s. Even if there is no damping, no energy lose, and the momentum is conservation for the collision system, the vessel can only obtain a velocity of 0.265m/s along the initial hitting direction of iceberg. Actually velocity of the oil tanker will be much smaller than 0.265m/s after the collision. As a consequence, the oil tanker can be treated static during the overall collision process.

Therefore, the only moving object in the collision simulation is the iceberg.
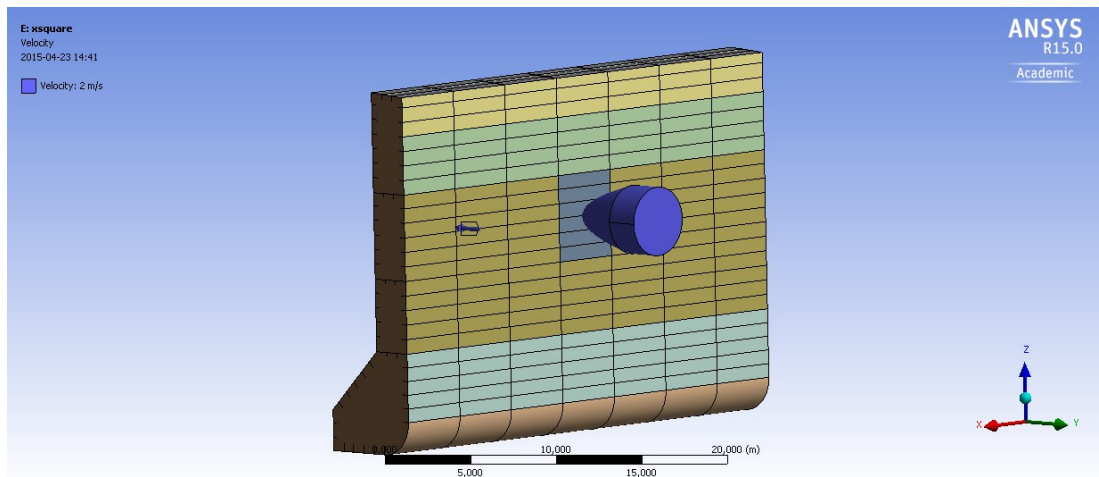

Figure 4-18 The iceberg heading to the side structure with the initial velocity of 2m/s along the negative Y direction

Table 4-9 Initial motion situation

	X	Y	Z	RX	RY	RZ
Iceberg	0	-2m/s	0	0	0	0
Oil Tanker	0	0	0	0	0	0

But for the iceberg only the transition of Y-direction is free but other degrees of freedom are fixed. In this case the iceberg is only partly simulated. The geometry of the iceberg is not in full scale. Therefore, during the collision the interaction forces may change the motion of the simulated iceberg easily. It is highly expected that the simulated iceberg may have pitch or roll motion after the collision, if all the degrees of freedom are free. However, those motions will not happen during the practical

collision. The rest geometry of iceberg, which has not been simulated, can limit the degrees of freedom on the simulated part. That is why only the degree of freedom on Y-direction is set to be free but others are fixed.

Table 4-10 Constrains on the degrees of freedom

	X	Y	Z	RX	RY	RZ
Iceberg	Fixed	Free	Fixed	Fixed	Fixed	Fixed
Oil Tanker	Fixed	Fixed	Fixed	Fixed	Fixed	Fixed

4.6 Frictional Coefficient

In the ANSYS Workbench, the frictional coefficient is required for the collision situation. However, it is also very hard to define the coefficient since the shape and also the surface roughness of both steel and ice are unknown. And if the collision happens underwater, it is highly expected that the water can lubricate the collision. Hence, a more 'smooth' collision will happen with a relatively low frictional coefficient.

But in some engineering manuals, the frictional coefficient of ice and steel has already indicated. Normally the frictional coefficient will be distinguished to dry and lubricated situation. However, in the cases related to ice there is no data showed in the lubricated situation. It is believed that during the collision, the frictional heat will melt the friction surface of ice. Actually it is a lubricated situation with the media of water melted from ice.

In the simulation carried out in this thesis report, the frictional coefficient will not be verified by the collision region. The above water and under water collision will share the same set of frictional coefficient.

The Engineering ToolBox (2015) has indicated the static frictional coefficient of ice and steel to be 0.03. And the dynamic coefficient is set to be the half value of the static frictional coefficient. Therefore, the dynamic frictional coefficient of ice and steel will set to be 0.015.
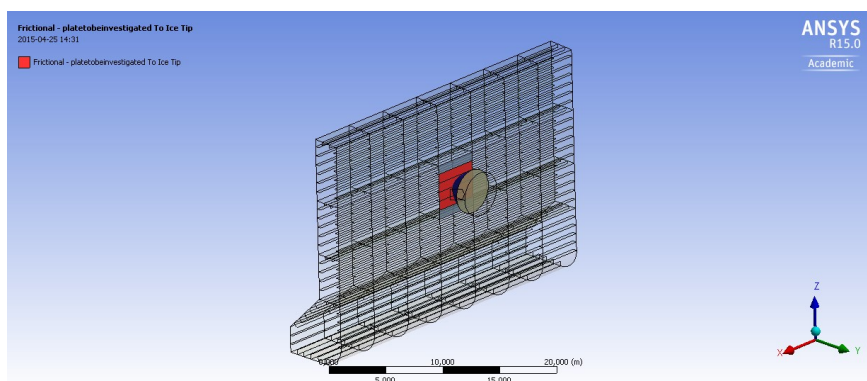

Figure 4-19 Frictional coefficient is assigned to the collision region

4.7 Meshing

In order to investigate the collision in a more accurate method, fine mesh is applied on the collision part. However, it is not possible to apply the fine mesh for the whole model, since it will cost much more time for the computation.

A mesh size of 100mm is assigned for the collision part in the vessel. And a mesh size of 500mm is assigned to the other part of the vessel.

And according to the recommendation from Professor Sören Ehlers, the mesh size ratio between two collision objects should be 1:1 but not exceed 1:4. However, in this case, the structure of the oil tanker is in interest. And in order to save time, the mesh size of the iceberg will be set rougher.

As a consequence, a mesh size of 200mm is assigned to the ice part of the iceberg. And a mesh size of 500mm is assigned to the other part of the iceberg.
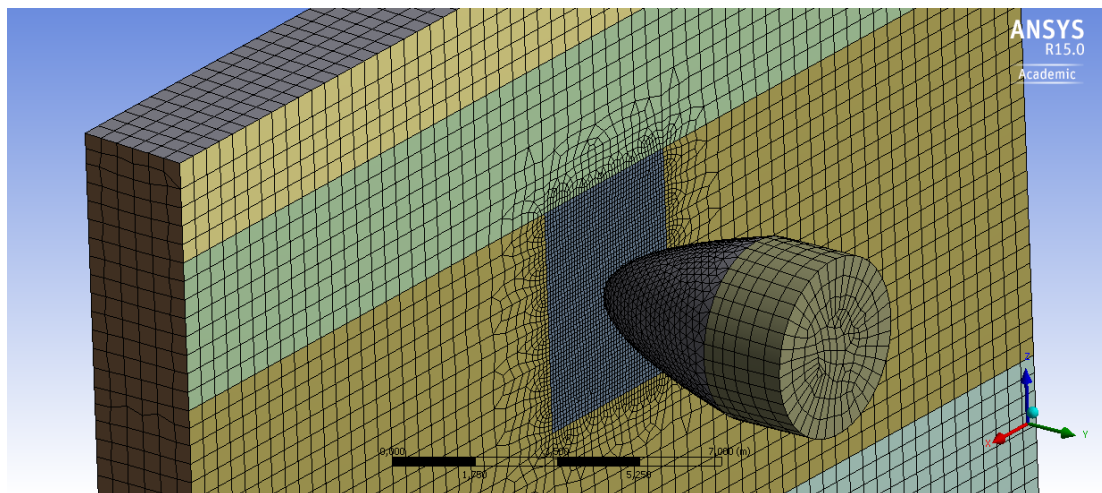

Figure 4-20 Mesh of the model

5 Results of Various Collision Scenarios Simulation

The collision simulation will follow the procedure introduced in *Section 4 Modelling*. Several ice-ship collision scenarios will be investigated.

Firstly, the shape sensitivity of the iceberg will be verified. It is known that the sharper hitting object can penetrate the target easily with the same energy. Therefore, the failure situation for the side structure intends to happen when hit by sharper iceberg.

And then the iceberg will hit both the under (0°C) and above water (-30°C) region of the side structure. When the iceberg hits underwater region, the steel in low temperature is the boundary for the collision. When the iceberg hits the above water region (the steel in low temperature), low temperature will be a factor to influence the collision directly.

5.1 Parameters to be Investigated

After the collision simulations are done, the following parameters will be investigated to measure the collision. Those parameters are only applied on the hit plate of the oil tanker.

Failure Area: The failure area focus on the failure happens on the hit plate of the side structure of the oil tanker. In the simulation, it refers the number of the elements that have been 'taken away' after the collision. This criterion can reflect the severe of the collision in a quite visible and direct way.

Deformation Area (Where deformation on Y axis >=100mm): This is an assistant parameter to measure the collision influence if the failure does not happen.

Maximum Deformation on Y axis: This parameter can reflect the level of being penetrated on the plate.

Plastic Strain Area (including Failure Area) where EPS (Equivalent Plastic Strain) > 0.05: It is a parameter to indicate the plastic strain. According to the data given in *Table 4-3* Multilinear isotropic hardening data for NVA steel, the yield points for the NVA steel in different temperatures are located near the region where EPS=0.05. That is the reason why EPS>0.05 is set as the critical value for plastic strain.

Number of Damaged Stiffeners (EPS>0.05): This parameter indicates the damage level of stiffeners.

Velocity of the Iceberg after Collision: It can indicate the energy loss of the iceberg with the initial velocity (2m/s, which is already known) after the collision.

Kinetic Energy Lose: Derive from the initial and end velocity of icebergs.

And the **Simulation Time**, **Computation Time** will also be recorded.

5.2 Scenarios and Summaries

The shape sensitivity check of the icebergs will be implemented firstly. The simulated icebergs will hit the underwater part. However, during the shape sensitivity check process, the failure criteria will not be assigned to the iceberg. Hence, the collision part in the target vessel can have failure easily. And there is no other variables to affect the results of the iceberg shape sensitivity check. Only the shape is the variable to be checked.

For the shapes that can cause the failure on the hitting plate of the vessel will be introduced to the next stage simulation tests. The failure criteria of the ice will be assigned to those models to simulate the practical situations. In those cases, the icebergs still hit the underwater region of the vessel. The only changed variables compared to the previous cases are the failure criteria of the ice.

And the icebergs will also hit the above water region with or without the ice failure criteria. Those simulations can show the collision performance of steel in the low temperature directly. The scenarios are also practical. During the sailing and operations in the Arctic region, the icebergs can be in various kind of shapes. It cannot be excluded that the above waterline part of the iceberg hit the vessel firstly. And the icebergs hit the above water region scenarios will simulate the situations.

The temperature distribution above the waterline will be also changed. But the icebergs still hit the underwater region of the vessel. As introduced before, the vessel structure above the waterline is going to be the boundary condition of the hitting. The change of the temperature distribution on this region also changes the mechanical performance of the steel in this region. Hence, the change of the temperature distribution above the waterline can reflect the influence of the temperature as a factor of boundary condition.

General introduction of individual simulations will be showed firstly. Then comes the summaries of the simulation results. To have a summary, there are 4 categories of the simulations:

Table 5-1 Categories of different scenarios

Category	Description
I	Collision Sensitivity Check of Iceberg Shapes
II	Failure Criteria Assigned to the Ice (More practical simulation)
III	The Iceberg Hit above Water Region (Low temperature steel collision simulation)
IV	Change the Temperature Distribution on the above Water Region. (Influence of temperature as the boundary condition).

The following context will discuss and make a comparison within different categories. Conclusion will also be followed. The detail results of the individual simulations will be listed in the *Appendix B: Detail Collision Results*.
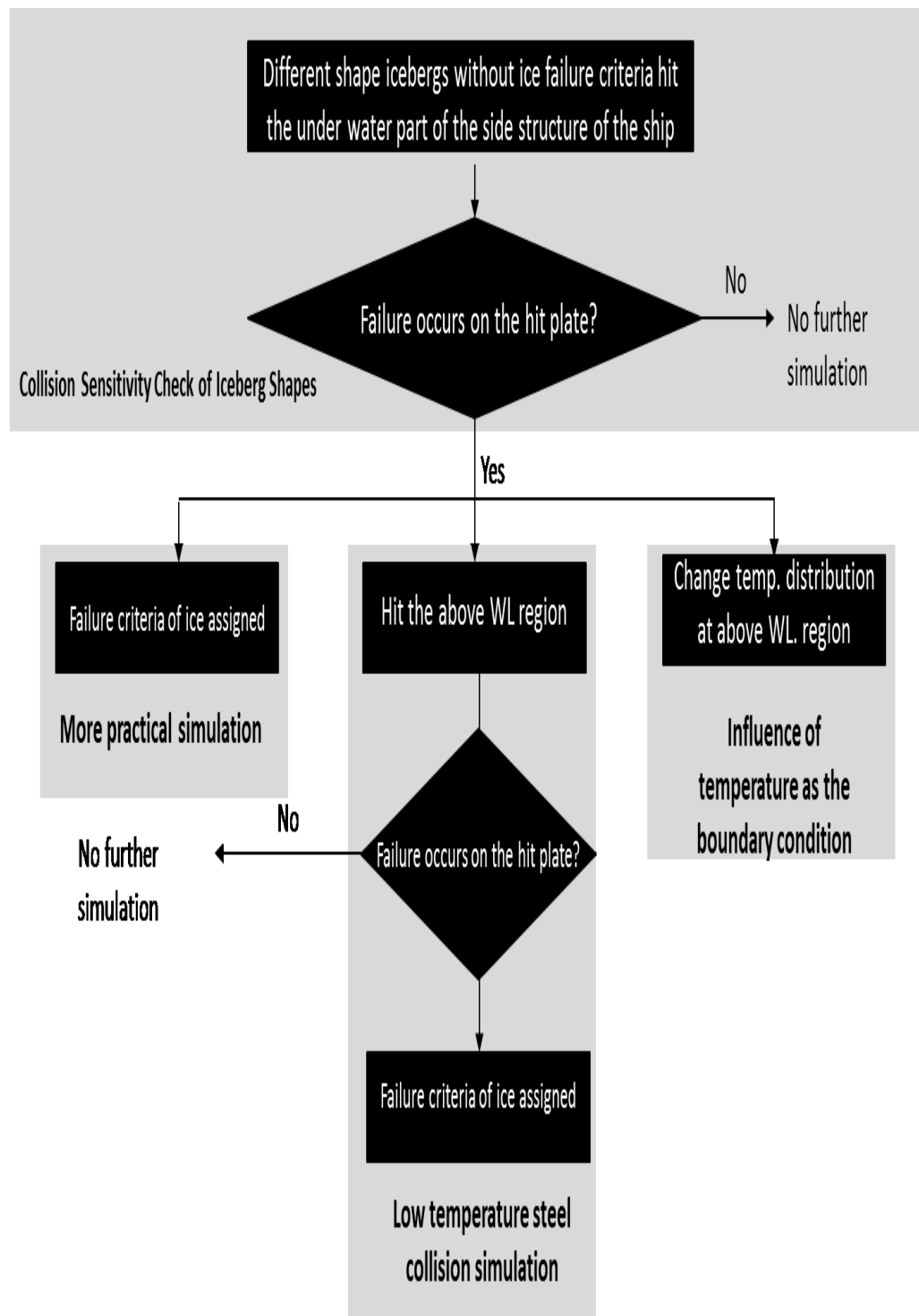

Figure 5-1 Simulation process

5.2.1 Collision Sensitivity Check of Iceberg Shapes

5.2.1.1 Introduction of the Shapes

As mentioned before, sharper icebergs will cause much bigger pressure on the tip where the collision happens. That is why it is easier for the sharper icebergs to penetrate the side plate of the vessel. However, it is unknown in what sharpness level can the failure on the hit plate on the vessel can happen.

In order to check the shape sensitivity of the iceberg, four iceberg models in different shapes are built. Those iceberg models are distinguished by their shape especially their sharpness at the tips. However, they have the same total mass and all the mechanical properties are the same in the ice parts.

No failure criteria of ice will be assigned to those icebergs' ice part. Therefore, the influence of the shape can be the only variable for the investigation.

The index of the sharpness is the curvature on the tip. Except a cubic case, all the other three iceberg models are rotating surfaces. And the axis passes through the tip point. Although the iceberg is a 3D geometry, the curvature on the tip can be calculated with the rotating curve functions.
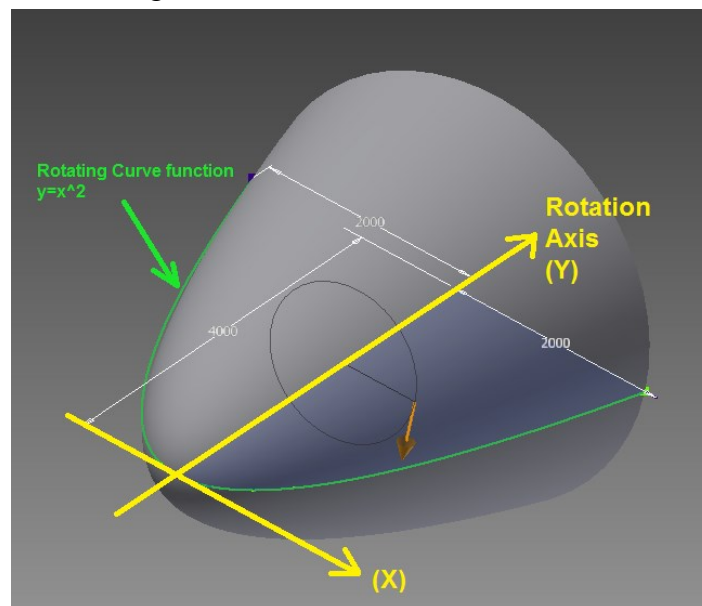

Figure 5-2 Rotating surface

If the rotating curve function is known, the curvature at a point can be obtained by the following equation:

$$\kappa = \frac{\left| f''(x) \right|}{\left[1 + (f'(x))^2 \right]^{3/2}}$$

(5-1.1)

To the curvature of circle, the *Equation 5-1* be simplified as

$$\kappa = \frac{1}{R}$$

(5-1.2)

Where

R =   Radius of the circle

The detail parameters of those four iceberg models are listed below:

a) Cubic iceberg

Table 5-2 Geometry parameters of the cubic iceberg

	Name of the parameters	Value or expression	Unit
Ice Part	Width (in X direction)	4	m
	Depth (in Y direction)	2	m
	Height (in Z direction)	2	m
	Curvature on the tip	0	m^{-1}
Mass Part	Width (in X direction)	4	m
	Depth (in Y direction)	2	m
	Height (in Z direction)	2	m
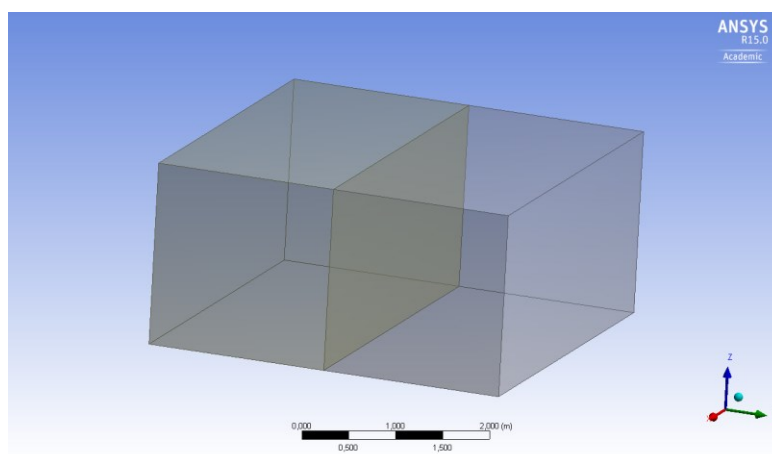
Figure 5-3 Cubic iceberg

b) Half sphere iceberg

Table 5-3 Geometry parameters of the half sphere iceberg

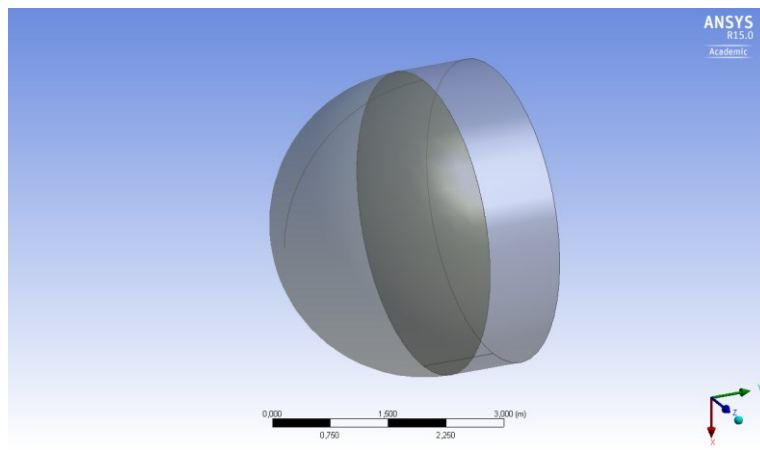|	Name of the parameters	Value or expression	Unit
Ice Part	Radius	2	m
	Curvature on the tip	0.5	m^{-1}
Mass Part	Radius	2	m
	Depth (in Y direction)	1	m

Figure 5-4 Half sphere iceberg

c) Bullet shape 1 iceberg

Table 5-4 Geometry parameters of the bullet shape 1 iceberg

	Name of the parameters	Value or expression	Unit
Ice Part	Rotating curve function	$y=0.5*x^2$	m
	Rotating axis	Y	-
	Depth (in Y direction)	2	m
	Curvature on the tip	1	m^{-1}
Mass Part	Radius	2	m
	Depth (in Y direction)	1	m
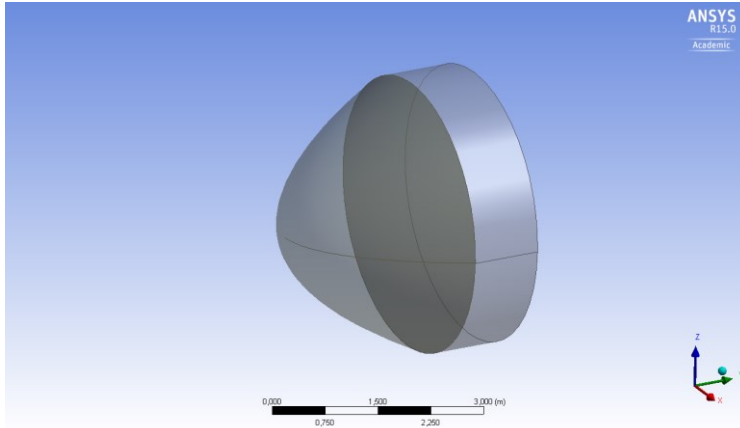
Figure 5-5 Bullet shape 1 iceberg

d) Bullet shape 2 iceberg

Table 5-5 Geometry parameters for the bullet shape 2 iceberg

	Name of the parameters	Value or expression	Unit
Ice Part	Rotating curve function	$y=x^2$	m
	Rotating axis	Y	-
	Depth (in Y direction)	4	m
	Curvature on the tip	2	m^{-1}
Mass Part	Radius	2	m
	Depth (in Y direction)	2	m
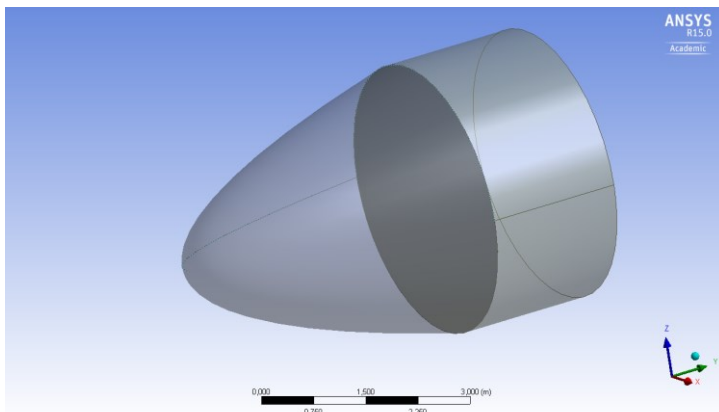
Figure 5-6 Bullet shape 2

5.2.1.2 Results and Discussion

The detail results of the shape sensitivity check illustrates in the Appendix B: case a), b), c) and d). In this section, the results of the shape sensitivity check will be summarized and have a comparison to have an insight view of the influence of the shape. The curvature at the tip of the iceberg will be set as the variables to represent the sharpness of the iceberg.

Failure Area

With the increasing of the curvature, the failure happens when the curvature is $1m^{-1}$ for the iceberg tip. And after the failure happens, the failure area will increase with the increment of the curvature.
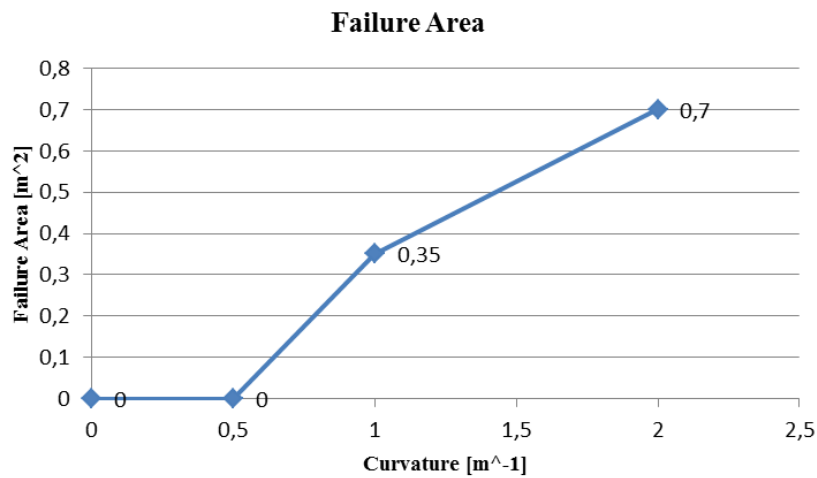
Figure 5-7 Failure Area vs. Curvature

Deformation Area (Where deformation on Y axis >=100mm)

Smaller curvature means the iceberg is blunter. When the collision happens, the energy disputes in larger area, hence the deformation area decreases with the increment of the iceberg curvature.
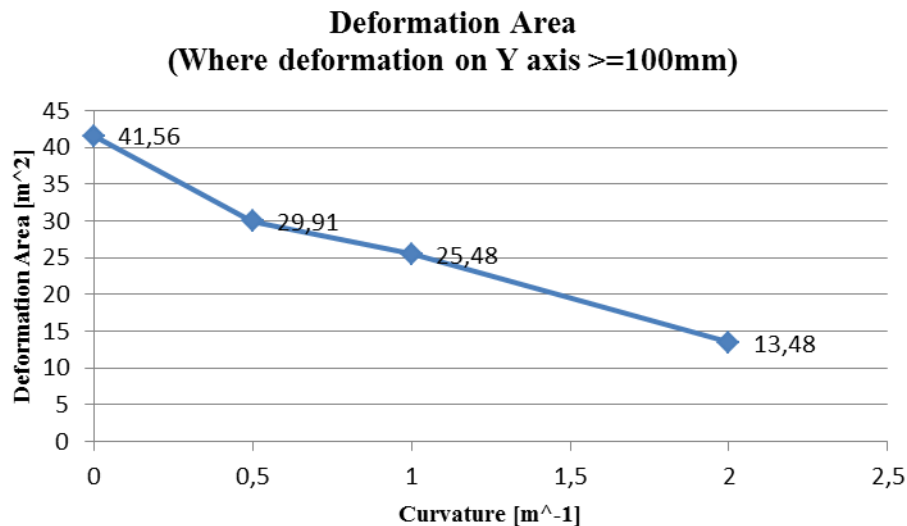

Figure 5-8 Deformation Area vs. Curvature

Maximum Deformation on Y axis

If the plate is not penetrated, the maximum deformation will increase with larger curvature on the iceberg tip. When the failure of the plate happens, the maximum deformation reaches its peak. But the value will not change too much with the increase of the curvature on the iceberg tip after the failure happens.
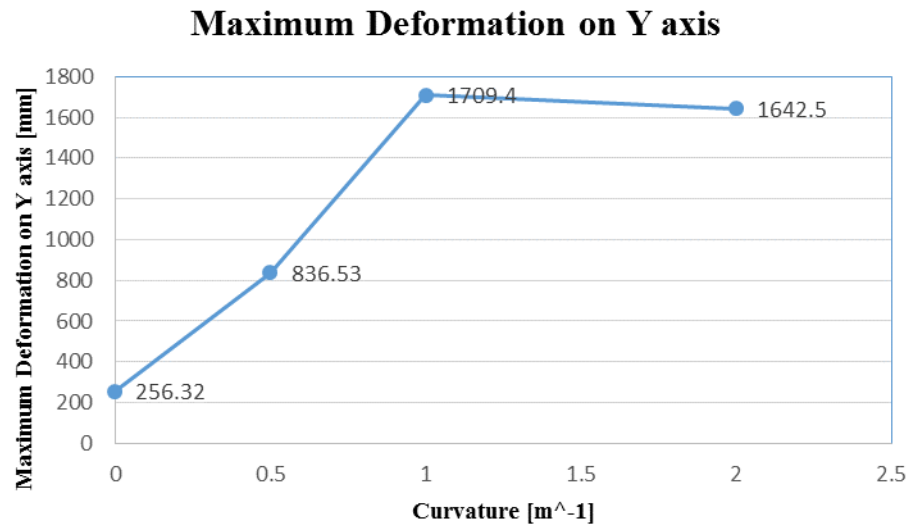

Figure 5-9 Maximum Deformation on Y axis vs. Curvature

Plastic Strain Area where EPS>0.05 (including Failure Area)

For the cubic iceberg, whose curvature is 0, the collision energy distributed on the large cubic surface. Hence, there is no area where EPS>0.05. But the half sphere iceberg, whose curvature is 0.5, causes the largest plastic strain. However, the largest plastic strain area dose not equal to the worst scenario. No failure happens when the half sphere iceberg hit the side structure. However, the plastic strain area does not change too much when failure happens on the plate.
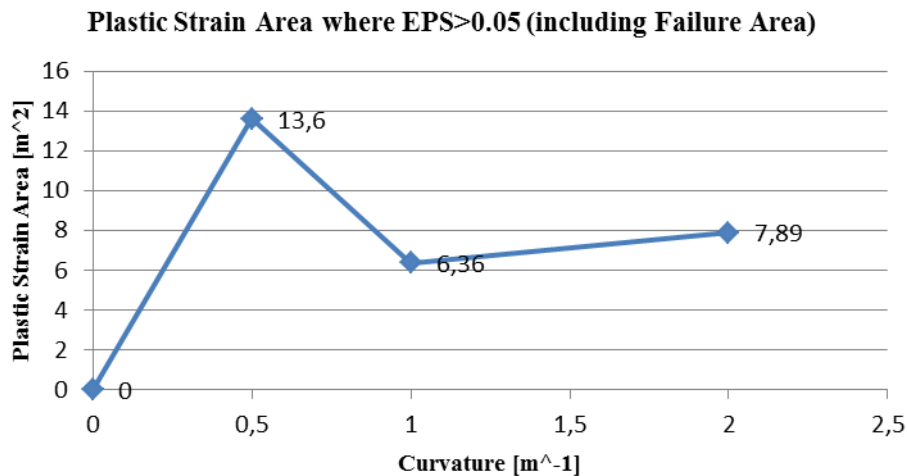

Figure 5-10 Plastic Strain Area where EPS>0.05 vs. Curvature

Number of Damaged Stiffeners

EPS>0.05 is set as the critical criterion for judging the damaged stiffeners. But there is not clear relationship between number of damaged stiffeners and curvature.
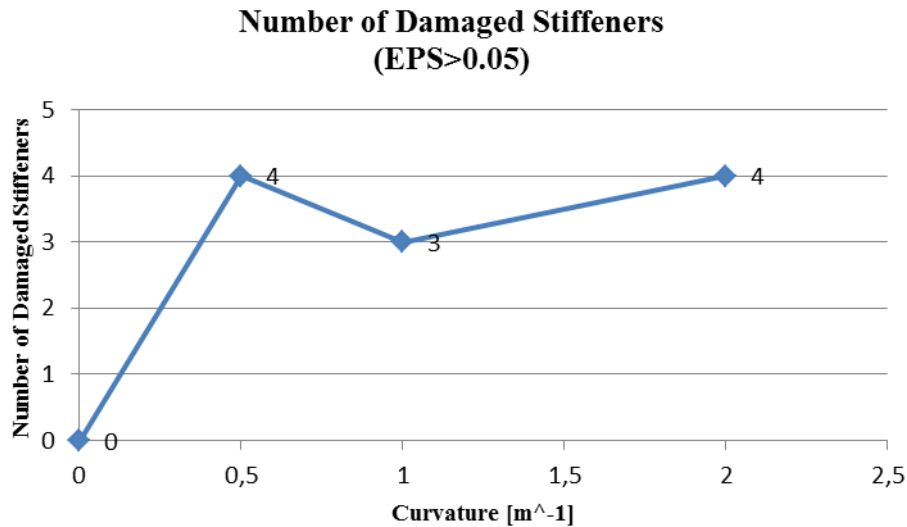

Figure 5-11 Number of Damaged Stiffeners vs. Curvature

Kinetic Energy Lose for the Iceberg

With the increase of the curvature on the iceberg tip, the collision will consume more energy. When the failure happens, the kinetic energy of the iceberg will be almost totally disputed. But no big difference on the energy lose when comparing two failure occur situation (Curvature are $1m^{-1}$ and $2m^{-1}$).
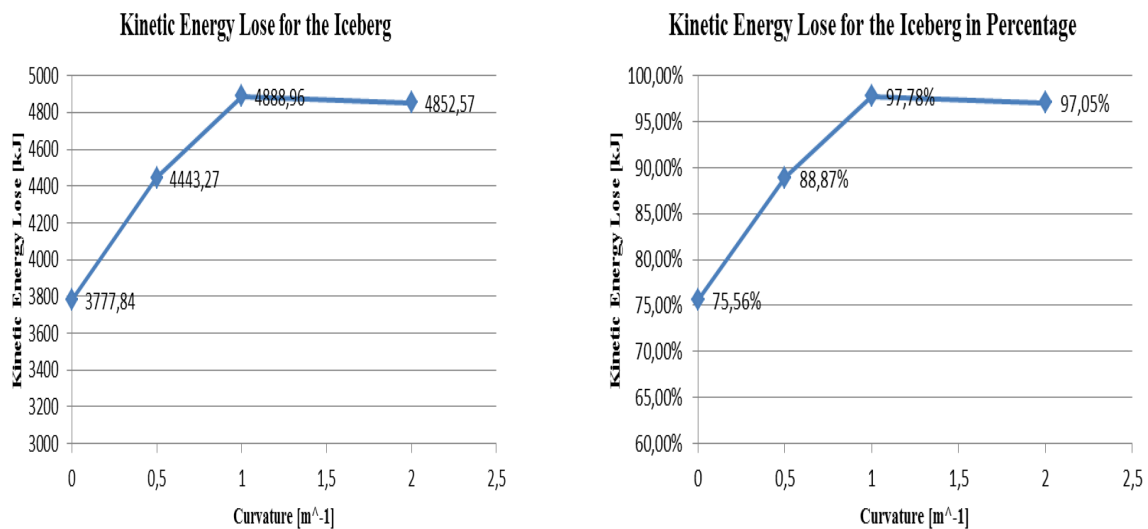

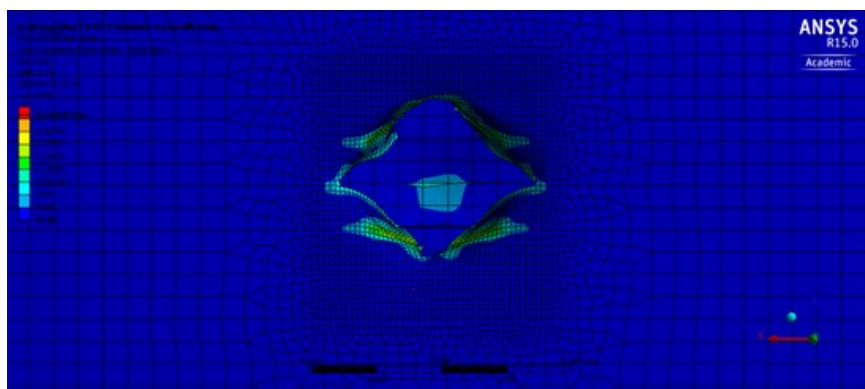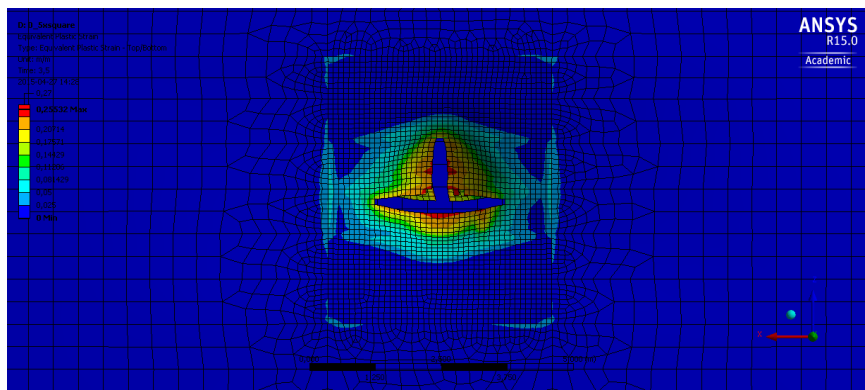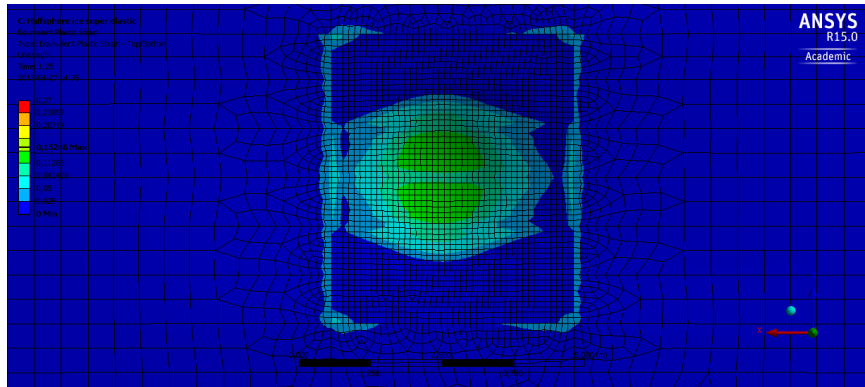*Figure 5-12 Kinetic Energy Lose for the Iceberg vs. Curvature*
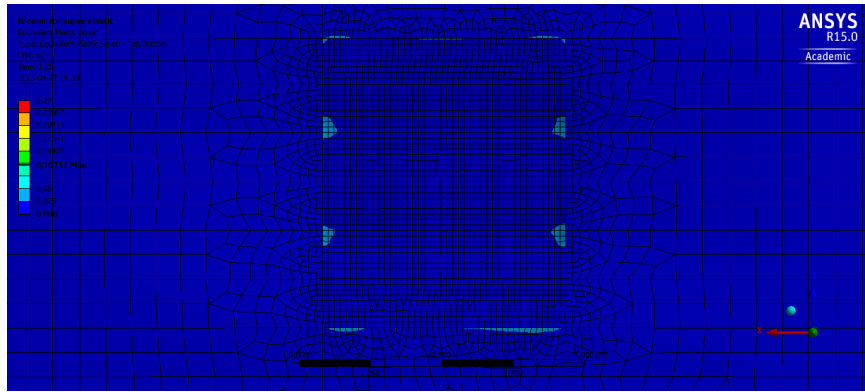
Figure 5-13 EPS illustration in the same scale of the shape sensitivity check, from top to bottom are case a), b), c) and d)

5.2.2 Failure Criteria Assigned to the Ice

5.2.2.1 General Introduction

From the result of *Section 5.2.1*, Bullet Shape 1 and Bullet Shape 2 can make failure happens on the plate of the side structure. And penetration phenomenon can also be observed from the simulation in these two cases. According to the strategy introduced in *Section 5.2*: *Figure 5-1 Simulation process*, the iceberg model in Bullet Shape 1 and 2 cases will be assigned the failure criteria of ice to the tip of the model. And the failure criteria follow the discussion in *Section 4.4.2*, Maximum Tensile Pressure will be defined as 7 MPa to the simulated ice. That is to say more practical scenario will be simulated. ´

In order to distinguish with the tested cases introduced in *Section 5.2.1*, the failure criteria assigned cases will be marked as

e) Bullet Shape 1 Iceberg with Failure Criteria and,

f) Bullet Shape 2 Iceberg with Failure Criteria.

Detail collision simulation results are in *Appendix B: Detail Collision Results*.

5.2.2.2 Results and Discussion

Although the failure criteria have been assigned to two iceberg models to make the ice fragile and brittle, the vulnerable iceberg can still penetrate the plate of the side structure due to the huge kinetic energy of the iceberg. Moreover, the failure seems to be more serious compared to the scenarios that failure criteria have not assigned to the ice. The sharp edges on the rest part of the icebergs may cause secondary hurt on the plate of the vessel.

The tables below show the comparison between scenarios c) Bullet Shape 1 Iceberg and e) Bullet Shape 1 Iceberg with Failure Criteria. Also the comparison of d) Bullet Shape 2 Iceberg and f) Bullet Shape 2 Iceberg with Failure Criteria is illustrated.

Table 5-6 Comparison between scenarios c) Bullet Shape 1 Iceberg and e) Bullet Shape 1 Iceberg with Failure Criteria

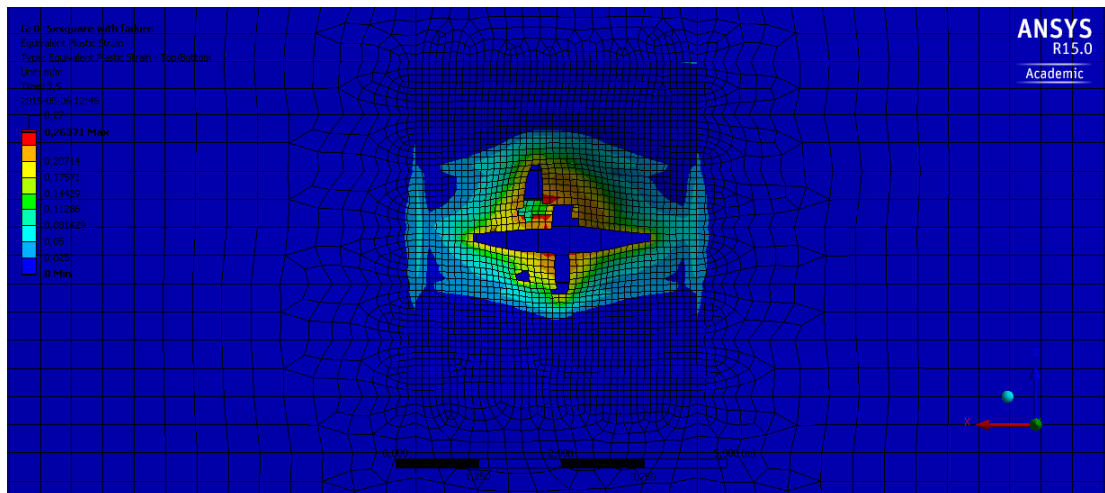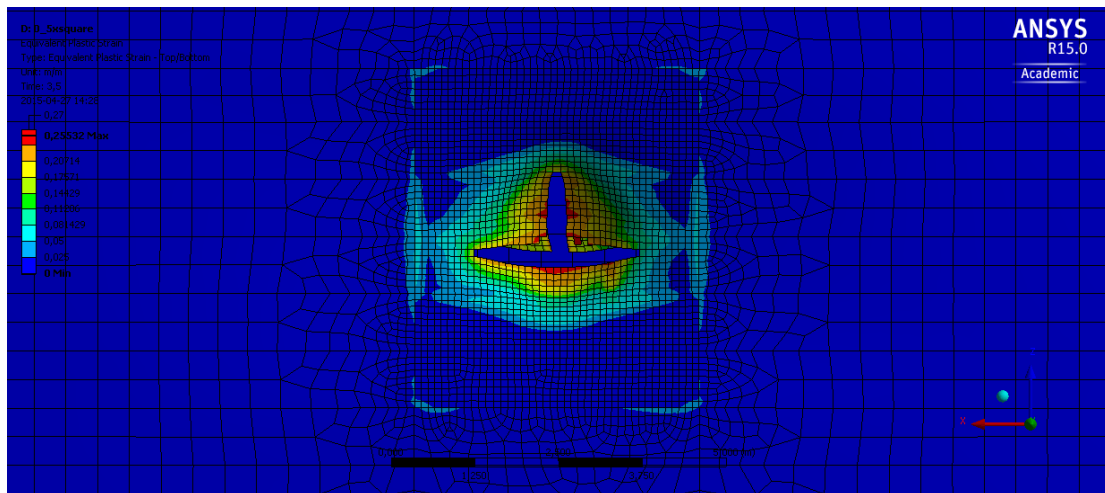| Name	Value of c)	Value of e)	Unit
Failure Area	0.35	0.49	m^2
Deformation Area (Where deformation on Y axis	25.48	22.04	m^2
Maximum deformation on Y axis	1709.40	1155.60	mm
Plastic Strain Area (including Failure Area)	6.36	6.46	m^2
Number of Damaged Stiffeners (EPS>0.05)	3	3	-
End Velocity of Iceberg	0.30	0.33	m/s
Kinetic Energy Lose for the Iceberg	4888.96	4863.83	kJ
Kinetic Energy Lose in Percentage	97.78%	97.28%	-
Time Span to be Simulated	3.5	3.5	s
Computation Time for Computer	767.38	791.31	min

Figure 5-14 EPS illustration in the same scale, from top to bottom are case c) and e)

Table 5-7 Comparison between scenarios d) Bullet Shape 2 Iceberg and f) Bullet Shape 2 Iceberg with Failure Criteria

| Name	Value of d)	Value of f)	Unit
Failure Area	0.70	1.04	m^2
Deformation Area (Where deformation on Y axis	13.48	20.55	m^2
Maximum deformation on Y axis	1642.50	1570.00	mm
Plastic Strain Area (including Failure Area)	7.89	7.81	m^2
Number of Damaged Stiffeners (EPS>0.05)	4	3	-
End Velocity of Iceberg	0.34	0.16	m/s
Kinetic Energy Lose for the Iceberg	4852.57	4967.47	kJ
Kinetic Energy Lose in Percentage	97.05%	99.35%	-
Time Span to be Simulated	2.75	3.5	s
Computation Time for Computer	736.15	904.43	min
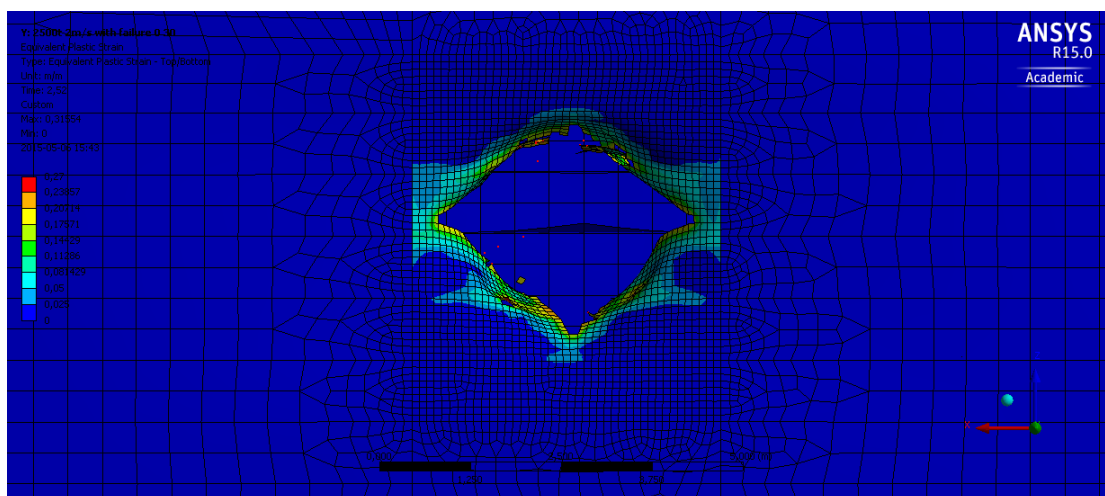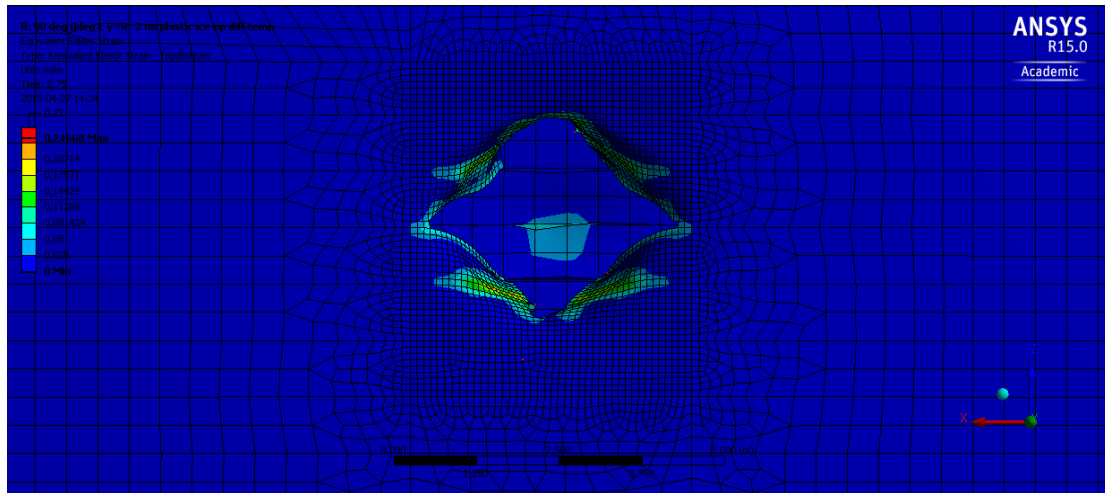
Figure 5-15 EPS illustration in the same scale, from top to bottom are case d) and f)

Based on the data provided in *Table 5-6* and *Table 5-7*, failure area differs mostly in the comparison. After the failure criteria of ice have been assigned to the iceberg models, the icebergs can make larger area of failure on the plate of the vessel. Although the ice becomes brittle and vulnerable, the huge kinetic energy still makes them powerful to penetrate the plate. Moreover, just because its brittle property, it is quite easy to have sharp edges in the front part of the iceberg. According to the result in *Section 5.2.1* , sharper iceberg is easier to penetrate or damage the plate on the vessel. As a consequence, the sharp local edges on the iceberg front also can damage the plate. That is the reason why the fragile and brittle iceberg models can cause larger failure area on the plate of the vessel. However, other data have not indicated so much difference between ice failure criteria assigned or not assigned scenarios.

In general, the failure criteria of the ice mainly influence the failure area on the collision target, the plate on the side structure of the vessel.

5.2.3 The Iceberg Hit above Water Region (Low Temperature Region)

5.2.3.1 General Introduction

In order to investigate the collision phenomenon on low temperature (-30°C) plate, the icebergs will hit the low temperature region of the side structure. Since the shape sensitivity check has already been implemented and results show the shapes that can penetrate the plate, the shapes of the icebergs will be as same as the models in case c) Bullet Shape 1 Iceberg and d) Bullet Shape 2 Iceberg.

Also firstly, the failure criteria of the ice will not be assigned to the icebergs to simplify the collision process. Hence, the shape influence of the iceberg can be investigated by this method. The cases will be named as

g) Bullet Shape 1 Iceberg Hits above Region and,

h) Bullet Shape 2 Iceberg Hits above Region.

Then, the failure criteria of the ice will be assigned to the icebergs to simulate more practical situations. The cases will be named for

i) Bullet Shape 1 Iceberg Hits above Region with Failure Criteria and,

j) Bullet Shape 2 Iceberg Hits above Region with Failure Criteria
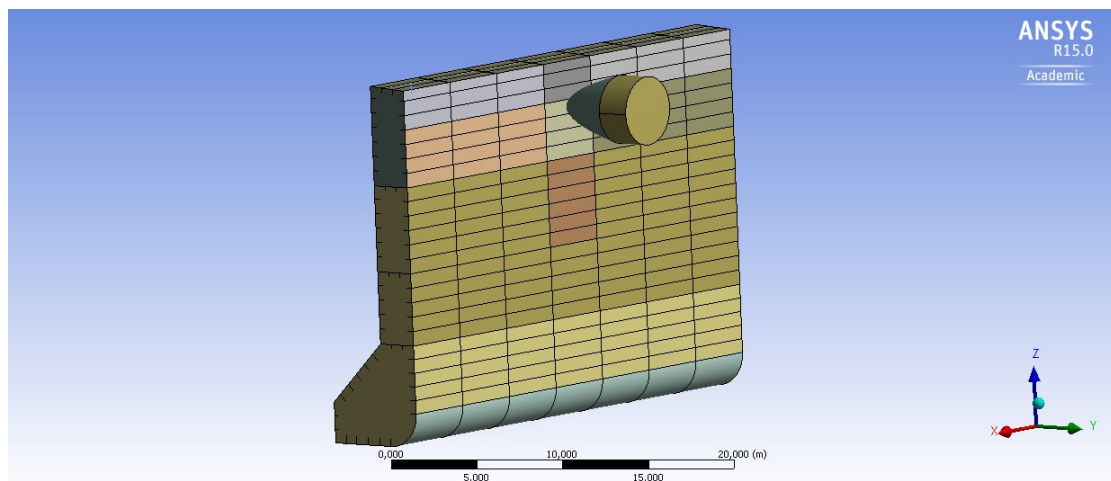

Figure 5-16 The iceberg hits the low temperature region of the side structure

5.2.3.2 Results and Discussion

A comparison between cases will be illustrated in this section. They are:

c) Bullet Shape 1 Iceberg/ g) Bullet Shape 1 Iceberg Hits above Region,

d) Bullet Shape 2 Iceberg/ h) Bullet Shape 2 Iceberg Hits above Region,

e) Bullet Shape 1 Iceberg with Failure Criteria/ i) Bullet Shape 1 Iceberg with Failure Criteria Hits above Region, and

f) Bullet Shape 2 Iceberg with Failure Criteria/ j) Bullet Shape 2 Iceberg with Failure Criteria Hits above Region.

Table 5-8 Comparison of the Results between c) Bullet Shape 1 Iceberg/ g) Bullet Shape 1 Iceberg Hits above Region

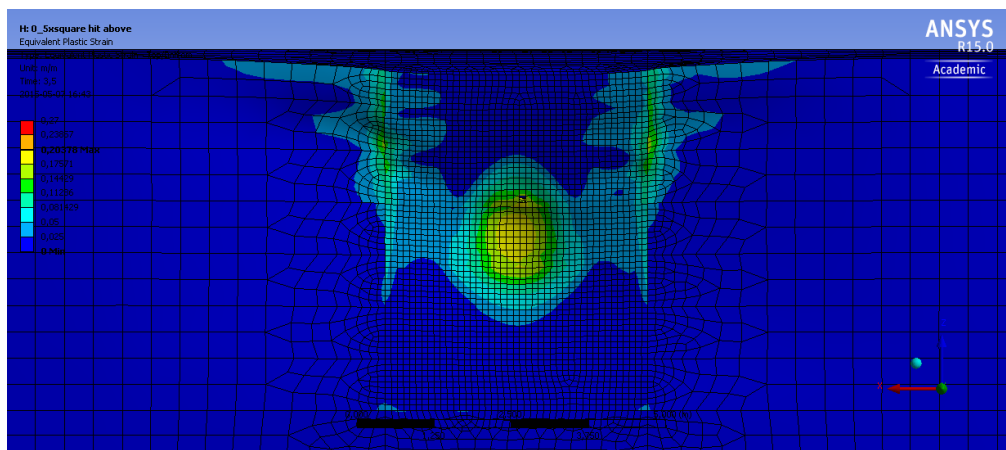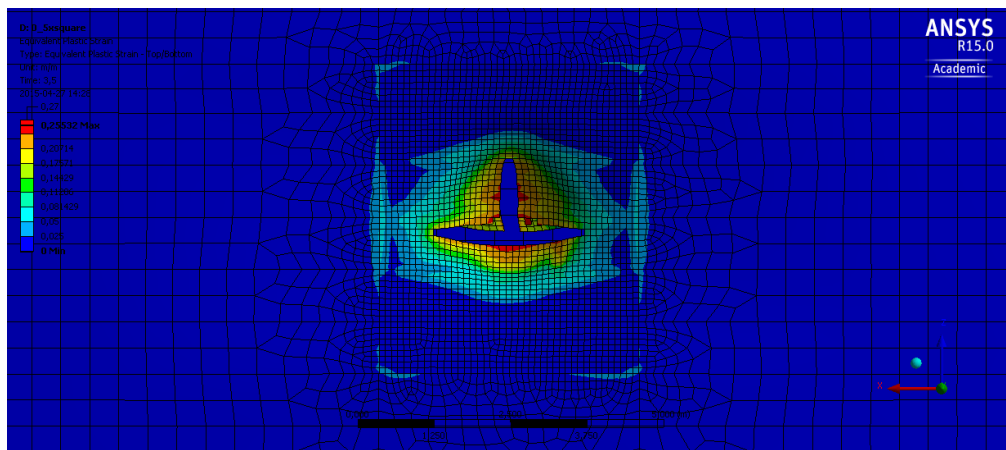| Name	Value in c)	Value in g)	Unit
Failure Area	0.35	0.01	m²
Deformation Area (Where deformation on Y axis >=100mm)	25.48	47.35	m²
Maximum Deformation on Y axis	1709.40	1187	mm
Plastic Strain Area (including Failure Area) where EPS> 0.05	6.36	6.46	m²
Number of Damaged Stiffeners (EPS>0.05)	3	4	-
End Velocity of Iceberg	0.30	0.41	m/s
Kinetic Energy Lose for the Iceberg	4888.96	4794.16	kJ
Kinetic Energy Lose in Percentage	97.78%	95.88%	-
Time Span to be Simulated	3.5	3.5	s
Computation Time for Computer	767.38	904.92	min

Figure 5-17 EPS illustration in the same scale, from top to bottom are case c) and g)

Table 5-9 Comparison of the Results between d) Bullet Shape 2 Iceberg/ h) Bullet Shape 2 Iceberg Hits above Region

Name	Value in d)	Value in h)	Unit
Failure Area	0.70	0.91	m²
Failure Area (Inner Side Shell)	0	0.06	m²
Deformation Area (Where deformation on Y axis >=100mm)	13.48	44.78	m²
Deformation Area (Inner Side Shell)	0	1.41	m²
Maximum Deformation on Y axis	1642.5	1385.7	mm
Maximum Deformation on Y axis (Inner Side Shell)	0		mm
Plastic Strain Area (including Failure Area) where EPS> 0.05	7.89	8.13	m²
Plastic Strain Area (Inner Side Shell)	0	0.21	m²
Number of Damaged Stiffeners (EPS>0.05)	4	4	-
Number of Damaged Stiffeners (Inner Side Shell)	0	1	-
End Velocity of Iceberg	0.34	0.20	m/s
Kinetic Energy Lose for the Iceberg	4852.57	4948.08	kJ
Kinetic Energy Lose in Percentage	97.05%	98.96%	-
Time Span to be Simulated	2.75	3.5	s
Computation Time for Computer	736.15	1232.29	min

Figure 5-18 EPS illustration in the same scale, from top to bottom are case d) and h)

Table 5-10 Comparison of the Results between e) Bullet Shape 1 Iceberg with Failure Criteria/ i) Bullet Shape 1 Iceberg with Failure Criteria Hits above Region

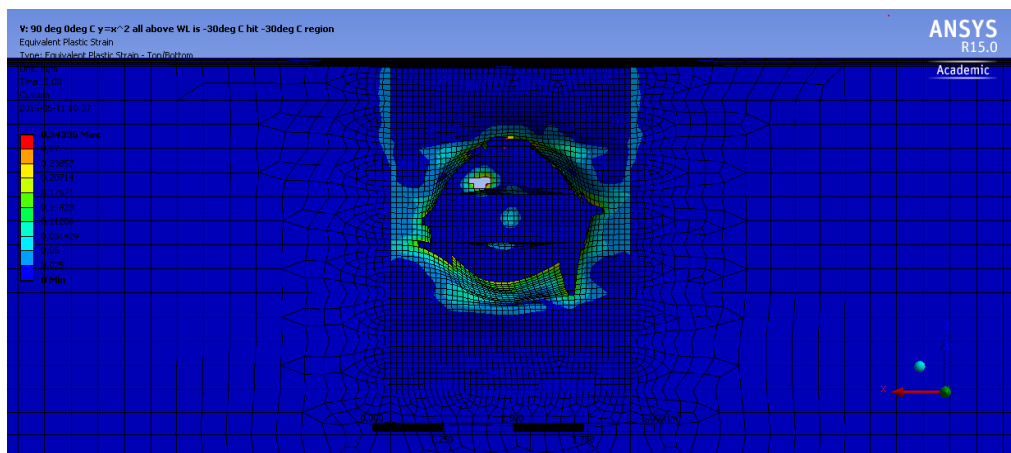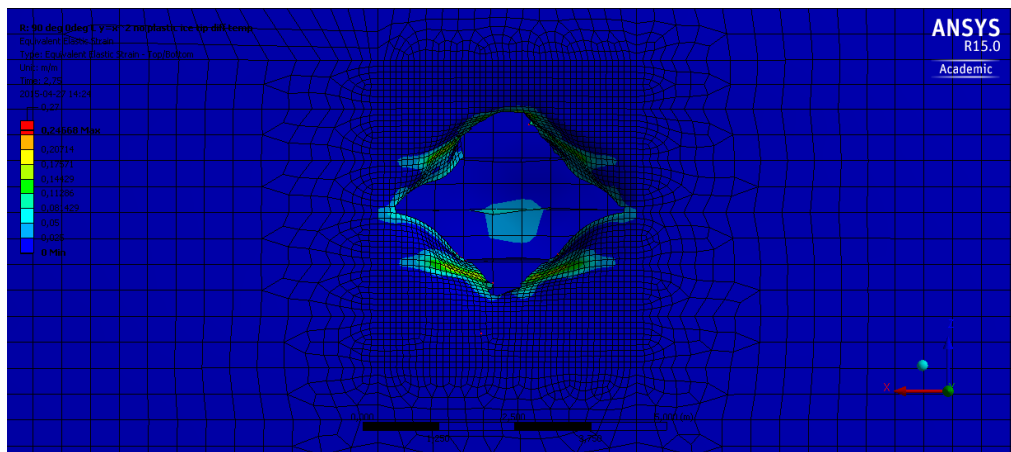| Name	Value in e)	Value in i)	Unit
Failure Area	0.49	0.00	m²
Deformation Area (Where deformation on Y axis >=100mm)	22.04	47.56	m²
Maximum Deformation on Y axis	1155.60	1199.50	mm
Plastic Strain Area (including Failure Area) where EPS> 0.05	6.46	5.96	m²
Number of Damaged Stiffeners (EPS>0.05)	3	4	-
End Velocity of Iceberg	0.33	0.51	m/s
Kinetic Energy Lose for the Iceberg	4863.83	4673.13	kJ
Kinetic Energy Lose in Percentage	97.28%	93.46%	-
Time Span to be Simulated	3.5	3.5	s
Computation Time for Computer	791.31	934.43	min
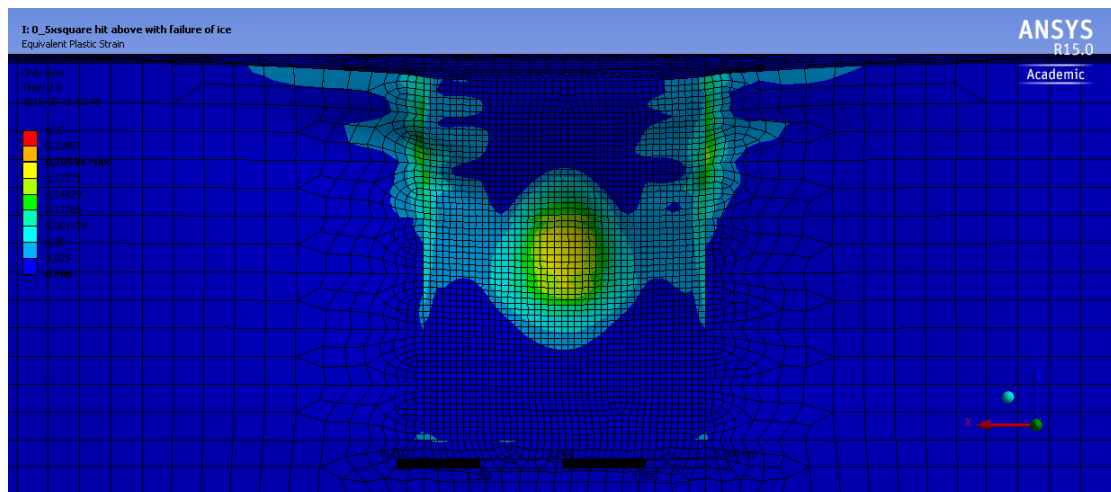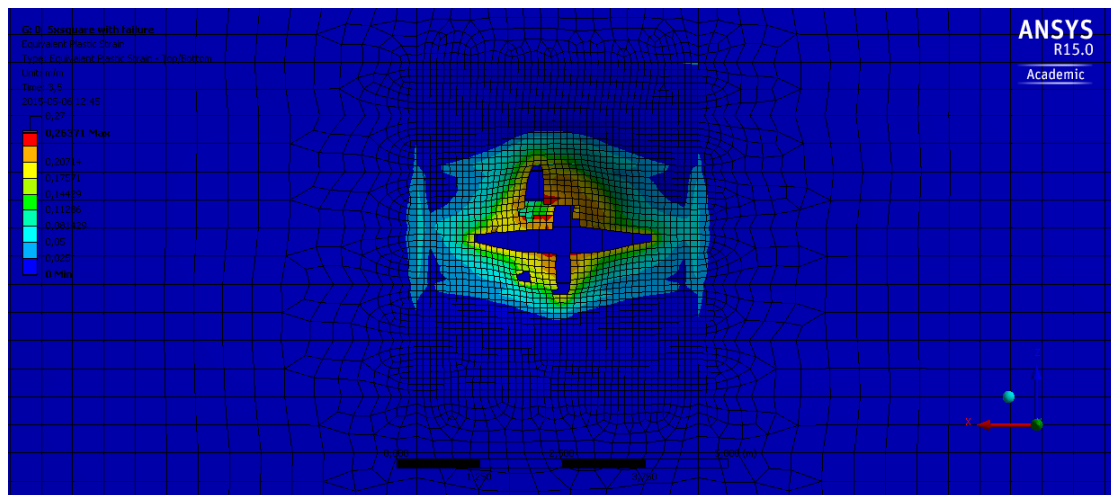
Figure 5-19 EPS illustration in the same scale, from top to bottom are case e) and i)

Table 5-11 Comparison of the Results between f) Bullet Shape 2 Iceberg with Failure Criteria/ j) Bullet Shape 2 Iceberg with Failure Criteria Hits above Region

| Name	Value in f)	Value in j)	Unit
Failure Area	1.04	1.19	m²
Deformation Area (Where deformation on Y axis >=100mm)	20.55	52.47	m²
Maximum Deformation on Y axis	1570.00	1433.6	mm
Plastic Strain Area (including Failure Area) where EPS> 0.05	7.81	7.39	m²
Number of Damaged Stiffeners (EPS>0.05)	3	4	-
End Velocity of Iceberg	0.16	0.20	m/s
Kinetic Energy Lose for the Iceberg	4967.47	4948.08	kJ
Kinetic Energy Lose in Percentage	99.35%	98.96%	-
Time Span to be Simulated	3.5	3.5	s
Computation Time for Computer	904.43	1232.29	min
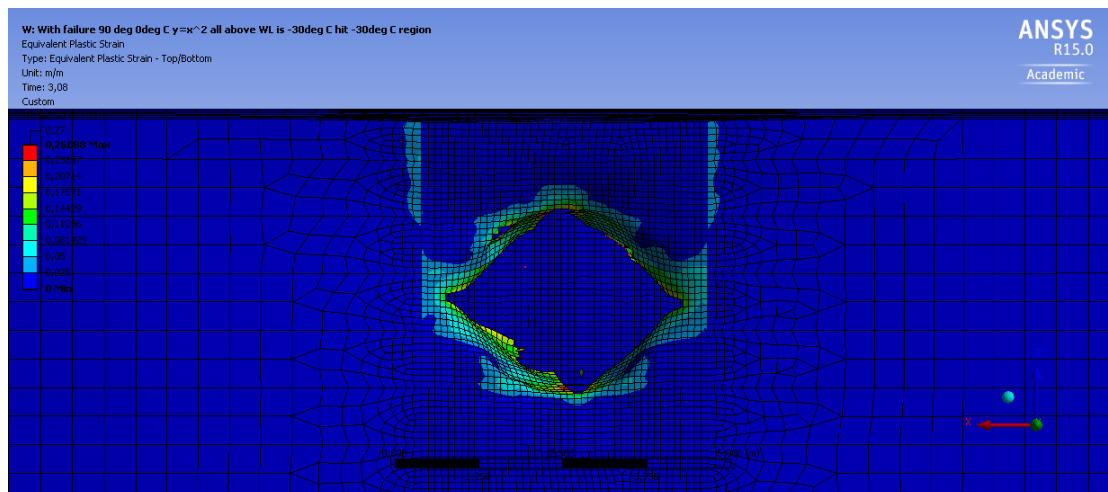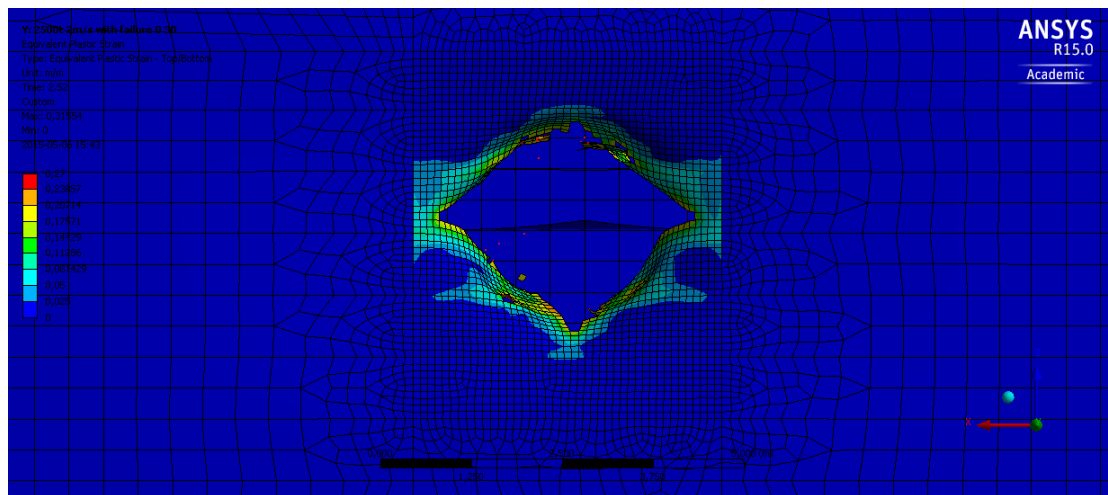
Figure 5-20 EPS illustration in the same scale, from top to bottom are case f) and j)

The four comparison groups show the difference of collision results between the steel in 0°C and -30°C. The steel in lower temperature has higher flow stress. Hence, if the blunt object hits the steel plate, it is not easy to have failure. But the deformation area for lower temperature collision is much bigger. However, the bigger deformation area can distribute the collision energy but prevent the failure.

On the other hand, once failure happens it is easier for the steel in low temperature to be penetrated or being damaged by the hitting objects. The NVA steel has lower failure strain values in -30°C compared to 30°C. It is easier for the steel in low temperature to reach the failure strain. The comparison groups d)/h) and f)/j) have clarified it.

5.2.4 Change the Temperature Distribution on the above Water Region

5.2.4.1 General Introduction

Similar models, which was used in case d), will be used in the following tests. In the *Section 5.2.1*, the Bullet Shape 2 Iceberg has already been verified as the most dangerous iceberg shape to hit the side structure. Serious damage will happen due to the large curvature at the tip of the iceberg. Hence, the geometry and kinetic model of case d) will be used to investigate the influence of the temperature as a change of the boundary condition. It is expected that clear result of failure will be indicated by using model in the case d). In order to simplify the problem, the failure criteria of the ice will not be assigned to the Bullet Shape 2 Iceberg.

Different from d) the temperature above the water line will change its distribution. But the iceberg will hit the near waterline region as indicated in the case d). The change of the temperature distribution affects the mechanical performance of the steel. But the temperature on the collision region will not be changed. Hence, the boundary condition of the collision region will be slightly changed.

Two cases will be tested:

k) Bullet Shape 2 Iceberg Hit with above Waterline Temperature is 0°C

All parts above the waterline of the side structure is in temperature of 0°C. The outer plates and their attached stiffeners are also in temperature of 0°C but no longer -30°C.

l) Bullet Shape 2 Iceberg Hit with above Waterline Temperature is -30°C

All parts above the waterline of the side structure is in temperature of -30°C. The inner side plates (above the water line) and their attached stiffeners are also in -30°C but no longer 0°C.

5.2.4.2 Results and Discussion

The comparison of case d) Bullet Shape 2 Iceberg, k) Bullet Shape 2 Iceberg Hitting with above Waterline Temperature is 0°C, and l) Bullet Shape 2 Iceberg Hitting with above Waterline Temperature is -30°C will be tabulated. A clear comparison will be showed in the table.

Table 5-12 Comparison of the Results for d) Bullet Shape 2 Iceberg k) Bullet Shape 2 Iceberg Hit with above Waterline Temperature is 0°C, and l) Bullet Shape 2 Iceberg Hit with above Waterline Temperature is -30°C

Name	Value in d)	Value in k)	Value in l)	Unit
Failure Area	0.70	0.78	0.81	m²
Deformation Area (Where deformation on Y axis >=100mm)	13.48	12.27	15.34	m²
Maximum deformation on Y axis	1642.50	1637.30	1600.6	mm
Plastic Strain Area (including Failure Area) where EPS> 0.05	7.89	7.96	8.0319	m²
Number of Damaged Stiffeners (EPS>0.05)	4	4	4	-
End Velocity of Iceberg	0.34	0.30	0.30	m/s
Kinetic Energy Lose for the Iceberg	4852.57	4888.70	4884.77	kJ
Kinetic Energy Lose in Percentage	97.05%	97.77%	97.70%	-
Time Span to be Simulated	2.75	2.75	2.75	s
Computation Time for Computer	736.15	743.53	743.53	min

From the data above, all items in three different cases share similar values. From the EPS figures of those three cases, the plastic deformation regions seldom reach the above waterline area. Therefore, most of the steel elements (plates and stiffeners) located above the water line is under linear deformation. It has been clarified that there is almost no difference for the steel regarding its linear mechanical performance if the temperature is not the same. Temperature mostly affects the non-linear mechanical properties of the steel. That is the reason why the collision results for the three cases are almost the same.

As a consequence, the change of the temperature distribution for the above waterline region dose not affects the collision results.
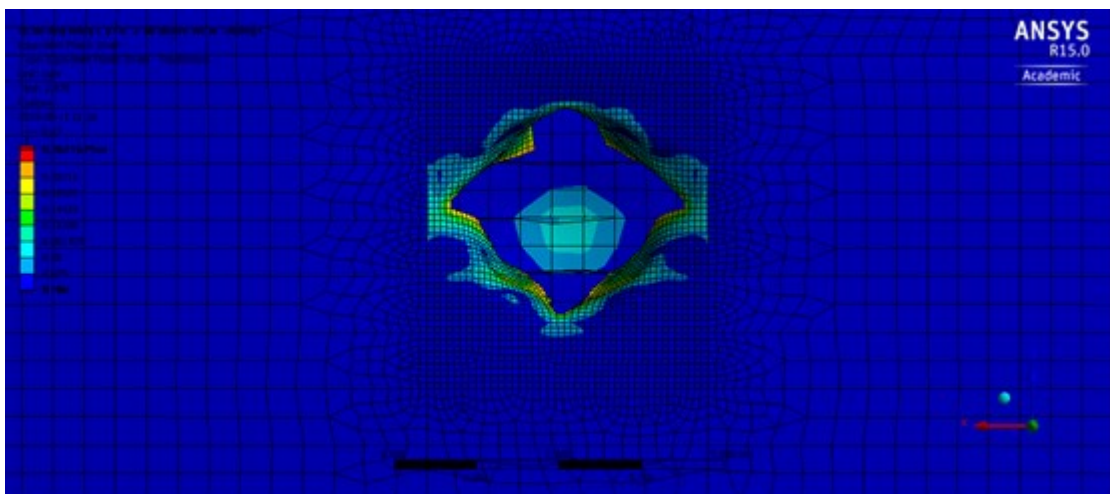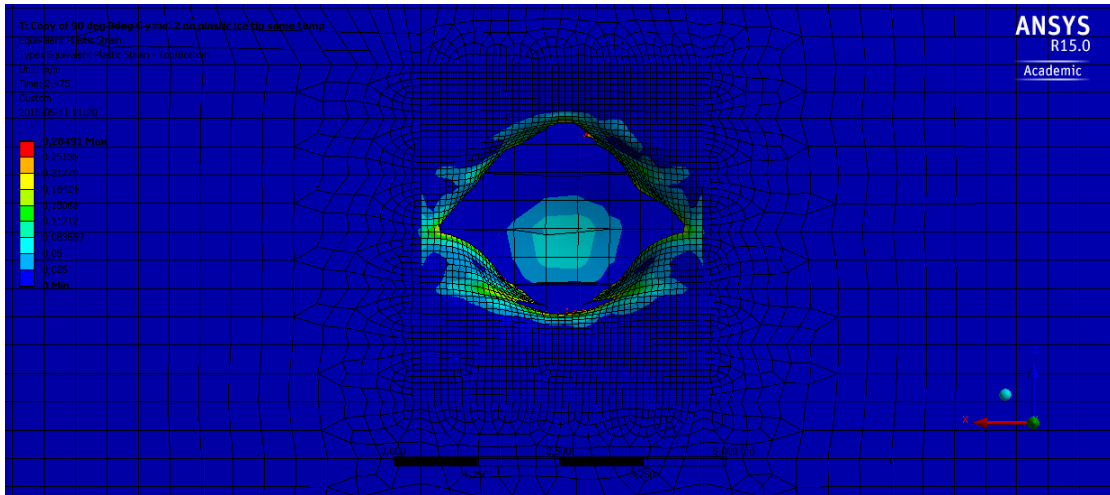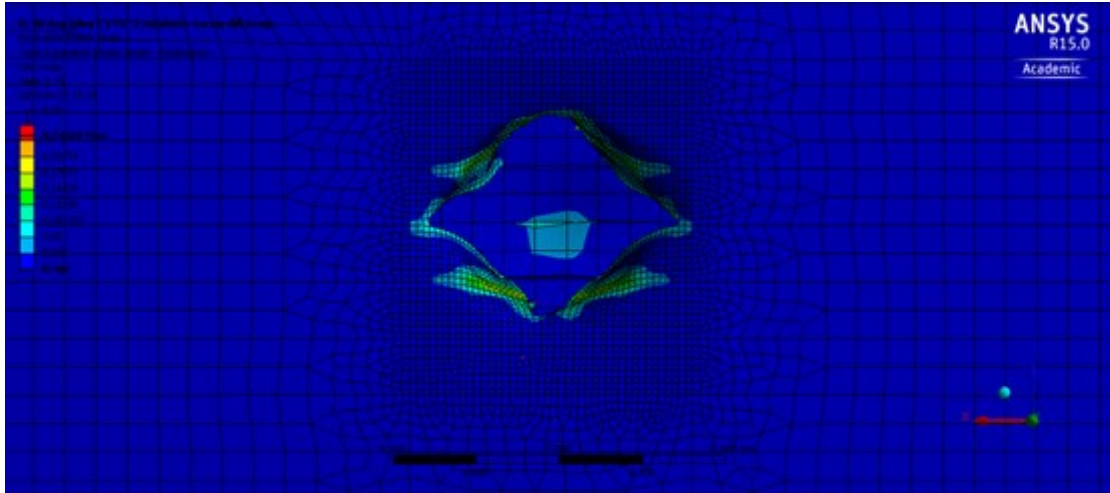
Figure 5-21 EPS illustration in the same scale, from top to bottom are case d), k) and l)

5.3 Conclusion of the Collision Simulations

From the result data given in the above simulations, several conclusions can be made:

1) The damage level of ship plate in the collision region is sensitive to the shape of the icebergs. Sharper icebergs lead more serious damage on the side structure of the vessel.

2) If the ice failure criteria is taken into account in the simulation, there are two consequences depend on the shape of the iceberg. If the shapes even cannot make failure on the plate in the simulation category I (shape sensitivity check), no further damage will happen if the iceberg is assigned failure criteria. But for the shapes which can penetrate the steel plate. More severe damage will occurs after assigning failure criteria of the ice. It is because the sharp edge of the broken ice may have a secondary cut on the plate of the vessel

3) If the collision happens on the low temperature area (-30°C), the steel plate is averagely in smaller EPS if no failure happens. It can be described that the structure in low temperature region is more stiffened. However, once failure happens, the damage situation will be worse than the 0°C situations.

4) The temperature distribution change on the non-collision part dose not influence the collision results so much.

And the kinetic energy loss of the iceberg is considered to be consumed by the following items:

1) The plastic deformation of the steel on the side structure.

2) The failures on the steel.

3) Friction.

4) The failures on the ice (if the ice has been assigned the failure criteria).
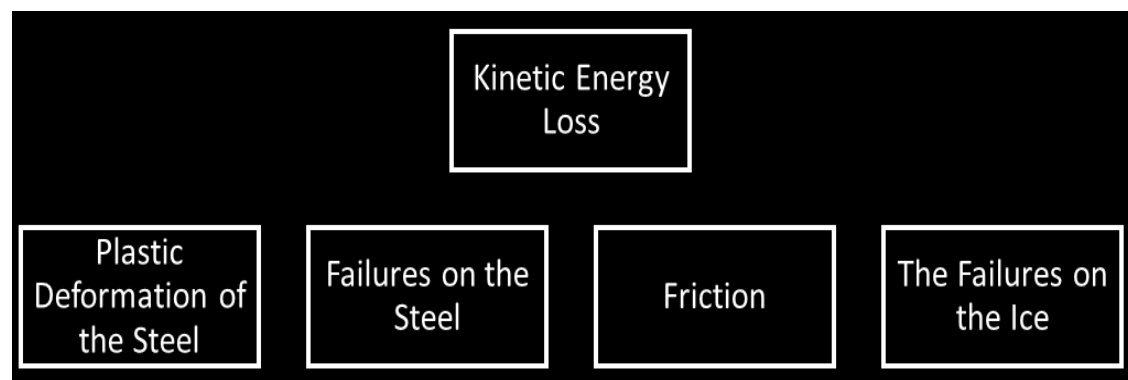
Figure 5-22 Kinetic energy loss flow

Case a) and case b) show the scenarios that failure not happens on the plates. But still the no failure criteria icebergs lose 77.56% and 88.87% kinetic energy respectively after the collision. Moreover, the cubic iceberg scenario in case a) is considered to have no or very little energy lose caused by friction. Therefore, the plastic deformation of the steel on the side structure can be taken as the priority reason for the kinetic energy loss of the iceberg during the collisions.

6 Methods to Reduce Damage

As indicated in the *Section 1.3*, the methods to reduce the damage caused by ice-ship collision in the Arctic region will focus on two aspects. They are operation and structure.

The operation is mainly focus on regulating the crew members. Based on the results of the simulations, it is possible to prevent the collision or rescue the vessel and crew members from the collision.

To optimize the structure, the vessel is expected to be more stiffened in the potential collision region. And according to the conclusion in *Section 5.3*, try to increase the plastic deformation but prevent failure of the steel is also an alternative to optimize the structure for the ice-ship collision.

6.1 Reduce Damage via Operation

First and the most priority thing is to prevent the collision of ice and ship. When sailing in the Arctic region, the route should be well planned and voyage should be in the summer season. The heavy ice routes must be avoided.

It is also not allowed for the vessels without ice class to sail in the icy region. The icebreakers should be employed for breaking the encounter floating ice if the ice condition is serious.

If the collision between ice and ship cannot be prevented, the crew should try their best to reduce the damage to the vessel during the collision. However, the under waterline region cannot be seen by the operators. That is to say it is not easy to prevent the ice-ship collision in the 0°C region on the vessel. Hence, it is practical to reduce the collision damage on the above waterline region, where the temperature is much lower.

From the results in case g), h), i) and j), sharp icebergs can easy penetrate the steel plates in low temperature. The NVA grade steel becomes brittle under low temperature. Once the failure happens on the plate, the damage will be catastrophic. Less energy will be needed for the iceberg to reach further deep, since the brittle steel cannot absorb energy when having plastic deformation. Hence, the iceberg penetration will be quite easy to reach the inner side shell. There is a high possibility for the inner side shell of the vessel to have failure too. Although the break on above waterline region may not cause the loss of buoyance for the vessel, serious environmental problems will occur. Once the inner side shell failure happens, there will be leakage of oil for the oil tankers and FPSOs. Since the environment in the Arctic region is very vulnerable.

The direction of the hitting iceberg should be better normal to the side of the vessel. It is known that tanks, including ballast tanks, are arranged along the vessel. If the iceberg cut the side structure along the x-direction of the vessel local coordinate system, more than one tank will be damaged and water floods into the vessel. However, if the iceberg hit the side structure along the y-direction of the vessel local

coordinate system, less number of tanks are in risk of damage. The buoyance of the vessel can be guaranteed.

6.2 Reduce Damage via Structural Optimization

For the structural aspect, the vessel should be strengthened for the ice load or the iceberg impact. However, the philosophy of strengthening vessel for the ice load is very general. There are many ways to strengthen the hull structure for the ice load. Many authorities and classification societies have carried out regulations regarding the design of the hull structure for the ice load. But those regulations normally set some critical sizes for the structural elements. Detail design and construction can be very flexible.

From the results and analysis of previous sections, the goal of the optimized structure is to have no failure or little. Hence, the collision energy should be discrete but not concentrated in a small area to make failure happen. Either make large deformation failure or distributes the collision energy in a large area on the side structure can achieve the goal of preventing failure. Based on this philosophy of optimization, the author comes up with two solutions:

1) Using high strength and high elongation steel for the collision plate,

2) Have more stiffeners for the collision plate.

The model in case d) will be modified to suit the requirements of the two methods above.

Simulations will be implemented for those two methods. The results of the simulations can show the differences of those two ways. Comparison will be illustrated. The results of the two optimization alternatives will also be compared with case d).

6.2.1 Using Exchange Steel for the Collision Plate

6.2.1.1 General Introduction

Normally the high strength steel is considered to be a good choice to stiffen the structure. But the purpose of using high strength steel is to increase the resistance for the global bending moment or local high stress. The utilization of high strength is still designed following the linear mechanical performance of the steel. However, the plastic deformation is seldom taken consideration.

Sperle from SSAB reported that the high strength steel normally has a much lower failure elongation compared to the ordinary steel. For example, the Dogal 350 YP steel has a yield stress of 350MPa, tensile strength of 420MPa but with a failure elongation of 22% tested on a specimen with size of 80mm. The Docal 1200 DP steel has a yield stress of 1000MPa and tensile strength of 1200MPa, but the failure strain elongation on an 800mm specimen is only 4%. Assume failure strain happens when the stress reach the tensile strength stress. A simple bilinear strain-stress plot is showed.
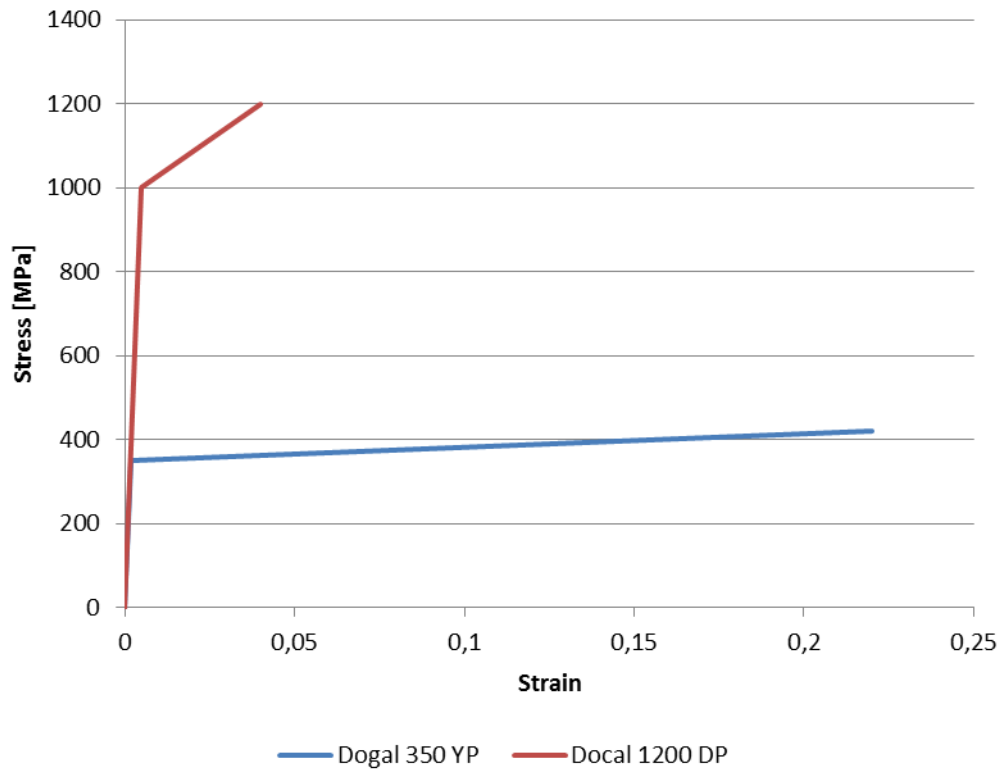
*Figure 6-1 Strain vs. Stress plot for Dogal 350 YP and Docal 1200 DP*

Sperle also indicates that the Young's Modulus for high strength steel and mild steel are the same. Therefore, before the yield stress both of them have the same linear elastic modulus.

Assume both Dogal 350 YP and Docal 1200 DP steels are tested on the specimen with the same size of 800mm. Therefore, when considering the energy they absorbed before failure. The Dogal 350 YP costs 67480MPa·mm energy to failure, but the high strength steel Docal 1200 DP only costs the energy of 32914MPa·mm. High strength steel needs less energy to get failure.

Under the collision scenario, there is a high possibility for the steel to have plastic deformation or even failure. Hence, to use a high strength but low elongation (failure strain) steel plate for the collision area is not a wise choice. As a consequence, high strength and high elongation steel is considered to be the optimum material choice for the plate located in the potential collision region.

In the automobile industry, the austenitic steel called Twinning-Induced Plasticity Steel (TWIP) is used for the door impact beam. Stuart Keeler and Menachem Kimchi (2014), indicates that TWIP steels have high strength with high stretchability also. That is the reason why TWIP steel is suitable for the door impact beam in automobiles.

Due to the advantage of the TWIP steels, TWIP can also be used to replace the NVA grade steel for the collision region on the vessel. However, only the plate for collision will have the material exchange. TWIP steels are very expensive. Even when the steel is used on the vessel, it can only be used for some certain regions.
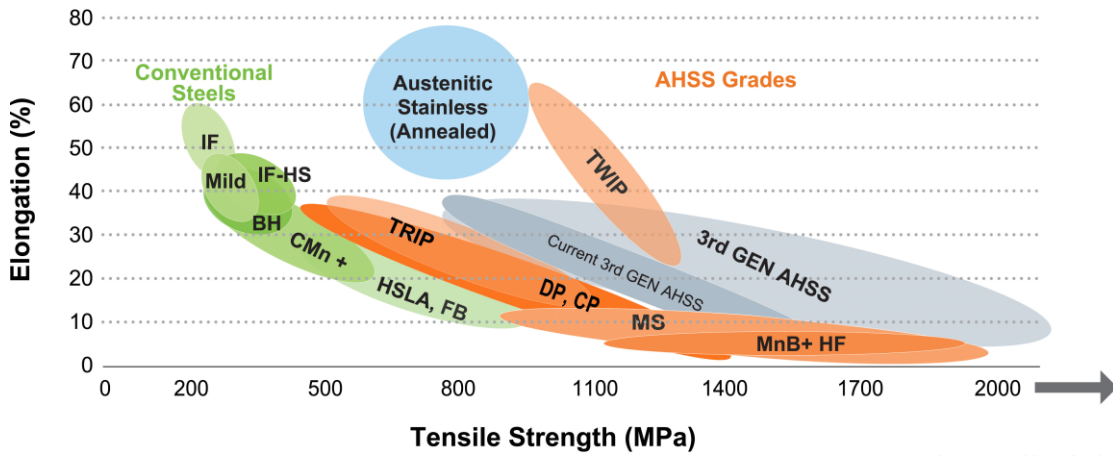
Figure 6-3 Range of properties available from Today's (Advanced High Strength Sheet Steel) AHSS grades steels, from Advanced High-Strength Steels Application Guidelines Version 5.0
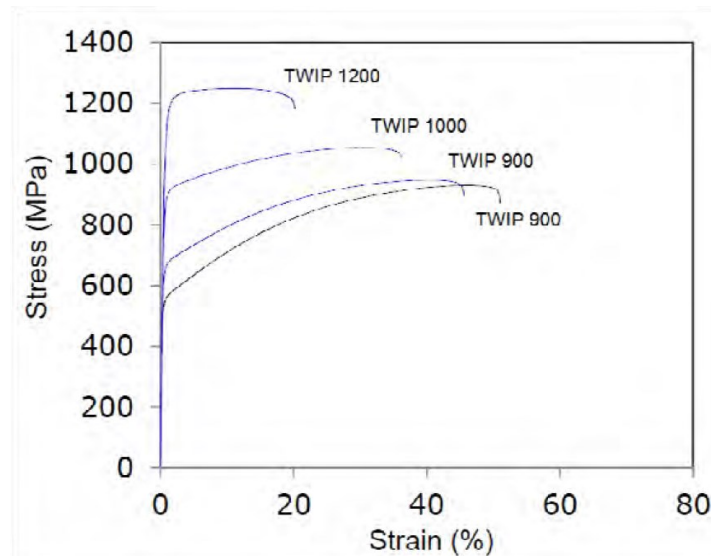
Figure 6-2 Engineering Stress-Strain Curve for TWIP

Figure 6-4 Door Impact Beam inside the Door of a Vehicle

In the FEM simulation, TWIP 1000 steel is used for replacing the collision plate on the side structure. Based on the data provided in the Advanced High- Strength Steels Application Guidelines, the data inputting of TWIP 1000 steel will be set as follows:

Yield stress is: 900MPa.

Tensile strength is: 1000MPa, and it is also set to be the stress at failure.

Failure criterion is: Maximum EPS= 0.35 for the element size of 100mm.

The TWIP replacement simulation will be named case m).

Figure 6-5 The plate in green color is replaced by TWIP 1000 steel

6.2.1.2 Results

From the results of the simulation, TWIP can reduce the damage caused by the collision. At least the iceberg cannot reach the inner side shell after the iceberg penetrates the outer plate. Similar to case d), the iceberg will be bounced by the side structure with a stable velocity of 0.27m/s along the pos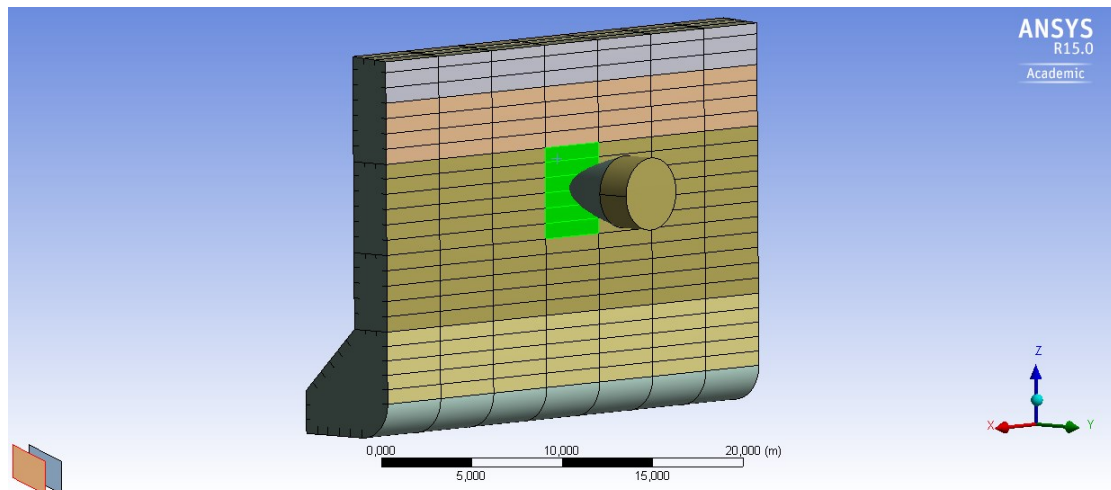itive Y-direction at the very end of the simulation. The detail results of the simulation are showed in the table below.

Table 6-1 Results of Case m) Optimization Solution: TWIP Steel

| Name	Value	Unit
Failure Area	0.45	m^2
Deformation Area (Where deformation on Y axis >=100mm)	20.89	m^2
Maximum deformation on Y axis	1354.8	mm
Plastic Strain Area (including Failure Area) where EPS> 0.05	7.48	m^2
Number of Damaged Stiffeners (EPS>0.05)	3	-
End Velocity of Iceberg	0.27	m/s
Kinetic Energy Lose for the Iceberg	4909.14	kJ
Kinetic Energy Lose in Percentage	98.18%	-
Time Span to be Simulated	3.5	s
Computation Time for Computer	928.54	min
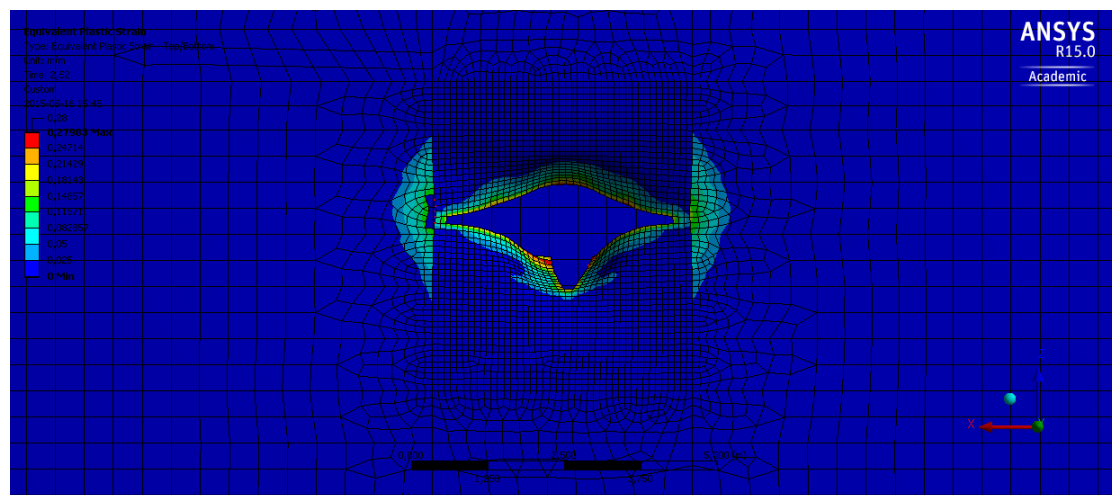
Figure 6-6 EPS illustration on the side structure after the collision with Case m) Optimization Solution: TWIP Steel

6.2.2 Have More Stiffeners on the Collision Plate

6.2.2.1 General Introduction

It is widely used in the ship construction that using more stiffeners to strengthen the plates. The stiffeners attached to the plates increase the moment of inertia for the entire plates plus stiffeners structure. And the attached stiffeners can also increase the distance for the plate to the neutral axis of the structure. When bending happens, the plates will take less stress.

Although from the global view the collision is not a bending issue, bending happens locally when the collision causing deformation on the plates. Therefore, it is considered to be an alternative to decrease the collision damage by locally increasing the moment of inertia (along the collision direction) of the collision region. And more collision energy will be discrete on the newly added stiffeners but less distributed on the plate.

The model in case d) will also be used to verify the solution. However, the number of stiffeners on the collision plate will be doubled. The size of the newly added stiffeners will be as same as the previous existing stiffeners. The other parts of the side structure of the vessel will not be changed and so will the other conditions.

It is reasonable to locally increase the stiffeners on the plates that will have the potential collision. Economy issue is one of the most important matters in shipbuilding process. The vessel cannot be strengthened unlimited but not considering the cost. And more stiffeners may also mean more weight. Generally, adding weight on the vessel is not a good choice in the design process. That is why the stiffeners should be added to the vessel locally.

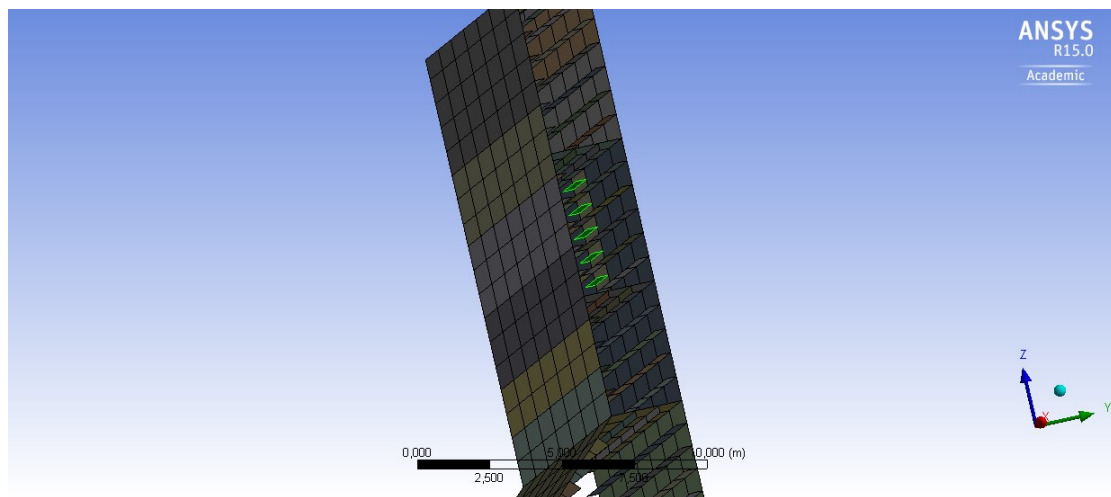The double stiffeners optimization will be named case n).

Figure 6-7 Stiffeners in green colors are newly added stiffeners to the potential collision plate

6.2.2.2 Results

By adding more stiffeners to the plate that will have potential collision, the collision damage will be reduced. The iceberg also has no chance to reach the inner side shell of the side structure. Similar to case d), the iceberg will be bounced by the side structure with a stable velocity of 0.23m/s along the positive Y-direction during the ending period of the simulation. The detail results of the simulation results are showed in the table below.

Table 6-2 Results of Case n) Optimization Solution: Double Stiffeners

| Name	Value	Unit
Failure Area	0.85	m²
Deformation Area (Where deformation on Y axis >=100mm)	21.25	m²
Maximum deformation on Y axis	1354.9	mm
Plastic Strain Area (including Failure Area) where EPS> 0.05	7.14	m²
Number of Damaged Stiffeners (EPS>0.05)	6	-
End Velocity of Iceberg	0.23	m/s
Kinetic Energy Lose for the Iceberg	4935,24	kJ
Kinetic Energy Lose in Percentage	98.70%	-
Time Span to be Simulated	3.5	s
Computation Time for Computer	1020.61	min
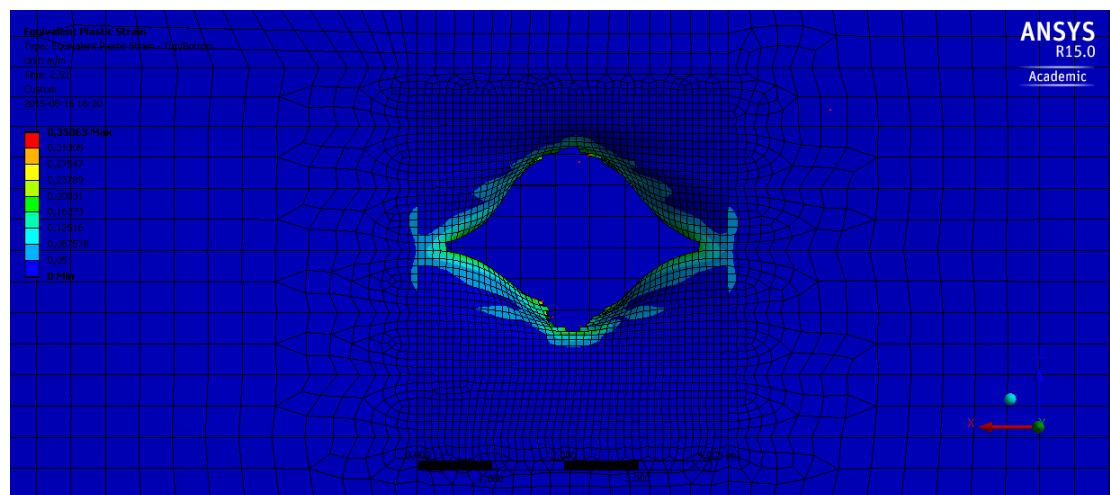
Figure 6-8 EPS illustration on the side structure after the collision with Case m) Optimization Solution: Double Stiffeners

6.2.3 Summary of the Structural Optimization

Since case m) and n) are the optimized solution for case d), a comparison will be listed for these three cases. And the advantages of the optimization solutions can be easily seen.

Table 6-3 Comparison of the Results for d) Bullet Shape 2 Iceberg, m) Optimization Solution: TWIP Steel and n) Optimization Solution: Double Stiffeners

Name	Value in d)	Value in m)	Value in n)	Unit
Failure Area	0.70	0.45	0.85	m^2
Deformation Area (Where deformation on Y axis >=100mm)	13.48	20.89	21.25	m^2
Maximum deformation on Y axis	1642.50	1354.8	1354.9	mm
Plastic Strain Area (including Failure Area) where EPS> 0.05	7.89	7.48	7.14	m^2
Plastic Strain on the inner side shell	YES	NO	NO	-
Number of Damaged Stiffeners (EPS>0.05)	4	3	6	-
End Velocity of Iceberg	0.34	0.27	0.23	m/s
Kinetic Energy Lose for the Iceberg	4852.57	4909.14	4935,24	kJ
Kinetic Energy Lose in Percentage	97.05%	98.18%	98.70%	-
Time Span to be Simulated	2.75	3.5	3.5	s
Computation Time for Computer	736.15	928.54	1020.61	min

From the comparison, it is easy to see that the both case m) and n) of the structural optimization solutions works well to reduce the damage of the collision. When comparing to case d), both of the optimization solutions can prevent the damage happens on the inner side shell of the side structure.

And the high strength plus high elongation steel (TWIP steel) solution can even have much smaller failure area. If the damage is levelled by the failure area, replacing the potential collision plate with TWIP steel is absolutely best alternative for the structural strengthening for the ice-ship collision. However, the welding issues of TWIP steel to NVA steels should be have more detail discussion. And TWIP is a kind of very expensive steel. The mass use of TWIP steel will increase the building cost a lot.

Actually in the shipbuilding industry, adding more stiffeners is a very common used way to strengthen the local structure. It is also not that so costly. And from the results in case n), it is also a good way to reduce collision damage. Hence, adding stiffeners is the most economical way to optimize the structure for the ice-ship collision or other collision situations. But the added stiffeners are located in the potential collision regions, the continuum of the structure may disturbed and it is easy for the stress concentration happens.
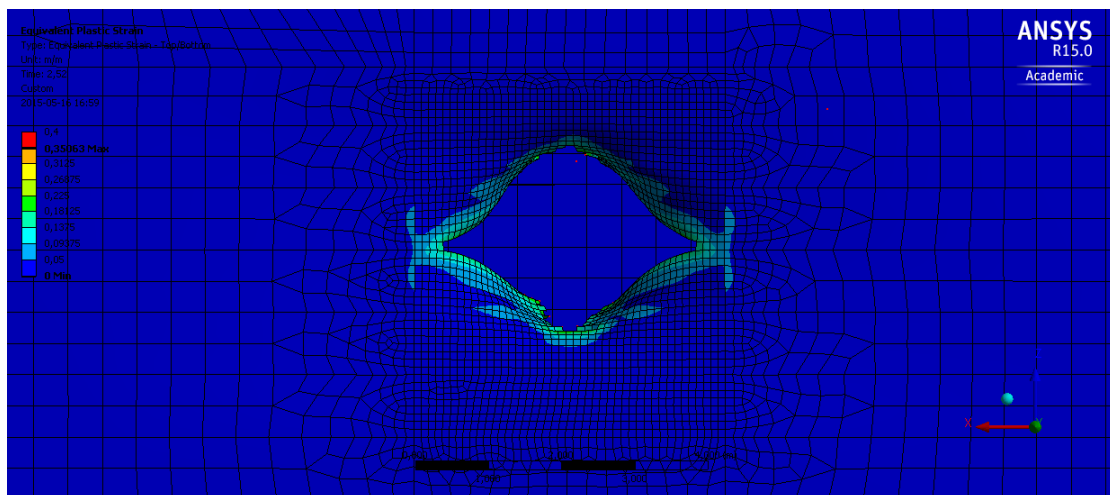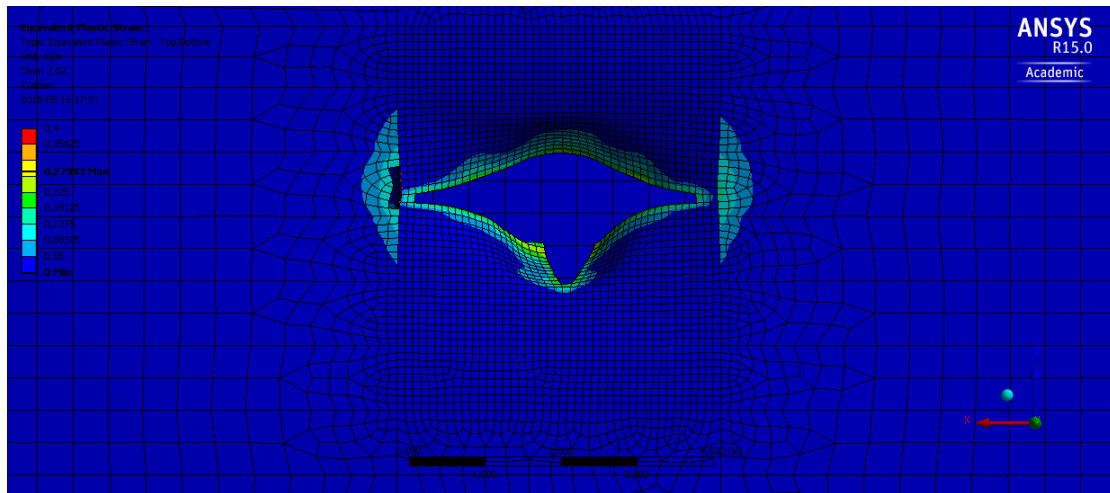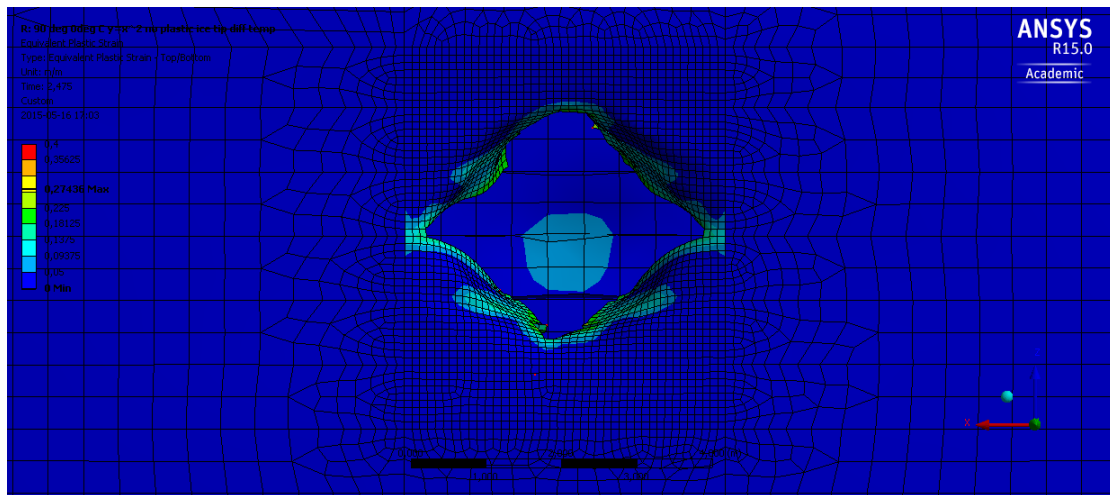
Figure 6-9 From top to the bottom are EPS illustrations in the same scale legend for case d), m) and n).

CHALMERS, *Shipping and Marine Technology*, Master's Thesis

7   Conclusion

The human beings need to explore new region with extreme climate condition. Arctic will be definitely the next front line for the energy or resource exploration. Sailing through the Arctic region is also considered possible in the summer due to the global warming. And it has been prove that sailing through Arctic will benefit a lot to the shipping between West Europe and East Asia. But the weather in the Arctic is extreme and the environment in the Arctic is also very vulnerable. In order to prevent the ice-ship collision accident happens, more sophisticated operation and structure are needed for the vessel.

The sailing and marine operations in the Arctic region may lead to great challenges to ship safety and environmental problems. Both the low temperature and ice load are the threats to the ship structures when operating in the region. The low temperature could lead to brittle metal ship structures which are easy to break, although the yield strength of the steel is higher in low temperature. The metal structures need less energy to be broken in low temperature. It means that the ship structures become vulnerable in the low temperature if the collision happens. While a ship's collision with floating ice or iceberg are always dangerous scenarios to challenge the ship's safety. Due to the large mass of the Arctic ice, the ice can have great inertia even with a very small speed. Hence, the collision energy is considered to be very huge when the ice hitting the vessel.

And during the collision, the tip shape of the iceberg is also critical when evaluating the damage of the collision. The results in *Section 5.2.1* illustrate that the sharper tip of the iceberg makes penetration easier, and then leads more severe damage to the structure itself. It is because the collision energy and forces will be concentrated on the sharper tips. The collision energy will be used efficiently to damage the structure. Like the sharp needle can even penetrate the metal sheet.

The break of the iceberg may also result in the secondary damage to the vessel after the collision happened. Ice is known as a brittle material. The break of the ice may also lead to sharp edges around the failure region. They can also cause further damages on the ship's side structure plates even the speed of the iceberg has been reduced during the collision.

The damage severity varies, if the collision happens in the low temperature region of the vessel (low temperature refers to -30°C in this thesis report). Normally it is the area above the water line for the vessel. If there is no damages on the plate, the side structure of the vessel is actually more stiffened to the collision. The equivalent plastic strain (EPS) is averagely smaller compared to the similar scenario happens at the underwater region. However, since the failure strain for the metal ship structures in lower temperature is smaller, iceberg with sharper tips may penetrate ship structures more easily due to the fact that the ship side structure plate can reach its failure strain easily. Consequently, more serious damage on the ship structures may happen.

It does not affect the collision results in the underwater area, if the temperature distribution has changed at the above water line region. It is a common sense that the temperature of ice water mixture is 0°C. Hence, the water temperature will be also

around 0°C in Arctic region. Since water has a very high specific heat capacity, the underwater outer shell of the vessel is also in temperature around 0°C. The mechanical performance of the DNV grade A (NVA) steel in 0°C can be applied to the underwater part of the outer shell regardless of the temperature at the above water area. The temperature change at the non-collision region does not affect the collision results happens on the underwater collision part.

The kinetic energy of the iceberg will mainly consume by four ways: 1) The plastic deformation of the steel, 2) Failure on the steel, 3) Friction due to the relative move of iceberg and vessels, 4) Failure of the iceberg. And the plastic deformation of steel during the collision consumes most energy for.

Based on the results of the collision analysis, the optimization aiming at safe arctic maritime activities is main carried out through operation and structure.

It is very important for the crew members to follow the navigation or sailing rules when having the Arctic sailings. Many regulations are often established based on the after-disaster analysis and set to prevent the similar tragedies. Sailing and operation in the Arctic should follow the corresponding regulations to avoid the ice-ship collision. Even when the collision cannot be avoided, trying to keep sharp iceberg away from the above waterline region can also reduce the damage.

Two ways have been used to optimize the structure: 1) Using high strength and elongation steel, 2) Strengthen the collision part with more stiffeners. Both of them can reduce the damage consequence in ice-ship collision phenomena.

Twinning-induced plasticity steel (TWIP) is considered to be the high strength and elongation steel for replacing the plate at the collision region. The simulation results have showed the replaced TWIP plate can have less failure area during the collision. However, twinning-induced plasticity steel is very expensive. It is not possible to mass use the material.

Adding more stiffeners to the collision part can also have a very good effect to reduce the collision damage. It is a more economical way to strengthen the structure. And in many regulations, to dense the arrangement of the stiffeners are claimed to be a strategy to build the ice belt for ice-ship collision. But the added stiffeners are located locally and may disturb the continuum of the structure. Therefore, it may be easier for the vessel structure to have more places with stress concentration effects.

8 Future Work

Many results and conclusions regarding the ice-ship collision in the Arctic region have been made in this thesis report. The mechanical performance, modelling, collision results and optimization solutions have been discussed in detail. But there is still many things can be continued and improved in the future work.

The failure criteria of the NVA grade steel

The maximum EPS is set to be the failure criteria of the NVA grade steel. And the maximum EPS of the NVA grade steel in this thesis report comes from the regression of empirical data. In order to make the simulation more accurate, the maximum EPS in different size of the NVA grade steel should be concluded from the experiment data. Hence, the material testing experiment can be carried out for more accurate failure criteria of the NVA grade steel.

The properties of ice

Since the properties of ice are too complicated, more investigation should be done to have the exact data of the mechanical properties of ice. It is more practical to have the ice data from the sailing or operation regions. Ice in some certain region is believed to have similar properties. Otherwise it will be too hard to give the exact data of ice. However, many experiments are needed to support the data.

The model can be in more details

In this thesis report, the model of the side structure has been simplified. If some hot spots need to be investigated, the model can be built in detail. Moreover, the boundary conditions and loading conditions can also be assigned to some local models. But the types of the elements can be kept the same.

Strain rate sensitivity

Mare Meyers and Krishan Chawla (2009) point out that many materials, especially steels, are sensitive to the strain rate. For different strain rate, the same material will have different strain vs. stress curves. Usually the flow stress will increase with the strain rate. And the failure strain will be lower when the material has higher strain rate.

Due to the limitation of the solver, ANSYS Workbench Explicit does not contain the influence of the strain rate sensitivity. The explicit method takes the strain rate into calculation in order to update the density of the element and the displacement of the vertexes. But the strain vs. stress curve is not changed based on the updated strain rate. The same situation happens to the failure strain.

It is highly expected that more sophisticated explicit solver can be introduced to take the strain sensitivity into consideration.

Collision experiments in practice is needed

This thesis report mainly concerns about the collision simulations by FEA. Actually, there are many differences between the simulation and reality. Although the current simulation solvers for collisions can perform the process and results exactly, full scale experiments are still needed to verify or update the simulation results.
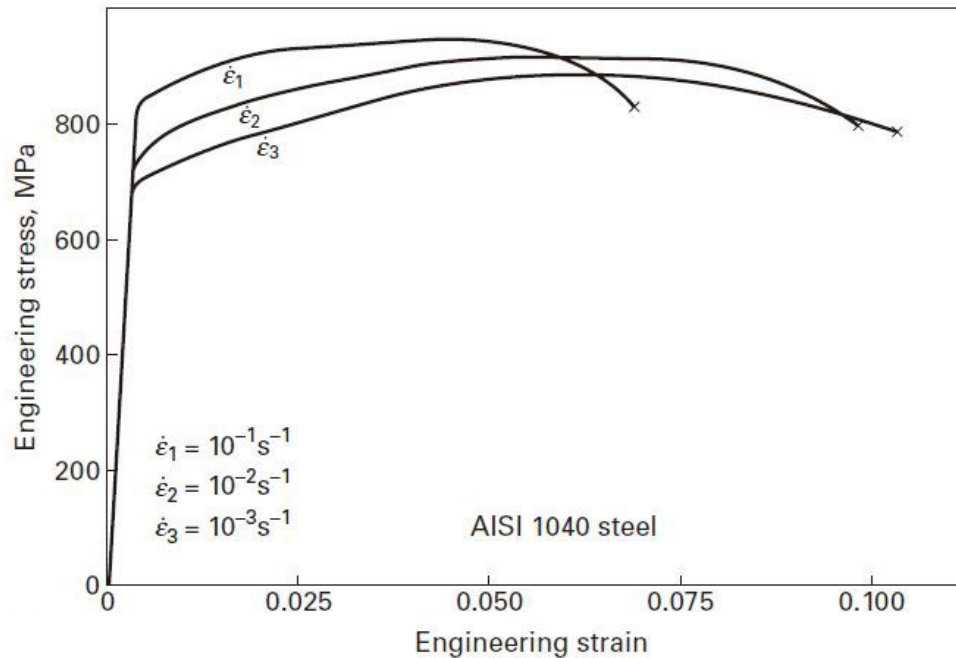

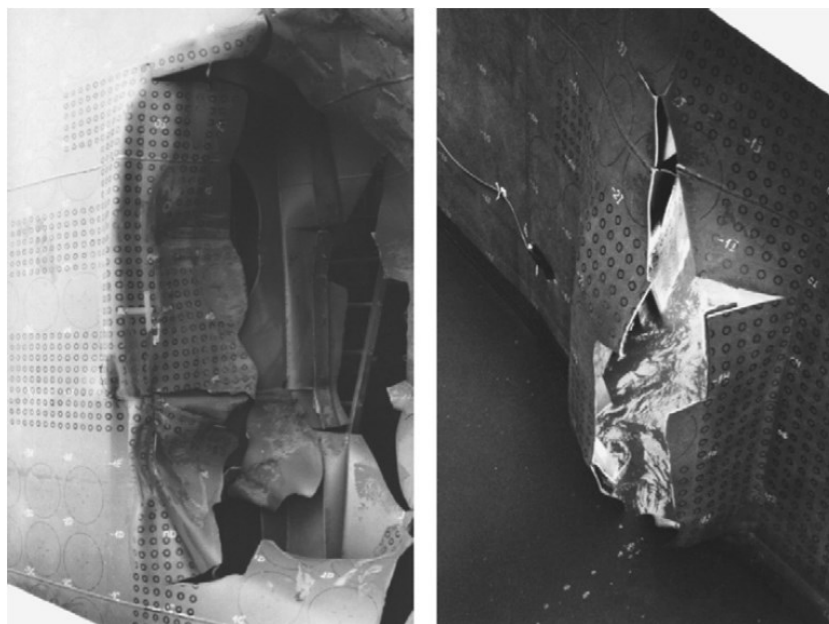*Figure 8-1 Strain rate sensitivity of AISI 1040 steel, from Mare Meyers and Krishan Chawla (2009)*

Figure 8-2The results of the collision experiment on a double hull structure, from Wolf (2003)

9 Reference

ANSYS, Inc. (2013). *ANSYS 15.0 Help Viewer*. ANSYS, Inc.

Baumans, P., Bøe, Å. (2012). *CSR Harmonisation-Direct Strength Analysis*. International Association of Classification Society.

Courant, R., Friedrich, K., Lwey, H., (1967). *On the partial difference equations of mathmatical physics*. IMB journal of Research and Development, 11(2), 215-234.

DNV. (2012). *DNV Rules for Ships*. Part 8 Chapter 1.

DNV. (2012). *Metallic Materials*. In: Offshore Standard: DNV, pp. 17

DNV GL. *Arctic- the next risk frontier*. Retrieved from DNV GL: https://www.dnvgl.com/technology-innovation/broader-view/arctic/the-arctic-risk-picture.html

Ehlers, S., & Østby, E. (2012). *Increased crashworthiness due to arctic conditions-The influence of sub-zero temperature*. Marine Structure(28), pp. 86-100.

Gold, L. W. (1988). *On the elasticity of ice plates.* Canadian Journal of Civil Engineering, 15(6), 1080-1084.

Haynes, F. (1978). *Effect of Temperature on the Strength of Snow-Ice. Hanover*, New Hampshire, USA: Department of the Army, Cold Regions Research and Engineering Laboratory, Corps of Engineers.

IACS. (2011). *Requirements conderning Polar Class*. International Association of Classification Societies.

Lin, M. W., Abatan, A. O. (1994). *Application of Commercial Finite Codes for the the Analysis of Induced Strain-Actuated Structures*. Intelligent Material Systems and Structures, 5(6), 869-875.

Liu, Z., Amdahl, J., Løset, S., (2010). Plasticity based material modelling of ice and its application to ship-iceberg impacts. *Cold Regions Science and Technology*, 65, 326-334.

Liu, Z. (2011). *Analytical and numerical analysis of iceberg collisions with ship structures*. Trondhiem, Norway: Norwegian Unviersity of Science and Technology.

Meyer, M., & Chawla, K. (2009). *Mechanical Behavior of Materials* [Second Edition]. Cambridge: Cambridge University Press.

Hogström, P., Ringsberg, J. W., Johnson, E., (2009). *Experimental verification of finite element failure criteria with respect to strain state and element size.* Twelfth International Conference on Fracture. Ottawa, Canada.

Petrovic, J. (2003). *Review-Mechanical properties of ice and snow.* Journal of Materials Science(38), 1-6.

Pett, A. (2011). *Introduction to Explicit Dynamics Using ANSYS Workbench*. Horsham, UK: ANSYS, Inc.

Sanderson, T. J. (1988). *Ice mechanics: risks to offshore structures.* London: Graham & Trotman.

Schulson, E. (2001). *Brittle Failure of Ice*. Engineering Fracture Mechanics(68), 1839-1887.

Sperle, J. O. *High Strength Sheet and Plate Steels for Optimum Strucutural Performance*. Borlänge, Sweden: SSAB Tunnplåt AB.

Keeler, S. & Kimchi, M. (2014). *Advanced High-Strength Steels Application Guidelines Version 5.0*. WorldAutoSteel.

The Engineering ToolBox. (2015). *Friction and Coefficients of Friction*. Retrieved April 25, 2015, from http://www.engineeringtoolbox.com/friction-coefficients-d_778.html

The Engineering ToolBox. (2015). *Thermal Conductivity of Metals*. Retrieved April 21, 2015, from http://www.engineeringtoolbox.com/thermal-conductivity-metals-d_858.html

Nelson, T. & Wang, E. (2004). *Reliable FE-Modeling with ANSYS*. Proceedings of the International ANSYS Conference. Munich.

U.S. Geological Survey. (2008, July 23). *90 Billiion Barrels of Oil and 1,670 Trillion Cubic Feet of Natural Gas Assessed in the Arctic.* Retrieved from USGS: http://www.usgs.gov/newsroom/article.asp?ID=1980#.VVsXFk377AU

Western Washington University. (2009, 4 17). *Thermal Expansion.* Retrieved from http://web.archive.org/web/20090417003154/http://www.ac.wwu.edu/~vawter/PhysicsNet/Topics/Thermal/ThermExpan.html

Wolf, M. (2003). *Full scale collision experiment,* X-type Sandwich side hull. EU Sandwich Project Report.

Yamada, Y., Endo, H., Pedersen, P. T., (2005). *Numerical Study on the Effect of Buffer Bow Structure in Ship-to-ship Collisions.* 15th International Offshore and Polar Engineering Conference. Seoul, Korea: Inernation Society of Offshore and Polar Engineers (ISOPE).

Zelko, F. (2013). M*ake It a Green Peace!-The Rise of Countercultural Environmentalism.* New York: Oxford University Press.

Appendix A: Detail Information of the Side Structure

Figure A-1 Midship section scantling

Table A-0-1 The profile data of the stiffeners

Number	Type	Dimensions in mm
Outer Shell		
1-23	Tbar	445*150*12*20
26-30	Tbar	420*150*12*20
32-35	Tbar	370*150*12*20
37-41	Tbar	370*125*12*20
43-45	Jap_L	350*100*12*17
46-48	Jap_L	350*100*12*17
25-24	Jap_L	300*90*13*18
22-1	Jap_L	400*100*13*18
Inner Bottom & Inner Side		
1-17	Tbar	420*150*12*20
26-30	Tbar	470*150*12*20
32-35	Tbar	370*150*12*20
37-41	Tbar	370*125*12*20
43-46	Jap_L	350*100*12*17
47-48	Jap_L	350*100*12*17
Bottom Girder 15300		
1-2	Jap_L	250*90*12*16
CL Bulkhead		
1-2	Jap_L	400*100*13*18
28-32	Tbar	370*150*12*20
33-38	Tbar	368*125*12*18
39-45	Tbar	343*125*12*18
46-49	Jap_L	350*100*12*17
Stringer 6000		
2-1	Jap_L	250*90*10*15
Stringer 10250		
2-1	Fbar	250*15
Stringer 15350		
2-1	Fbar	250*15

Table A-0-2 The exchange from T-bars to flat bars

APPLY TO OUTER SHELL PROFILE 26-30, INNER SIDE PROFILE 26-30					
T-bar 420*150*12*20				**Substitution of a flat bar**	
Name	**Symbol**	**Value**	**Unit**	**Value**	**Unit**
Height	H	420	mm	420	mm
Width	B	150	mm	0	mm
Thickness of the web	b	12	mm	24	mm
Thickness of the flange	t	20	mm	0	mm
Height of the web	h	400	mm	0	mm
Area	A	78,0	cm^2	100,8	cm^2
Position of Centroid to top	y_1	139,2	mm	210,0	mm
Position of Centroid	y_2	280,8	mm	210,0	mm
Moment of Inertia to x-x	I_{xx}	14551,538	cm^4	14817,600	cm^4
Difference between moment of inertia *(I_{xx}_flat bar- I_{xx}_ T-bar)/I_{xx}_flat bar*100%*					1,83%

APPLY TO OUTER SHELL PROFILE 32-35, INNER SIDE PROFILE 32-35					
T-bar 370*150*12*20				**Substitution of a flat bar**	
Name	**Symbol**	**Value**	**Unit**	**Value**	**Unit**
Height	H	370	mm	370	mm
Width	B	150	mm	0	mm
Thickness of the web	b	12	mm	24	mm
Thickness of the flange	t	20	mm	0	mm
Height of the web	h	350	mm	0	mm
Area	A	72,0	cm^2	88,8	cm^2
Position of Centroid to top	y_1	117,9	mm	185,0	mm
Position of Centroid	y_2	252,1	mm	185,0	mm
Moment of Inertia to x-x	I_{xx}	10286,875	cm^4	10130,600	cm^4
Difference between moment of inertia *(I_{xx}_flat bar- I_{xx}_ T-bar)/I_{xx}_flat bar*100%*					-1,52%

T-bar 370*125*12*20				Substitution of a flat bar	
Name	Symbol	Value	Unit	Value	Unit
Height	H	370	mm	370	mm
Width	B	125	mm	0	mm
Thickness of the web	b	12	mm	24	mm
Thickness of the flange	t	20	mm	0	mm
Height of the web	h	350	mm	0	mm
Area	A	67,0	cm^2	88,8	cm^2
Position of Centroid to top	y_1	126,0	mm	185,0	mm
Position of Centroid	y_2	244,0	mm	185,0	mm
Moment of Inertia to x-x	I_{xx}	9659,453	cm^4	10130,600	cm^4
Difference between moment of inertia $(I_{xx}$ flat bar- I_{xx}_T-bar)/I_{xx}_flat bar*100%					4,88%

APPLY TO BULK PROFILE 26-30

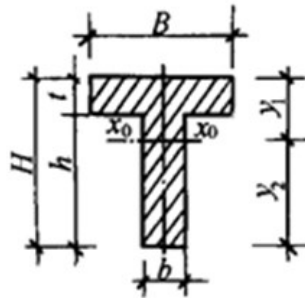| T-bar 470*150*12*20				Substitution of a flat bar	
Name	Symbol	Value	Unit	Value	Unit
Height	H	470	mm	470	mm
Width	B	150	mm	0	mm
Thickness of the web	b	12	mm	23	mm
Thickness of the flange	t	20	mm	0	mm
Height of the web	h	450	mm	0	mm
Area	A	72,0	cm^2	88,8	cm^2
Position of Centroid to top	y_1	117,9	mm	185,0	mm
Position of Centroid	y_2	252,1	mm	185,0	mm
Moment of Inertia to x-x	I_{xx}	10286,875	cm^4	10130,600	cm^4
Difference between moment of inertia $(I_{xx}$ flat bar- I_{xx}_T-bar)/I_{xx}_flat bar*100%					0,64%

Figure A-2 Illustration of the dimension of the T-bar

Table A-0-3 The exchange from L-bars to flat bars

APPLY TO OUTER SHELL PROFILE 43-48, INNER SIDE PROFILE 43-48					
L-bar 350*100*12*17				**Substitution of a flat bar**	
Name	**Symbol**	**Value**	**Unit**	**Value**	**Unit**
Height	H	350	mm	350	mm
Width	B	100	mm	0	mm
Thickness of the web	b	12	mm	20	mm
Thickness of the flange	t	17	mm	0	mm
Height of the web	h	333	mm	0	mm
Area	A	57,0	cm^2	70,0	cm^2
Position of Centroid to top	y_1	218,7	mm	175,0	mm
Position of Centroid	y_2	131,3	mm	175,0	mm
Moment of Inertia to x-x	I_{xx}	7349,116	cm^4	7145,833	cm^4
Difference between moment of inertia *(Ixx_flat bar- Ixx_L-bar)/Ixx_flat bar*100%*					-2,77%

APPLY TO DECK PROFILE 24-25					
L-bar 300*90*13*17				**Substitution of a flat bar**	
Name	**Symbol**	**Value**	**Unit**	**Value**	**Unit**
Height	H	300	mm	300	mm
Width	B	90	mm	0	mm
Thickness of the web	b	13	mm	22	mm
Thickness of the flange	t	17	mm	0	mm
Height of the web	h	283	mm	0	mm
Area	A	52,09	cm^2	66	cm^2
Position of Centroid to top	y_1	185,558	mm	150	mm
Position of Centroid	y_2	114,442	mm	150	mm
Moment of Inertia to x-x	I_{xx}	4890,441	cm^4	4950,000	cm^4
Difference between moment of inertia *(Ixx_flat bar- Ixx_L-bar)/Ixx_flat bar*100%*					1,22%
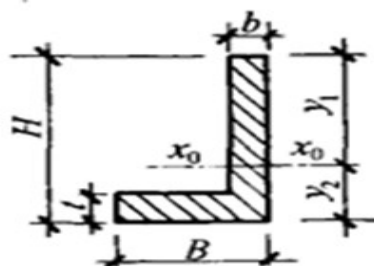
Figure A-3 Illustration of the dimension of the L-bar

APPLY TO BOTTOM GIRDER 15300   1-2

Name	Symbol	Value	Unit	Value	Unit
L-bar 250*90*12*16				**Substitution of a flat bar**	
Height	H	250	mm	250	mm
Width	B	90	mm	0	mm
Thickness of the web	b	12	mm	22	mm
Thickness of the flange	t	16	mm	0	mm
Height of the web	h	234	mm	0	mm
Area	A	42,48	cm^2	55	cm^2
Position of Centroid to top	y_1	159,373	mm	125	mm
Position of Centroid	y_2	90,627	mm	125	mm
Moment of Inertia to x-x	I_{xx}	2771,651	cm^4	2864,583	cm^4
Difference between moment of inertia $(I_{xx}\_flat\ bar - I_{xx}\_L\text{-}bar)/I_{xx}\_flat\ bar*100\%$					3,35%

APPLY TO STRINGER 6000   1-2

Name	Symbol	Value	Unit	Value	Unit
L-bar 250*90*12*15				**Substitution of a flat bar**	
Height	H	250	mm	250	mm
Width	B	90	mm	0	mm
Thickness of the web	b	10	mm	18	mm
Thickness of the flange	t	15	mm	0	mm
Height of the web	h	235	mm	0	mm
Area	A	37	cm^2	45	cm^2
Position of Centroid to top	y_1	163,108	mm	125	mm
Position of Centroid	y_2	86,892	mm	125	mm
Moment of Inertia to x-x	I_{xx}	2423,759	cm^4	2343,750	cm^4
Difference between moment of inertia $(I_{xx}\_flat\ bar - I_{xx}\_L\text{-}bar)/I_{xx}\_flat\ bar*100\%$					-3,30%

Appendix B: Detail Collision Results

Exclude the simulations for the optimizations, there are 12 cases are simulated in this thesis report to have a detail investigate to the ice-ship collision in the Arctic region.

The 12 cases are:

Category 1: Collision Sensitivity Check of Iceberg Shapes

a) Cubic shape iceberg,

b) Half sphere iceberg,

c) Bullet Shape 1 Iceberg,

d) Bullet Shape 2 Iceberg

Category 2: Failure Criteria Assigned to the Ice

e) Bullet Shape 1 Iceberg with Failure Criteria,

f) Bullet Shape 2 Iceberg with Failure Criteria,

Category 3: The Iceberg Hit above Water Region (Low Temperature Region)

g) Bullet Shape 1 Iceberg Hits above Region,

h) Bullet Shape 2 Iceberg Hits above Region,

i) Bullet Shape 1 Iceberg Hits above Region with Failure Criteria,

j) Bullet Shape 2 Iceberg Hits above Region with Failure Criteria.

Category 4: Change the Temperature Distribution on the above Water Region

k) Bullet Shape 2 Iceberg Hitting with above Waterline Temperature is 0°C

l) Bullet Shape 2 Iceberg Hitting with above Waterline Temperature is -30°C

And the detail results of the collision simulations are illustrated as below:

a) Cubic Shape Iceberg

It is expected that cubic ice has the lowest possibility to make the failure on the hit plate. And the result also meets the expectation.

The iceberg hit the plate with the initial speed of 2m/s. And after the collision the iceberg bounces back with a lower speed of 0.989m/s at the very end of the simulation.

There is no failure happened on the hit plate. The plastic strain happens on the area where the corners of the iceberg hit the plate. All the plastic strain is under the EPS (Equivalent Plastic Strain) of 0.05.

Table B-0-1 The collision result with a) Cubic shape iceberg

Name	Value	Unit
Failure Area	0	m²
Deformation Area (Where deformation on Y axis >=100mm)	41.56	m²
Maximum deformation on Y axis	256.32	mm
Plastic Strain Area (including Failure Area) where EPS> 0.05	0	m²
Number of Damaged Stiffeners (EPS>0.05)	0	-
End Velocity of Iceberg	0.99	m/s
Kinetic Energy Lose for the Iceberg	3777.84	kJ
Kinetic Energy Lose for the Iceberg in Percentage	75.56%	
Time Span to be Simulated	1.25	s
Computation Time for Computer	367.46	min
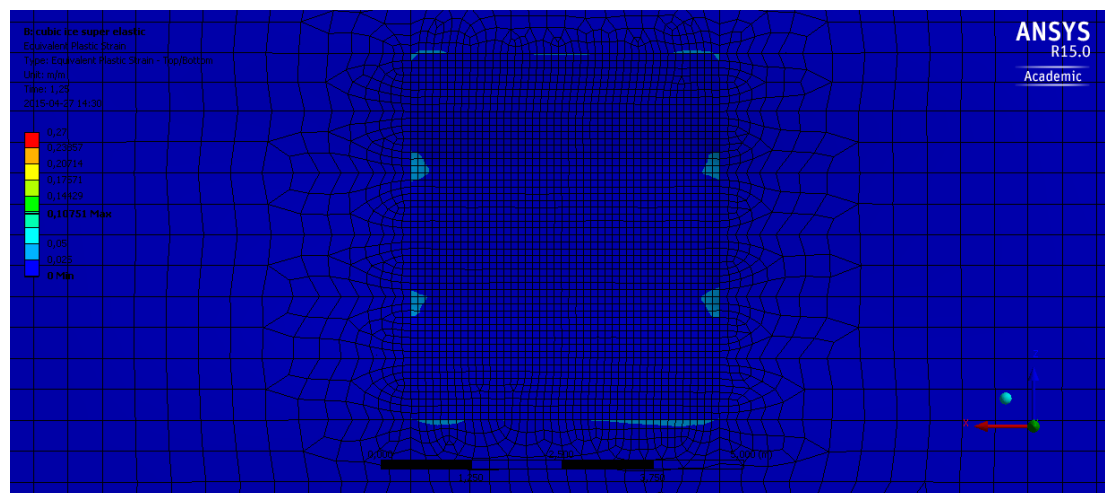
Figure B-1 EPS illustration on the side structure after the collision with a) Cubic shape iceberg

b) Half Sphere Iceberg

Compared to the collision caused by the cubic iceberg, the half sphere shape iceberg can have more serious damage. The shape of sphere is much 'shaper'.

The iceberg hit the plate with the initial speed of 2m/s. And after the collision the iceberg bounces back with a lower speed of 0.67m/s.

But still there is no failure happened on the hit plate. But the plastic strain with EPS>0.05 occurs. And some stiffeners also have the EPS>0.05.

Table B-0-2 The collision result with b) Half sphere iceberg

| Name	Value	Unit
Failure Area	0	m^2
Deformation Area (Where deformation on Y axis >=100mm)	29.91	m^2
Maximum deformation on Y axis	836.53	mm
Plastic Strain Area (including Failure Area) where EPS> 0.05	13.60	m^2
Number of Damaged Stiffeners (EPS>0.05)	3	-
End Velocity of Iceberg	0.67	m/s
Kinetic Energy Lose for the Iceberg	4443.27	kJ
Kinetic Energy Lose for the Iceberg in Percentage	88.87	-
Time Span to be Simulated	1.25	s
Computation Time for Computer	332.79	min
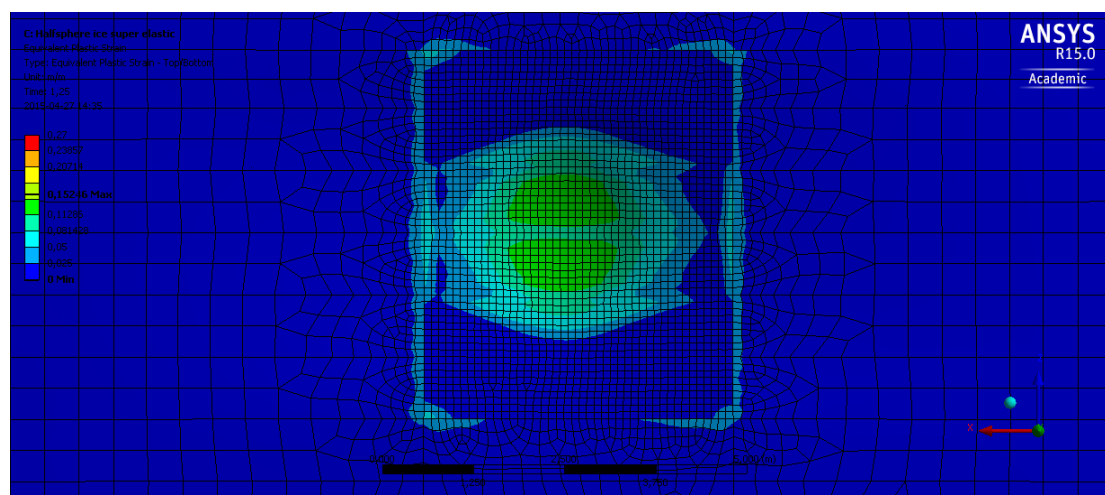
Figure B-2 EPS illustration on the side structure after the collision with b) Half sphere iceberg

c) Bullet Shape 1 Iceberg

It is a shape with the curvature of 1m^{-1} at the tip. And the penetration scenario happens in this case. The iceberg will penetrate the plate on the outside and failure happens on the plate.

But in the end the iceberg will also bounce back due to the stiffness of the side structure. The iceberg hit the plate with the initial speed of 2m/s. And after the collision the iceberg bounces back with a lower stable speed of 0.30m/s in the positive Y direction at the very end of the simulation.

Table B-0-3 The collision result with c) Bullet shape 1 iceberg

| Name	Value	Unit
Failure Area	0.35	m^2
Deformation Area (Where deformation on Y axis >=100mm)	25.48	m^2
Maximum deformation on Y axis	1709.40	mm
Plastic Strain Area (including Failure Area) where EPS> 0.05	6.36	m^2
Number of Damaged Stiffeners (EPS>0.05)	3	-
End Velocity of Iceberg	0.30	m/s
Kinetic Energy Lose for the Iceberg	4888.96	kJ
Kinetic Energy Lose in Percentage	97.78%	-
Time Span to be Simulated	3.5	s
Computation Time for Computer	767.38	min
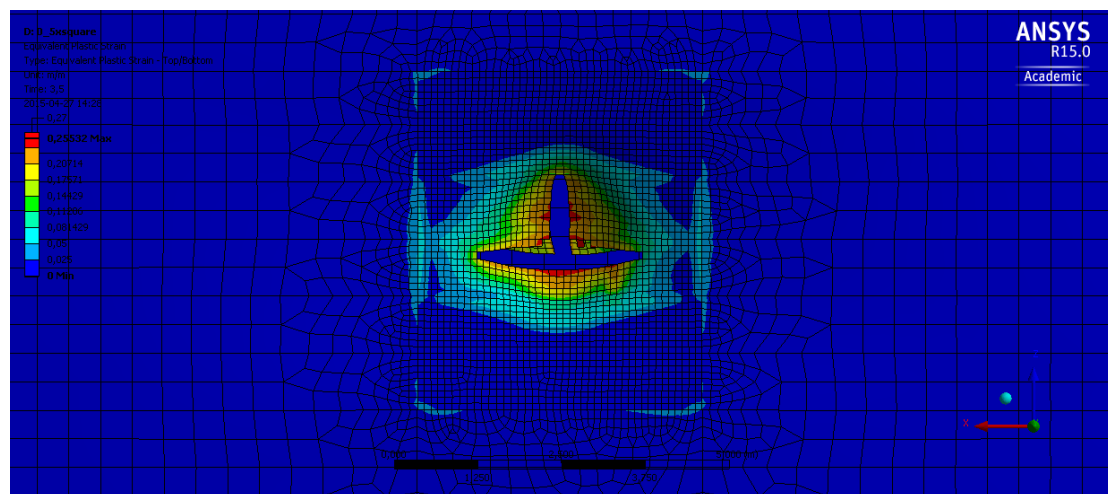
Figure B-3 EPS illustration on the side structure after the collision with c) Bullet shape 1 iceberg

d) Bullet shape 2 iceberg

This is an iceberg shape with an increasing curvature on the tip with the value of $2m^{-1}$. The iceberg penetrates the hit plate. Failure scenario is more serious in this case. That is to say the hole made by iceberg penetration is much bigger. The tip of the iceberg reaches the inner side of the side structure and caused plastic strain.

Still due to the stiffness of the side structure, the iceberg also bounces back. The initial speed of the iceberg is 2m/s. After the collision, the iceberg bounces back with a lower speed of 0.34m/s.

Table B-0-4 The collision result with d) Bullet shape 2 iceberg

Name	Value	Unit
Failure Area	0.70	m²
Deformation Area (Where deformation on Y axis >=100mm)	13.48	m²
Maximum deformation on Y axis	1642.50	mm
Plastic Strain Area (including Failure Area) where EPS> 0.05	7.89	m²
Number of Damaged Stiffeners (EPS>0.05)	4	-
End Velocity of Iceberg	0.34	m/s
Kinetic Energy Lose for the Iceberg	4852.57	kJ
Kinetic Energy Lose in Percentage	97.05%	-
Time Span to be Simulated	2.75	s
Computation Time for Computer	736.15	min
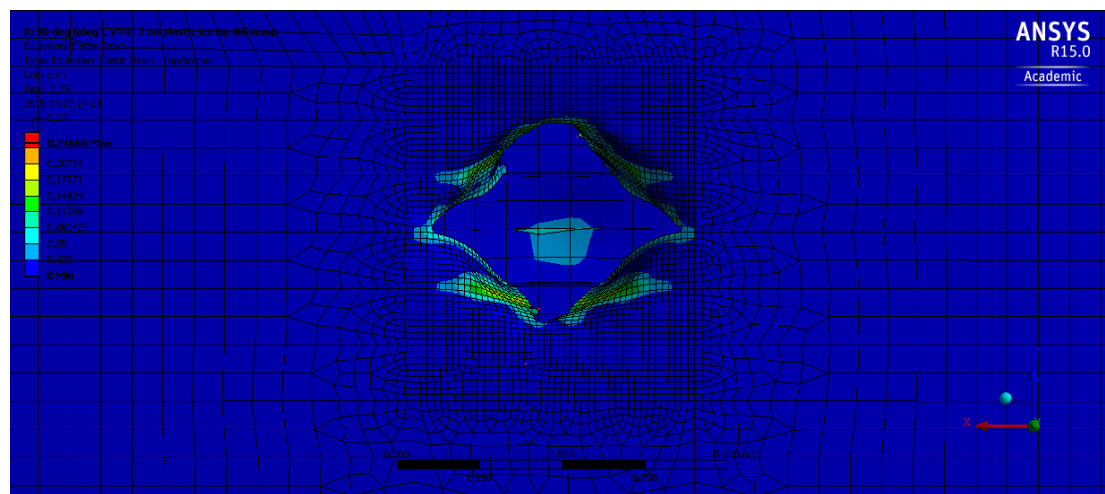
Figure B-4 EPS illustration on the side structure after the collision with d) Bullet shape 2 iceberg

e) Bullet Shape 1 Iceberg with Failure Criteria

After the failure criteria assigned to the ice, the iceberg can still make failure happens on the plate of the side structure. However, the tip of the iceberg will have the failure also.

It can be understood and more like the practical situation. In the practical situations, the ice will crack after the collision with steel structure such as vessels. And the failure of the ice is distributed about 0.75m along the Y direction from the tip.

Also due to the stiffness of the side structure, the iceberg bounces back. In the end the iceberg will move at a stable velocity of 0.33m/s in the positive Y direction.

Table B-0-5 Collision Result for e) Bullet Shape 1 Iceberg with Failure Criteria

Name	Value	Unit
Failure Area	0.49	m²
Deformation Area (Where deformation on Y axis >=100mm)	22.04	m²
Maximum deformation on Y axis	1155.60	mm
Plastic Strain Area (including Failure Area) where EPS> 0.05	6.46	m²
Number of Damaged Stiffeners (EPS>0.05)	3	-
End Velocity of Iceberg	0.33	m/s
Kinetic Energy Lose for the Iceberg	4863.83	kJ
Kinetic Energy Lose in Percentage	97.28%	-
Time Span to be Simulated	3.5	s
Computation Time for Computer	791.31	min
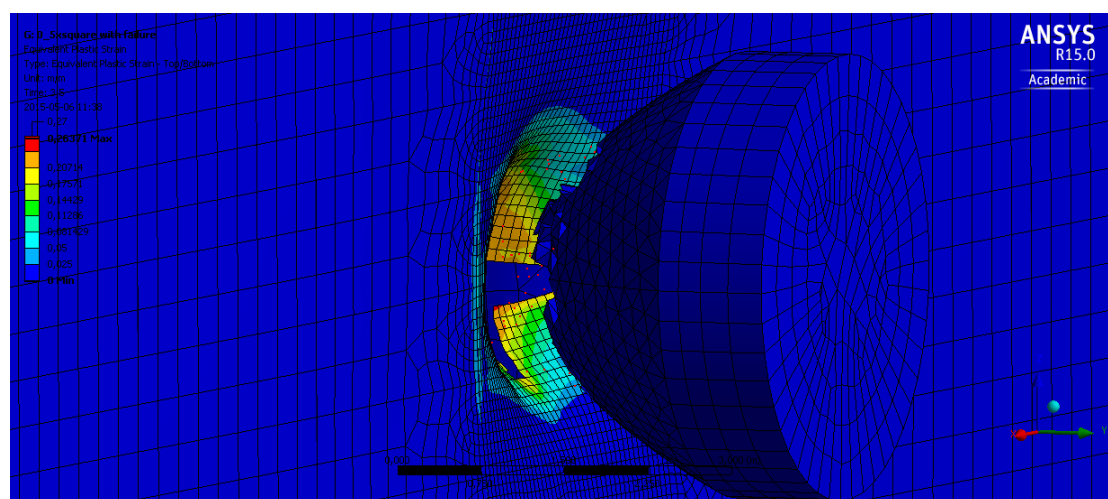
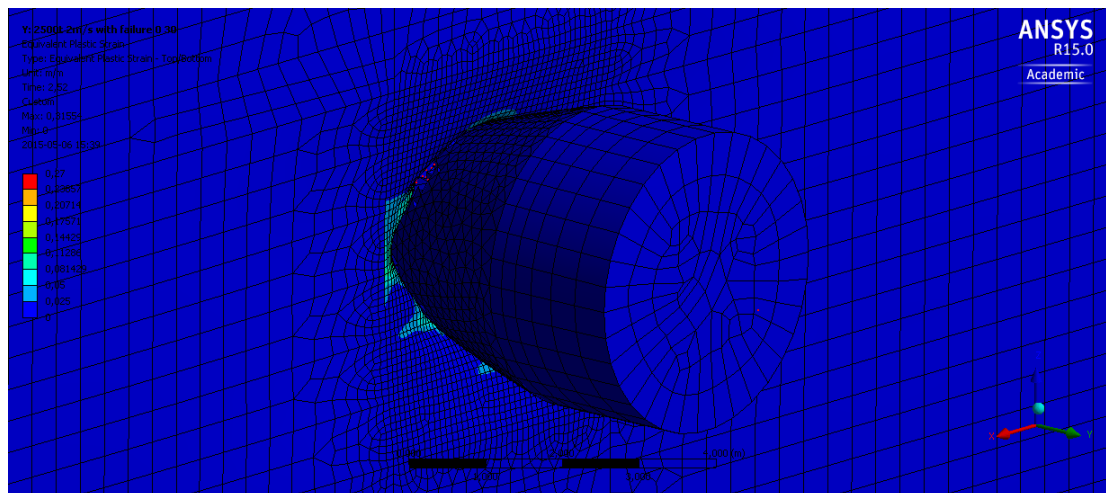*Figure B-5 The scenario after collision of e) Bullet Shape 1 Iceberg with Failure Criteria at 3.5s*
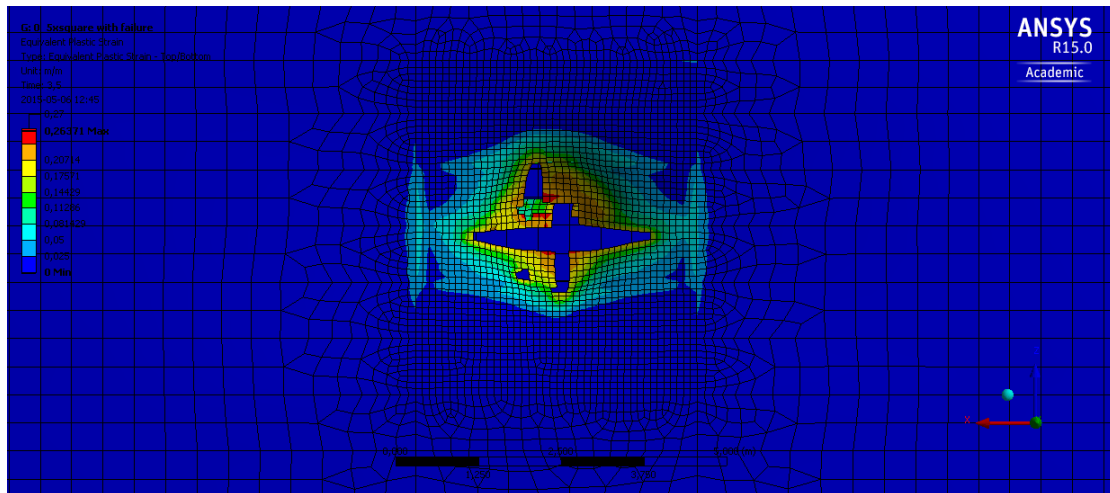
Figure B-6 EPS illustration on the side structure after the collision with e) Bullet Shape 1 Iceberg with failure criteria

The failure area in case e) is relatively larger compared to the case c) Bullet Shape 1 Iceberg without failure criteria on the ice tip. Moreover, the failure area is not continuous. There is a smaller failure area beside the main failure region.

After the iceberg failure happens in some part of the iceberg, the failed elements will be 'taken away'. Normally, they are elements at the tip. But the rest iceberg will have a coarse new front. Since the elements formed the ice tip are generally in tetrahedral or pyramid shape, the vertexes of the elements will be sharp. It is easier for them to destroy the plate. Moreover, the failure area will also be random since the failure happens on the ice tip is irregular.

However, the failure happens on the iceberg tip and the interaction on the plate of the side structure are in practical. Since the ice is known to be fragile and brittle, it is high possibility for the ice to have sharp edges after collision. And the sharp edges distributed quite randomly inside the collision region. Therefore, there is a chance for the sharp edges to cut the plate.
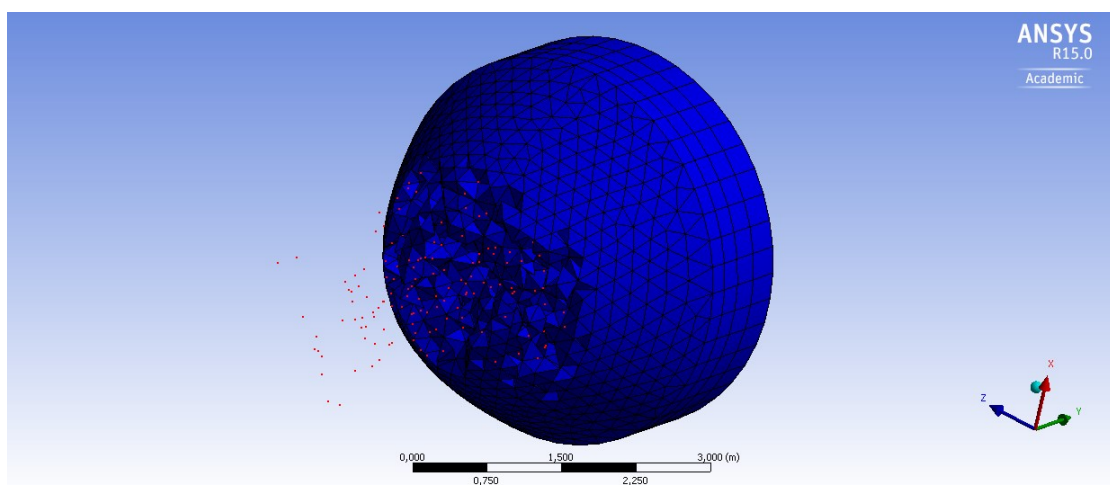
Figure B-7 Coarse front of the broken iceberg after collision in e) Bullet Shape 1 Iceberg with Failure Criteria at 3.5s

f) Bullet Shape 2 Iceberg with Failure Criteria

After the failure criteria have been assigned to the case d), the fragile iceberg can still penetrate the plate of the side structure. Failure happens on both the plate of the side structure and the iceberg.

Similar as the case e), the failure area on the plate of the side structure is not continuous. It is believed to be the same reasons, which has been clarified in the case e).

Also due to the stiffness of the side structure, the iceberg bounces back with a stable velocity of 0.16m/s along the Y positive direction at the very end of the simulation process.

Table B-0-6 Collision Result for f) Bullet Shape 2 Iceberg with Failure Criteria

Name	Value	Unit
Failure Area	1.04	m²
Deformation Area (Where deformation on Y axis >=100mm)	20.55	m²
Maximum deformation on Y axis	1570.00	mm
Plastic Strain Area (including Failure Area) where EPS> 0.05	7.81	m²
Number of Damaged Stiffeners (EPS>0.05)	3	-
End Velocity of Iceberg	0.16	m/s
Kinetic Energy Lose for the Iceberg	4967.47	kJ
Kinetic Energy Lose in Percentage	99.35%	-
Time Span to be Simulated	3.5	s
Computation Time for Computer	904.43	min

Figure B-8 The scenario after collision of e) Bullet Shape 1 Iceberg with Failure Criteria at 3.5s
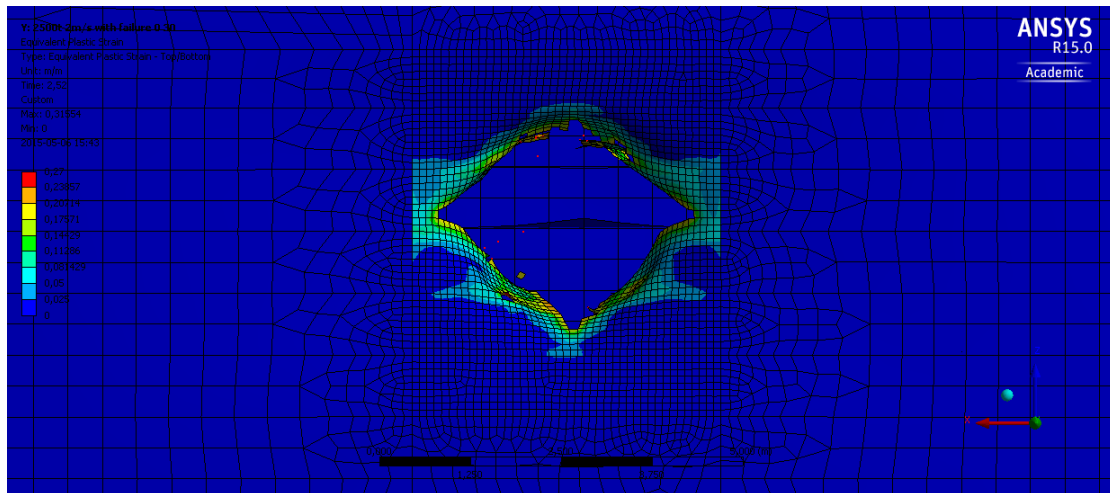
Figure B-9 EPS illustration on the side structure after the collision with f) Bullet Shape 2 Iceberg with failure criteria
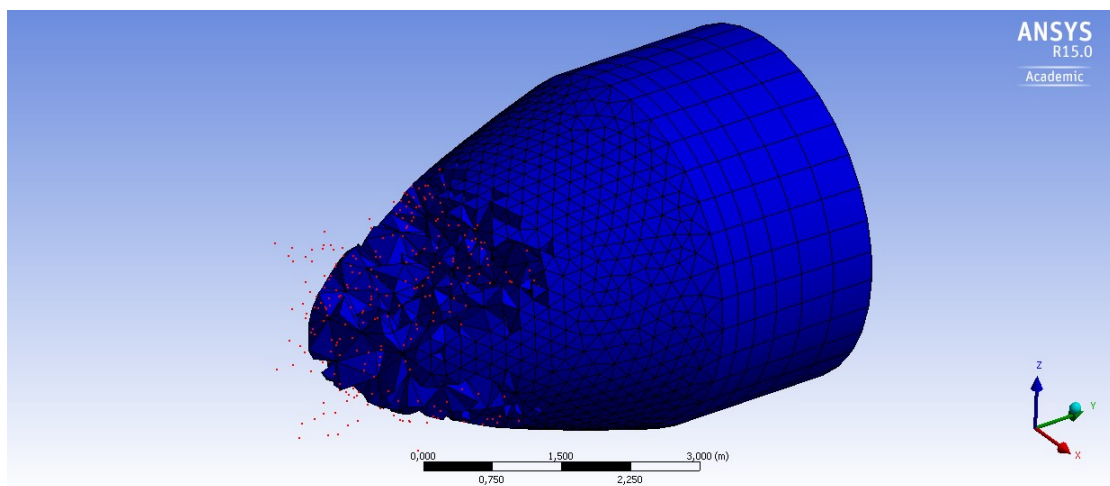

Figure B-10 Coarse front of the broken iceberg after collision in e) Bullet Shape 1 Iceberg with Failure Criteria at 3.5s

Also the iceberg failed at the front of the iceberg. There is also coarse front area after the collision. And the failure region distributed randomly from the tip to the bottom in the failure of the ice is distributed about 2.00m along the Y direction from the tip.

g) Bullet Shape 1 Iceberg Hits above Region

Different from the results in c) Bullet Shape 1 Iceberg, the iceberg change the hitting position to the above region where parts of the side structure are in low temperature (-30°C). However, almost no failure happens on the hit plate of the side structure in case g). The simulation shows that only one mesh element has been 'taken away', which means failure happens on the element.

Also still due to the stiffness of the side structure, the iceberg bounces back with a stable velocity of 0.41m/s in Y positive direction at the end period of the simulation time.

Table B-0-7 Collision Result for g) Bullet Shape 1 Iceberg Hits above Region

| Name	Value	Unit
Failure Area	0.01	m^2
Deformation Area (Where deformation on Y axis >=100mm)	47.35	m^2
Maximum deformation on Y axis	1187	mm
Plastic Strain Area (including Failure Area) where EPS> 0.05	6.46	m^2
Number of Damaged Stiffeners (EPS>0.05)	4	-
End Velocity of Iceberg	0.41	m/s
Kinetic Energy Lose for the Iceberg	4794.16	kJ
Kinetic Energy Lose in Percentage	95.88%	-
Time Span to be Simulated	3.5	s
Computation Time for Computer	904.92	min
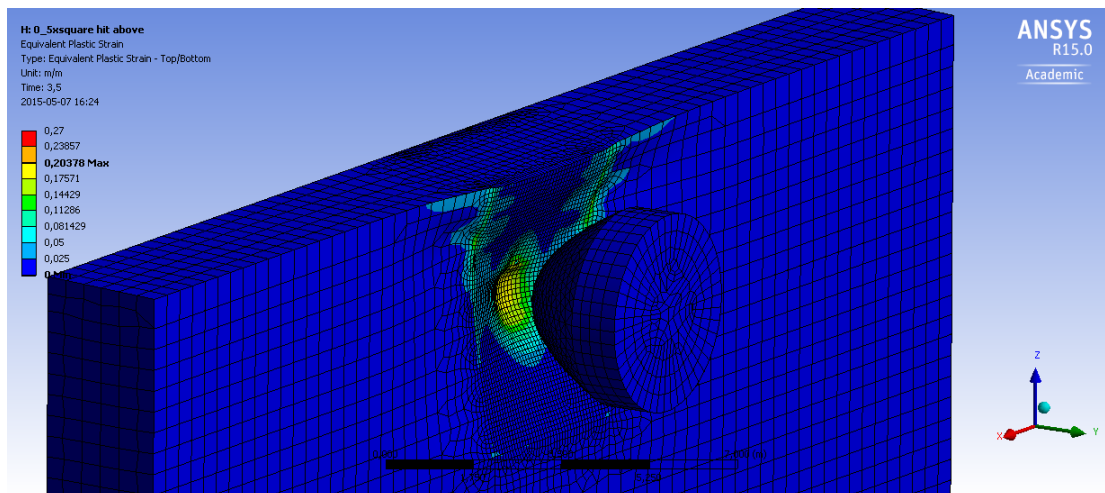
Figure B-11 The scenario after collision of g) Bullet Shape 1 Iceberg Hits above Region at 3.5s
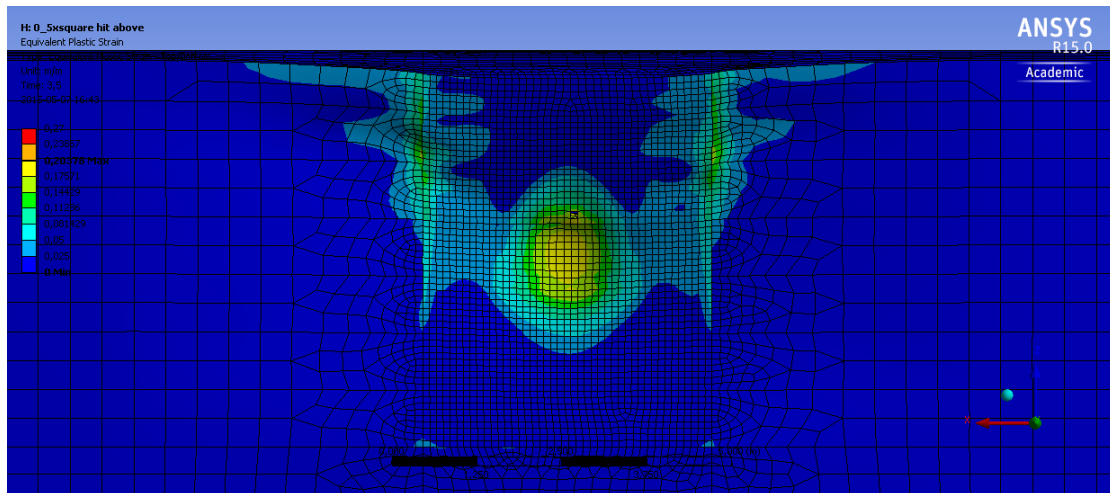
Figure B-12 EPS illustration on the side structure after the collision with g) Bullet Shape 1 Iceberg Hits above Region

It is believed that the NVA steel in low temperature has a higher flow stress. That is to say the steel becomes 'tougher'. This character has already been indicated in *Figure 2-2 Local Stress vs. Local Strain of the NVA Steel.*

If the steel have not reached its failure criteria, the steel in the low temperature will absorb more energy when having deformation at the same strain level. As a consequence, the collision energy is also expected to be absorbed much by the side structure if plastic happens but not reach the failure criteria. According to the data showed in *Figure B-12*, the highest EPS on the hit plate is 0.204. It is smaller to the failure criteria (Maximum EPS=0.239 for NVA steel in mesh size of 100mm under temperature of -30°C) introduced in *Table 4-5 Maximum EPS of NVA grade steel.* Therefore, little failure happens in the case g).

h) Bullet Shape 2 Iceberg Hits above Region

In this case, the damage seems to be more serious than case d) Bullet Shape 2 Iceberg. The iceberg penetrates not only the outer side shell but also make failure on the inner side shell. Although serious damage occurs in this case, the iceberg still bounces back with a stable velocity of 0.20m/s along the positive direction on Y at time of 3.5s. The reason for it is still the stiffness of the side structure of the vessel.

Table B-0-8 Collision Results for Bullet Shape 2 Iceberg Hits above Region

| Name	Value	Unit
Failure Area	0.91	m²
Failure Area (Inner Side Shell)	0.06	m²
Deformation Area (Where deformation on Y axis >=100mm)	44.78	m²
Deformation Area (Inner Side Shell)	1.41	m²
Maximum Deformation on Y axis	1385.7	mm
Maximum Deformation on Y axis (Inner Side Shell)		mm
Plastic Strain Area (including Failure Area) where EPS> 0.05	8.13	m²
Plastic Strain Area (Inner Side Shell)	0.21	m²
Number of Damaged Stiffeners (EPS>0.05)	4	-
Number of Damaged Stiffeners (Inner Side Shell)	1	-
End Velocity of Iceberg	0.20	m/s
Kinetic Energy Lose for the Iceberg	4948.08	kJ
Kinetic Energy Lose in Percentage	98.96%	-
Time Span to be Simulated	3.5	s
Computation Time for Computer	1232.29	min
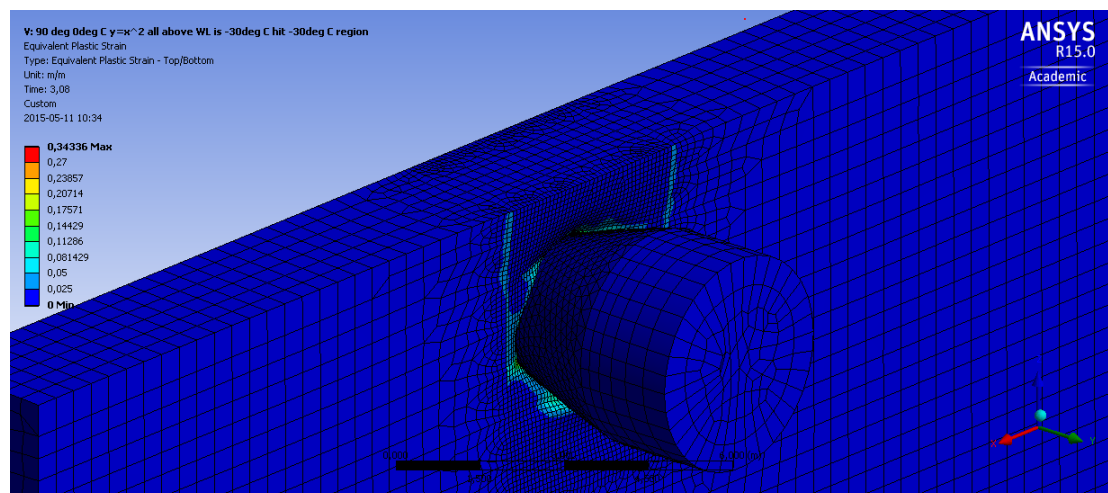
Figure B-13 The scenario after collision of h) Bullet Shape 2 Iceberg Hits above Region at 3.5s (ISO view)
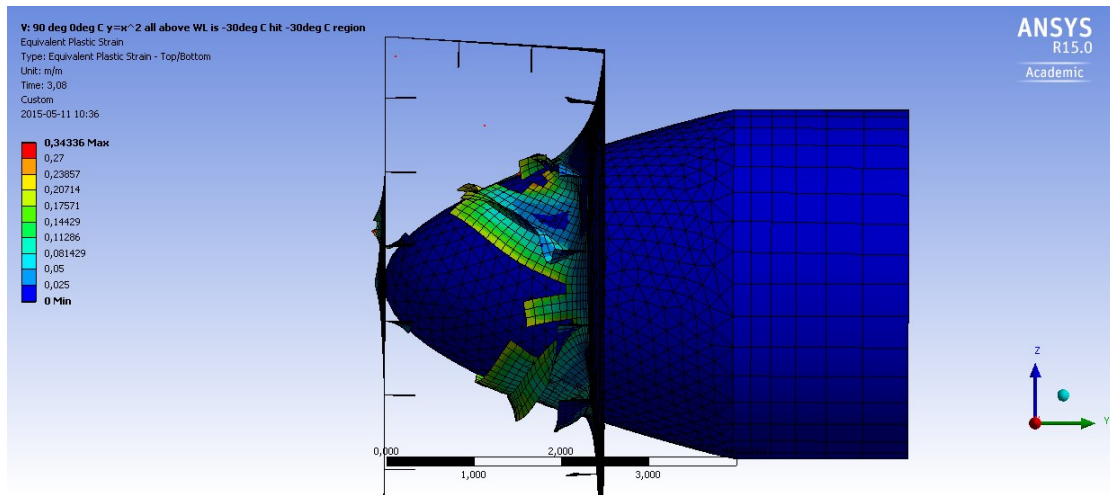
Figure B-14 The scenario after collision of h) Bullet Shape 2 Iceberg Hits above Region at 3.5s (side view)
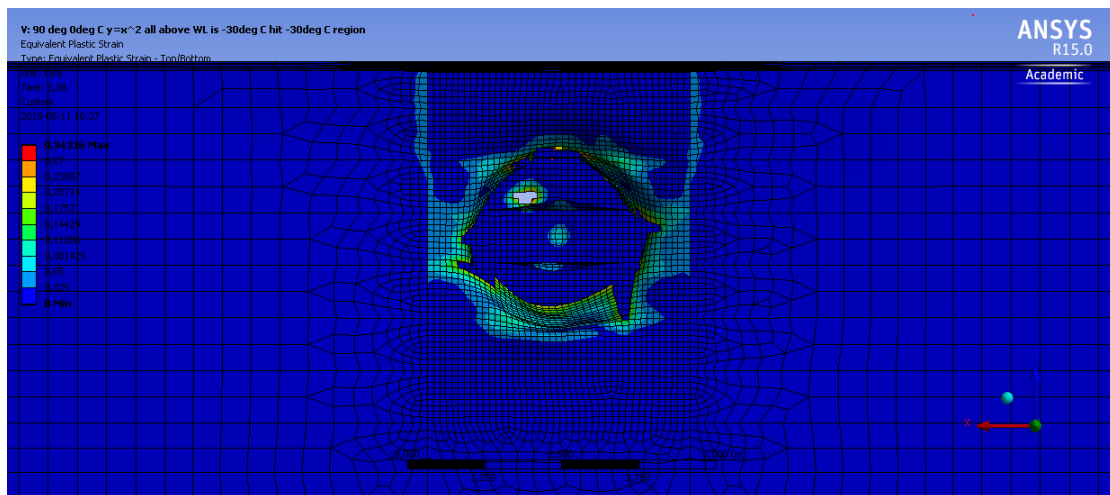

Figure B-15 EPS illustration on the side structure after the collision with g) Bullet Shape 2 Iceberg Hits above Region

The result in this case has verified that the steel in low temperature is easier to have failure. Although in the low temperature the steel becomes 'tougher' if the strain has not reached the maximum EPS, the low temperature also lower the maximum EPS of the steel. It has been indicated in the *Table 4-5 Maximum EPS of NVA grade steel.* Therefore, if the failure once happens, the damage scenario will be relatively more serious compared to the higher temperature if other conditions are not changed.

i) Bullet Shape 1 Iceberg with Failure Criteria Hits Above Region

When the failure criteria of ice has been assigned to the ice tip of bullet shape 1 iceberg, it is more difficult for the iceberg to make failure on the plate of the side structure. In this case, the 'tougher' steel seems to be a stone and the iceberg is more or less like a fragile egg. Therefore, failure happens on the tip of the iceberg. However, due to the geometry of the iceberg, the failure area of the iceberg is not very big when comparing to case e).

But still due to the huge inertia of the iceberg, the iceberg can make plastic deformation on the steel plate. And in the end of the collision process, the iceberg is bounced back by the side structure of the vessel. The end velocity of the iceberg is 0.51m/s in positive Y direction.

Table B-0-9 Collision Results for i) Bullet Shape 1 Iceberg with Failure Criteria Hits above Region

| Name	Value	Unit
Failure Area	0.00	m²
Deformation Area (Where deformation on Y axis >=100mm)	47.56	m²
Maximum deformation on Y axis	1199.50	mm
Plastic Strain Area (including Failure Area) where EPS> 0.05	5.96	m²
Number of Damaged Stiffeners (EPS>0.05)	4	-
End Velocity of Iceberg	0.51	m/s
Kinetic Energy Lose for the Iceberg	4673.13	kJ
Kinetic Energy Lose in Percentage	93.46%	-
Time Span to be Simulated	3.5	s
Computation Time for Computer	934.43	min
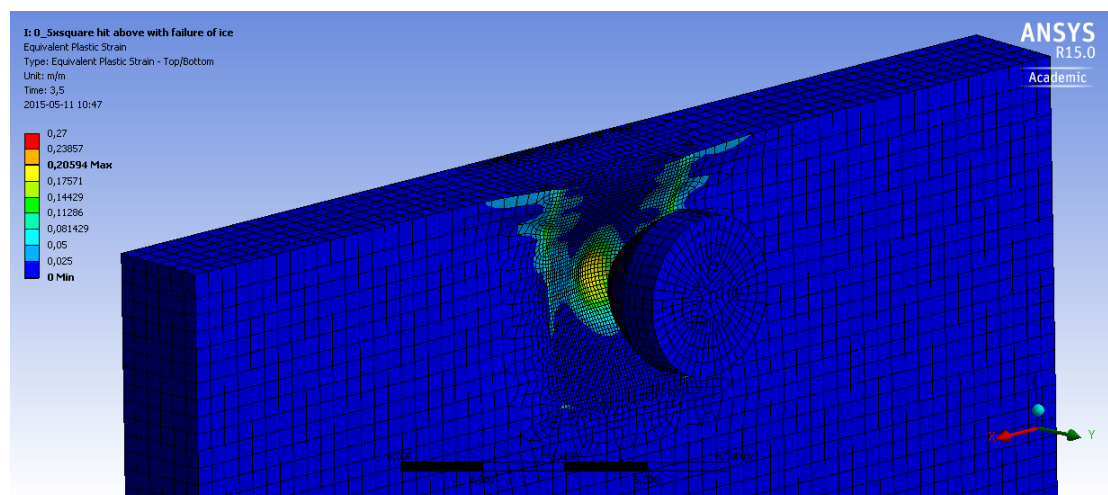
Figure B-16 The scenario after collision of i) Bullet Shape 1 Iceberg with Failure Criteria Hits above Region at 3.5s
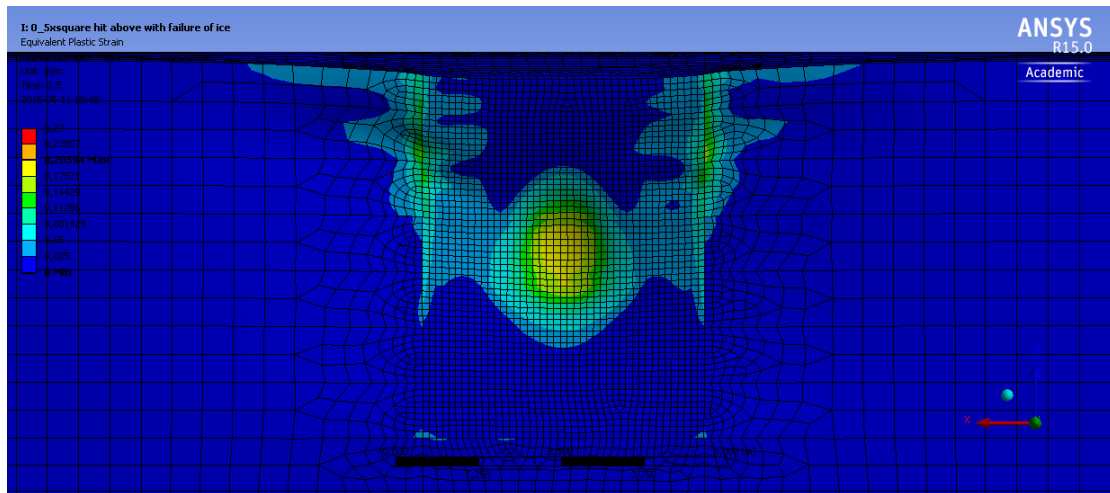
Figure B-17 EPS illustration on the side structure after the collision with i) Bullet Shape 1 Iceberg with Failure Criteria Hits above Region
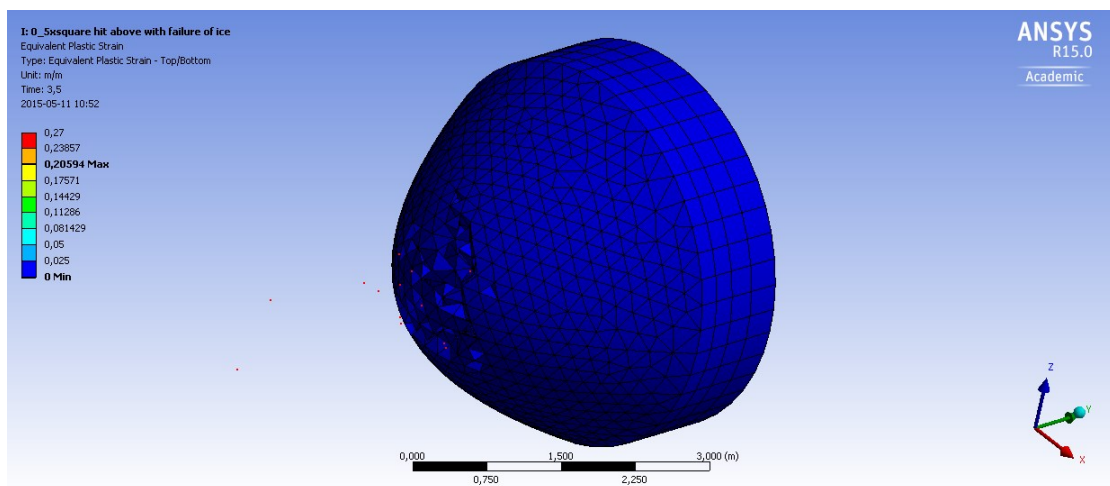

Figure B-18 The Iceberg in Case i) after Collision

j) Bullet Shape 2 Iceberg with Failure Criteria Hits above Region

When failure criteria of the ice are assigned to the Bullet Shape 2 Iceberg, it is not easy for the Bullet Shape 2 Iceberg to penetrate the inner side of the vessel. Since the tip part of the iceberg has been destroyed during the collision, the iceberg can no longer reach the inner side during the collision process.

Still due to the low temperature makes the plate brittle, serious damage or failure happens on the outer plate of the side structure also. But the iceberg also bounced back after the collision with a stable velocity of 0.28m/s along the positive Y direction at the period near 3.5s.

Table B-0-10 Collision Results in j) Bullet Shape 2 Iceberg with Failure Criteria Hits above Region

| Name	Value	Unit
Failure Area	1.19	m^2
Deformation Area (Where deformation on Y axis >=100mm)	52.47	m^2
Maximum deformation on Y axis	1433.6	mm
Plastic Strain Area (including Failure Area) where EPS> 0.05	7.39	m^2
Number of Damaged Stiffeners (EPS>0.05)	4	-
End Velocity of Iceberg	0.20	m/s
Kinetic Energy Lose for the Iceberg	4948.08	kJ
Kinetic Energy Lose in Percentage	98.96%	-
Time Span to be Simulated	3.5	s
Computation Time for Computer	1232.29	min
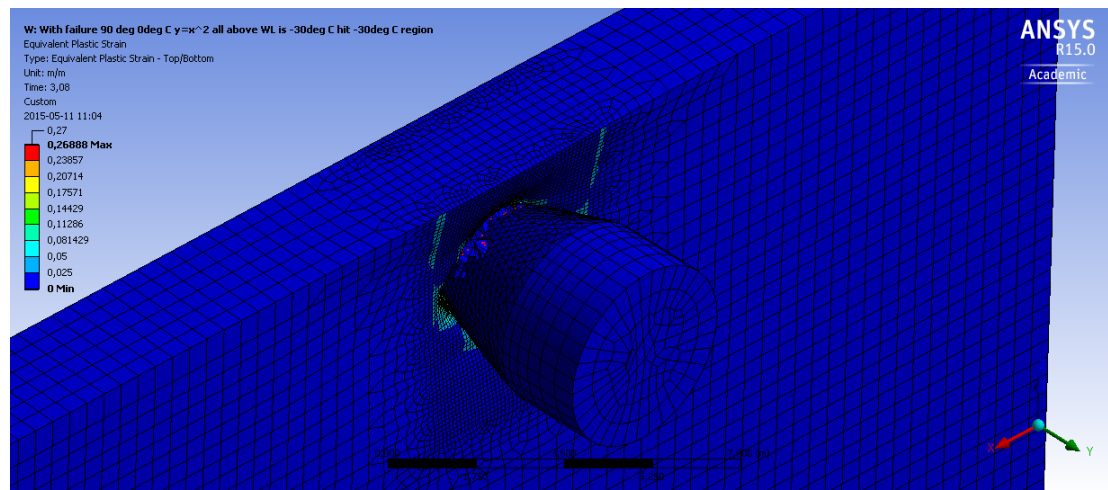
Figure B-19 The scenario after collision of j) Bullet Shape 2 Iceberg with Failure Criteria Hits above Region at 3.5s
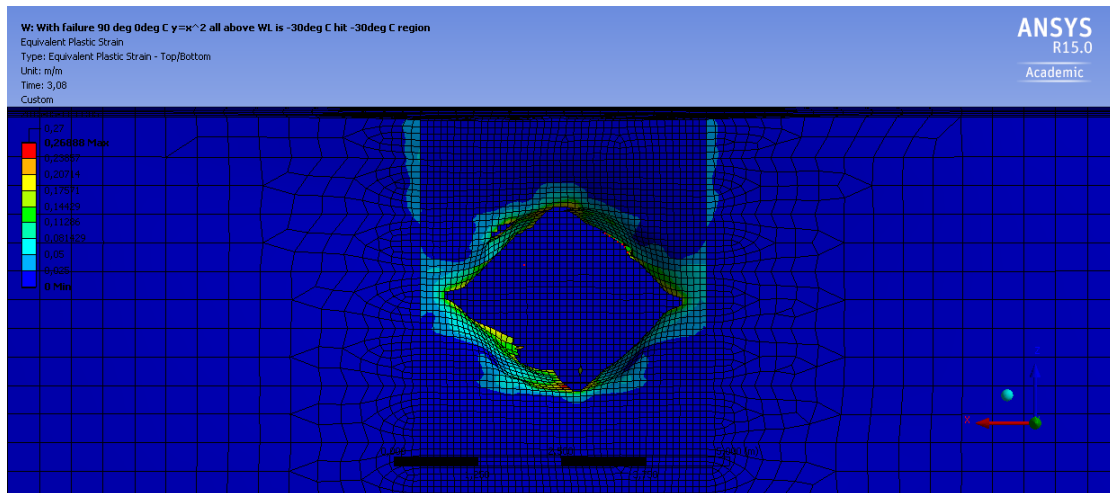
Figure B-20 EPS illustration on the side structure after the collision with j) Bullet Shape 2 Iceberg with Failure Criteria Hits above Region
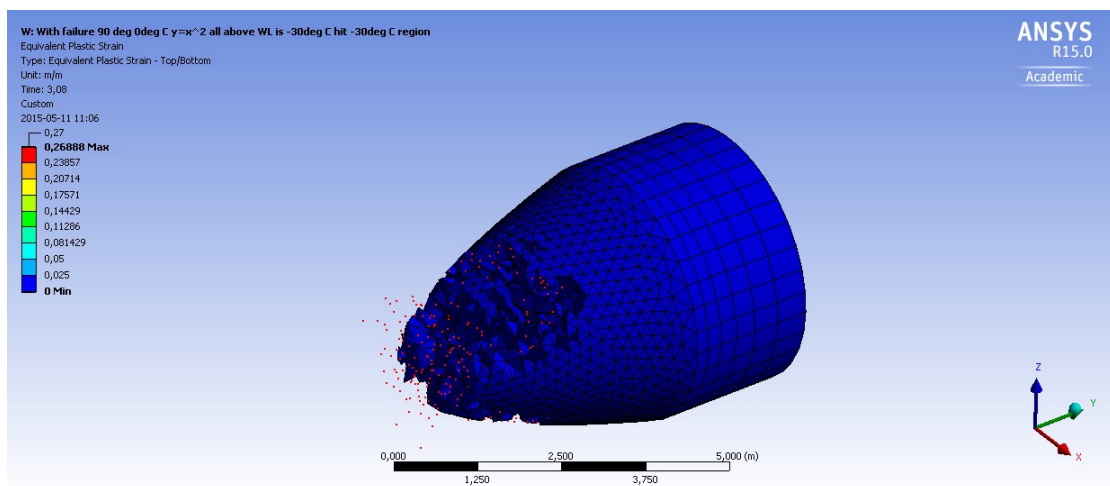

Figure B-21 The Iceberg in Case j) after Collision

k) Bullet Shape 2 Iceberg Hit (above Waterline Temperature is 0°C)

Quite similar results as in the case d), and the iceberg also bounced by the side structure with a stable velocity of 0.30m/s during the end period of the simulation. The detail results are showed in the table below.

Table B-0-11 Collision Results in k) Bullet Shape 2 Iceberg Hitting with above Waterline Temperature is 0°C

| Name	Value	Unit
Failure Area	0.78	m²
Deformation Area (Where deformation on Y axis >=100mm)	12.27	m²
Maximum deformation on Y axis	1637.3	mm
Plastic Strain Area (including Failure Area) where EPS> 0.05	7.96	m²
Number of Damaged Stiffeners (EPS>0.05)	4	-
End Velocity of Iceberg	0.30	m/s
Kinetic Energy Lose for the Iceberg	4888.70	kJ
Kinetic Energy Lose in Percentage	97.77%	-
Time Span to be Simulated	2.75	s
Computation Time for Computer	743.53	min
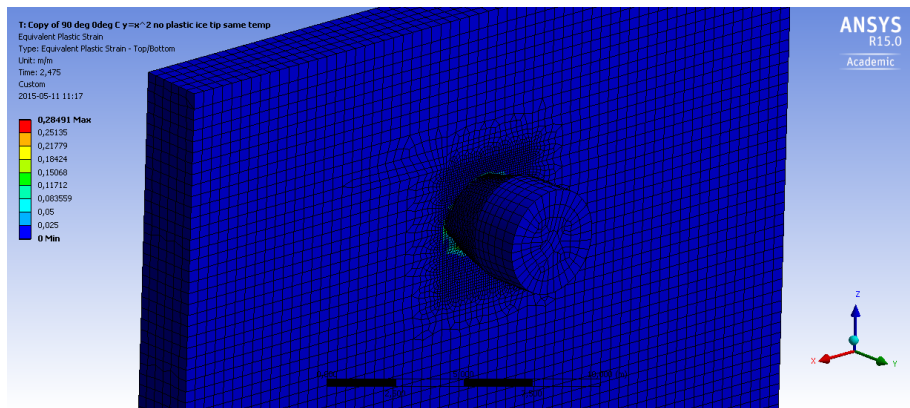
Figure B-22 The scenario after collision of k) Bullet Shape 2 Iceberg Hit with above Waterline Temperature is 0°C at 2.75s
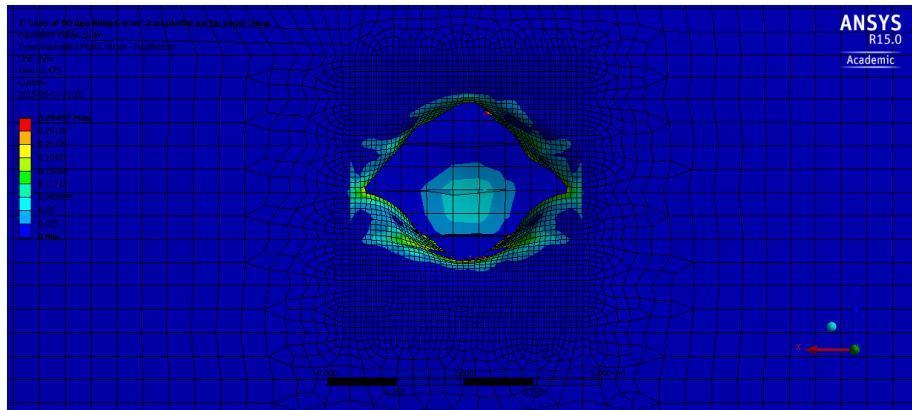
Figure B-23 EPS illustration on the side structure after the collision with k) Bullet Shape 2 Iceberg Hit with above Waterline Temperature is 0°C.

l) Bullet Shape 2 Iceberg Hit (above Waterline Temperature is -30°C)

Still quite similar results as case d), and the iceberg bounced by the side structure with a stable velocity of 0.30m/s during the end period of the simulation. The detail results are showed in the table below.

Table B-0-12 Collision Results in l) Bullet Shape 2 Iceberg Hit with above Waterline Temperature is -30°C

| Name	Value	Unit
Failure Area	0.81	m²
Deformation Area (Where deformation on Y axis >=100mm)	15.34	m²
Maximum deformation on Y axis	1600.6	mm
Plastic Strain Area (including Failure Area) where EPS> 0.05	8.0319	m²
Number of Damaged Stiffeners (EPS>0.05)	4	-
End Velocity of Iceberg	0.30	m/s
Kinetic Energy Lose for the Iceberg	4884.77	kJ
Kinetic Energy Lose in Percentage	97.70%	-
Time Span to be Simulated	2.75	s
Computation Time for Computer	743.53	min
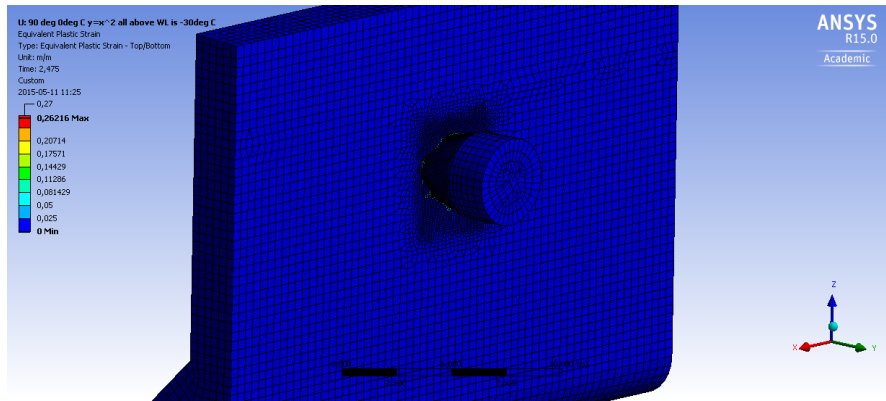
Figure B-24 The scenario after collision of l) Bullet Shape 2 Iceberg Hit with above Waterline Temperature is -30°C at 2.75s
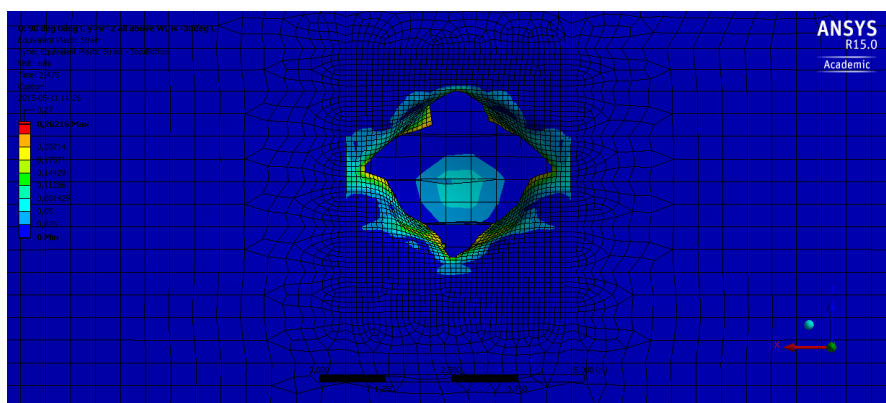

Figure B-25 EPS illustration on the side structure after the collision with l) Bullet Shape 2 Iceberg Hit with above Waterline Temperature is -30°C